ENVIRONMENTAL INFLUENCES ON MARINE BACTERIAL DIVERSITY AND ACTIVITY

Cansu Bayındırlı

Thesis submitted for the degree of
Master of Philosophy

University of East Anglia
School of Environmental Sciences
June, 2016

ABSTRACT

In order to facilitate the conservation of biological diversity, a comprehensive knowledge of the microbial ecology of an ecosystem is required. As the vast majority of microbes are not readily culturable, it is necessary to use molecular tools to investigate their diversity and function in the marine ecosystem. Although it provides a vast quantity of data, the information obtained by molecular tools alone is not sufficient to understand the drivers behind the changes in bacterial communities.

This study aims to characterize changes in the diversity and activity of the heterotrophic bacterial community in relation to a changing environment, in time and space. Two different sampling strategies were used in order to achieve this goal; an annual time series study at a coastal station (station L4, Western English Channel Observatory (WECO)) and a Lagrangian study following an upwelling plume on its track to off shore (2nd filament, Surface Ocean-Lower Atmosphere Study (SOLAS) - Impact of coastal upwelling on the air-sea exchange of climatically important gases (ICON) cruise).

Surface water samples were collected from the time series station L4 of the Western Channel Observatory (50º15'N, 04º13'W; www.westernchannelobservatory.org) every week between 6th April 2009 and 26th April 2010. The respiration rate of the heterotrophic community was determined using Winkler titration to measure the dissolved oxygen content of the < 0.8 µm size-fraction of the seawater. This dataset sits within the larger framework of the Western English Channel bacterial diversity

time series (2003-2009) and the seasonal metagenomic and metatranscriptomic studies associated with this site.

The second approach was to investigate the bacterial diversity and activity in a dynamic environment, such as an upwelling region. The upwelling region off the coast of Mauritania is one of the most productive areas of the world ocean, yet little is known of the temporal and spatial variability in prokaryotic community structure and metabolic activity there, and crucially how this contributes to global elemental cycles.

During a Natural Environmental Research Council (NERC) SOLAS-funded Lagrangian study, we determined bacterial community structure and production together with total community respiration and production. This part of the study describes the temporal changes in bacterial community structure and its activity, in relation to the complex upwelling environmental conditions (mixing, chlorophyll, dissolved organic and inorganic nutrients). Turbulence and dissolved organic carbon appear to play an important role.

1 TABLE OF CONTENTS

ABSTRACT 1

Table of Figures 7

ACKNOWLEDGEMENTS 17

ABBREVIATIONS AND CHEMICAL SYMBOLS 19

1 Introduction 25

1.1 Marine Microorganisms and Their Ecological Importance 25

1.1.1 ..... The Microbial Loop 27

1.1.2 ..... Marine Bacteria 29

1.2 Bacterial Respiration in the marine environment 36

1.2.1 ..... Factors Affecting Bacterial Respiration 37

1.3 Bacterial community structure 39

1.3.1 ..... Factors Affecting Bacterial Diversity 43

1.4 Objectives of the study 44

2. Methodology 45

2. 1. Study Sites 46

2. 1. 1. ..... Time Series Study at Station L4 46

2. 1. 2. ..... Lagrangian Sampling at an Upwelling Plume off the Mauritanian Coast 47

2. 2. Hydrographic Measurements 50

2. 3. Inorganic Nutrients 51

2. 4. Chlorophyll α and Primary Production 52

2. 5. Abundance by Flow Cytometry 53

2. 6. Radioactively labelled amino acid dilution bioassays 55

2. 7. Dissolved Oxygen Content of the Water 56

2. 7. 1. ..... Sampling and Automated Titration Apparatus 57

2. 7. 2. ..... Preparation of the reagents 58

2. 7. 3. ..... Calibration of Sodium Thiosulphate and Calculation of the Dissolved Oxygen 60

2. 8. Respiration Rate Measurements 62

2. 9. Microbial community structure 64

2. 9. 1. ..... Sample Collection, Filtering and Storage 64

2. 9. 2. ..... Nucleic Acid Extraction 65

2. 9. 3. ..... RNA Purification 67

2. 9. 4. ..... Reverse Transcription Polymerase Chain Reaction (RT-PCR) and Polymerase Chain Reaction (PCR) 67

2. 9. 5. ..... Sequence Clean-up, Annotation and Statistical Analysis 69

3. Annual Time-Series Study on the Bacterial Diversity and Activity 71

3. 1. Sea Surface Temperature and Salinity 71

3. 2. Inorganic Nutrients 74

3. 3. Dissolved Oxygen 81

3. 4. Chlorophyll *α* 82

3. 5. Eukaryotic and Bacterial Cell Abundance 84

3. 6. Respiration Rates 96

3. 7. Bacterial Diversity and the Active Groups 102

4. Microbial Community Structure During an Upwelling Event off the North West African Coast 107

4. 1. Mauritanian Upwelling Region 107

4. 2. Sea Surface Temperature 110

4. 3. Inorganic Nutrients 111

4. 4. Chlorophyll *a* 113

4. 5. Eukaryotic and Bacterial Abundance 115

4. 6. Community Respiration and Production 118

4. 7. Bacterial Production 118

4. 8. Bacterial Diversity and the Active Groups 119

5. Conclusion and Future Perspectives 123

APPENDIX A: MANUFACTURERS' PROTOCOLS 125

Bibliography 127

TABLE OF FIGURES

Figure 1.1. The three domains of life. (A) Phylogenetic tree based on ribosomal RNA sequences of Bacteria, Archaea and Eukarya. The root of this tree is based on a hypothetical common ancestor. (B) Phylogenetic tree representation of the three-domain tree, taking into account likely horizontal gene transfer. (Munn, 2011). 26

Figure 1.2**.** Simplified representation of the microbial loop and its relation with the rest of the food web in the ocean. The green (photosynthetic) and yellow (heterotrophic) boxes are the organisms making up the microbial loop, and the blue boxes are the rest of the organisms of the ocean's food web that are in immediate contact with microbes. Straight lines represent the major fluxes of energy and carbon, while the dotted lines represent less dominant ones. (Image from Pomeroy et al., 2007). 28

Figure 1.3. Relative abundances of different groups of bacteria (in %DAPI) at 24 stations around the world. Red numbers indicate the stations between 0 to 35° N and blue numbers indicate the higher latitudes (>35°). (Image from Wietz et al., 2010). 31

Figure 1.4. Representation of organic matter in seawater in micro scale, made up of polymers, fibrils and particles (all black) with bacteria (red) and algae (green), creating microniches, or "hot spots" of microbial activity. (Image from Azam, 1998). 33

Figure 1.5. Relationship between bacterial respiration (BR) and abundance (BA). ($BR=1.62BA^{0.81}$, $n=260$, $p<0.001$, $r^2=0.27$, Robinson, 2008). 39

Figure 1.6. Secondary structure of a 16S rRNA based on *E. coli*. Highly variable regions are drawn red and labelled with their names. Highly conservative regions are shown in green and the binding sites of primers used in PCR amplification of the rRNA gene are shown in blue. Arrows indicate the directions of amplification. The rest of the nucleotides are drawn black. (Adapted from Stackebrandt et al., (2001); available in the public domain Ribosomal Database Project)..... 41

Figure 2.1. Location of the station L4 of Western Channel Observatory..... 46

Figure 2.2. The study site and station locations, with dates of sampling marked on the map, overlaid on the sea surface temperature data taken on 20th May 2009. (Image courtesy of NEODAAS)..... 49

Figure 2.3. Workflow for the metagenome sequencing. 65

Figure 3.1. The mean SST (—), maximum and minimum values (·····) recorded between 2000 and 2008, and the SST data recorded during the present study, from April 2009 to April 2010, shown in red squares. Solid square is used (■) for data collected in 2009 and empty square (□) for data collected in 2010..... 71

Figure 3.2. The temperature depth profile during the study period..... 72

Figure 3.3. The salinity measurements (—■—) at L4, from 07th January 2002 to 26th April 2010. 73

Figure 3.4. The mean (—) and the maximum (·····) nitrate concentrations recorded between 2000 and 2009, with the concentrations recorded during the present study, in 2009 (♦) and 2010 (◇)..... 75

Figure 3.5. The mean (—) and the maximum (·····) nitrite concentrations recorded from 2000 to 2009, with the concentrations recorded during the present study, in 2009 (▲) and 2010 (▲). 76

Figure 3.6. The mean (—) and the maximum (·····) ammonia concentrations recorded from 2000 to 2009, with the concentrations recorded during the present study, in 2009 (●) and 2010 (●). 77

Figure 3.7. The mean (—) and the maximum (·····) silicate concentrations recorded from 2000 to 2009, with the concentrations recorded during the present study, in 2009 (■) and 2010 (■). 78

Figure 3.8. The mean (—) and the maximum (·····) phosphate concentrations from 2000 to 2009, with the concentrations recorded during the present study, in 2009 (◆) and 2010 (◆). 79

Figure 3.9. The dissolved oxygen content (—◆—) of the surface waters at station L4. 81

Figure 3.10. The chlorophyll *a* measurements (—●—) at station L4, from beginning of 2000 to end of April 2010..... 83

Figure 3.11. The mean chlorophyll *a* (—), the maximum and minimum values since 2000 (·····), and the chlorophyll *a* measurements recorded during the present study, samples from 2009 (●) and 2010 (●). 83

Figure 3.12. The mean (—), the maximum and the minimum (·····) cell counts for phototrophic picoeukaryotes, together with the abundances observed during the present study, samples from 2009 (■) and 2010 (■). 84

Figure 3.13. The mean (—), the maximum and the minimum (·····) cell counts for phototrophic nanoeukaryotes, together with the abundances observed during the present study, samples from 2009 (●) and 2010 (○). 86

Figure 3.14. The mean (—), the maximum and the minimum (·····) coccolithophore cell counts with the abundances observed during the present study, samples from 2009 (●) and 2010 (○). 87

Figure 3.15. The mean (—), the maximum and the minimum (·····) heterotrophic nanoeukaryote cell counts with the abundances observed during the present study, samples from 2009 (▲) and 2010 (△). 88

Figure 3.16. The mean (—), the maximum and the minimum (·····) cryptophyta cell counts with the abundances observed during the present study, samples from 2009 (●) and 2010 (○). 88

Figure 3.17. The mean (—), the maximum and the minimum (·····) *Synechococcus* spp. cell counts with the abundances observed during the present study, from 2009 (♦) and 2010 (◇). 89

Figure 3.18. The mean (—), the maximum and the minimum (·····) cell counts for heterotrophic bacteria together with the abundances observed during the present study, from 2009 (♦) and 2010 (◇). 90

Figure 3.19. The changes in the percentages of the HNA (dark blue) vs LNA (light blue) heterotrophic bacteria during the sampling period. 91

Figure 3.20. The sea surface temperature (-●-) and the chlorophyll *a* concentrations (-●-) throughout the sampling period. 92

Figure 3.21. The ammonia (), nitrate (), nitrite (), phosphate (), and silicate () concentrations throughout the sampling period. 92

Figure 3.22. The dissolved oxygen () and the chlorophyll *a* () concentrations at the surface waters at station L4. The shaded area between the dashed lines represents the period of SST above 14ºC..... 93

Figure 3.23. The changes in the respiration rates of the total () and the bacterial () community, with the SST (), throughout the sampling period at station L4. 93

Figure 3.24. The picoeukaryote () and the nanoeukaryote () cell counts by flowcytometry during the sampling period..... 94

Figure 3.25. The coccolithophore () and the heterotrophic nanoeukaryote () abundances during the sampling period. 94

Figure 3.26. The *Synechococcus* spp. () and the cryptophyta () abundances during the sampling period..... 95

Figure 3.27. The change in the heterotrophic bacterial () abundance during the sampling period. 95

Figure 3.28. The relation between the total community (a) and bacterial respiration (b) with sea surface temperature, during the study period, at station L4. 97

Figure 3.29. The relation between the bacterial respiration with HNA (a) and LNA (b) bacteria, during the study period, at station L4. 97

Figure 3.30. The changes in the respiration rates of the total (→) and the bacterial (→) community, from 22nd September to end of the sampling period. Please note the scale. 100

Figure 3.31. The percent bacterial respiration in relation to the community respiration. 100

Figure 3.32. The relative abundance of actinobacteria (■), bacteriodetes (■), cyanobacteria (■), proteobacteria (alphaproteobacteria (■), betaproteobacteria (■), gammaproteobacteria (■), and other proteobacterial groups (■) and other bacteria (■) in the unfiltered water, from 6th April 2009 to 26th April 2010, a) 16S rDNA and b) rRNA (cDNA). 103

Figure 3.33. The relative abundance of actinobacteria (■), bacteriodetes (■), cyanobacteria (■), proteobacteria (alphaproteobacteria (■), betaproteobacteria (■), gammaproteobacteria (■), and other proteobacterial groups (■) and other bacteria (■) in the >0.8 µm size fraction, from 6th April 2009 to 26th April 2010, a), 16S rDNA and b) rRNA (cDNA). 104

Figure 3.34. MDS plot for the DNA sequences of the unfiltered water. (Bacterial OTUs only). 105

Figure 3.35. MDS plot for the RNA sequences of the unfiltered water. (Bacterial OTUs only). 105

Figure 3.36. MDS plot for the DNA sequences of the <0.8 µm fraction. (Bacterial OTUs only). 106

Figure 3.37. MDS plot for the RNA sequences of the <0.8 µm fraction. (Bacterial OTUs only). 106

Figure 4.1. The study site and station locations, with dates of sampling marked on the map, overlaid on the sea surface temperature data taken on 20th May 2009. (Image courtesy of NEODAAS). 108

Figure 4.2. The wire-walker data showing the relative proportions of the two water masses. Warm colours indicate higher percentage of the NACW (max being 1 (red) is 100% NACW) and colder colours indicate higher percentage of the SACW. The thick black line indicates NACW front. The thin black line above is the euphotic layer, and the thin black line below is the mixing layer. (Image courtesy of Ricardo Torres). 109

Figure 4.3. Vertical section of temperature (°C) from 15th May to 22nd May 2009. Black line represents the mixed layer depth. Please note the upwelled plume travelled from east (coast) to west (off shore); the direction of the transit is from east to west. 110

Figure 4.4. The distribution of the concentrations of (a) nitrate + nitrite and (b) phosphate in the upper 500 m of the transect. The unit of measurement is µmol L^{-1}. (Image courtesy of Ricardo Torres). 112

Figure 4.5. Inorganic phosphate (—●—), nitrite+nitrate (—◆—), ammonia (—■—), silicate (—●—) and chl *a* (—◆—) concentrations at the sampling depth (55% irradiance, ca 8 m). 113

Figure 4.6. Vertical profile of chlorophyll *a* (mg m^{-3}) from 15th to 22nd May 2009. Note the upwelled plume travelled from east (coast) to west (off shore); the direction of the transit is from east to west. 114

Figure 4.7. MDS plot for the temperature, inorganic nutrients and chlorophyll *a*. . 115

Figure 4.8. Abundance of (a) picoeukaryotes and (b) nanoeukaryotes (cells ml^{-1}) along the transect. 116

Figure 4.9. Abundance of (a) *Synechococcus* and (b) *Prochlorococcus* (cells ml^{-1}) along the transect. 116

Figure 4.10. Abundance of (a) HNA and (b) LNA bacteria (cells ml^{-1}) along the transect. 117

Figure 4.11. Heterotrophic bacterial abundance (cells ml^{-1}). 117

Figure 4.12. Community respiration (—●—), GPP (—■—) and NCP (—◆—) at the 55% light intensity. 118

Figure 4.13. Bacterial amino acid turnover times (leucine (blue), methionine (red) and tyrosine (purple)). Samples collected from 55% light intensity, at pre-dawn. 118

Figure 4.14. Relative Abundance of Archaea and major bacterial groups collected between 15th and 22nd May 2009. 119

Figure 4.15 Relative abundance of subphyla within the Proteobacteria, collected between 15th and 22nd May 2009. 120

Figure 4.16 Relative abundance of Archaea and major bacterial OTUs, obtained from cDNA, collected between 15th and 22nd May 2009. 121

Figure 4.17 Relative abundance of subphyla within the Proteobacteria OTUs, obtained from cDNA, collected between 15th and 22nd May 2009. 121

ACKNOWLEDGEMENTS

I would like to express gratitude to my advisors Dr Carol Robinson, Professor Dr. Colin Murrell, and Dr Jack Gilbert. Carol, you have been an incredible mentor over the years; always there to help, encourage, and motivate, always with the right questions and best solution. I would like to thank you for supporting me in every way possible, both academically and mentally. I also would like to thank you for believing in me even at the times that I didn't. But mostly, I would like to thank you for giving me the chance in the first place. Colin, you didn't hesitate to offer your help when I needed the most. I appreciated all the support and the patience. Jack, thank you for making half of this research possible, adopting me as one of your students when I needed a supervisor and half a research project. Thanks to you, funding was never an issue when it came to ordering the latest extraction kits or participating the biggest conferences. I also would like to thank Dr Graham Savidge and Professor Alastair Grant for letting my viva be an enjoyable moment. Thank you both for your brilliant comments and suggestions. I thoroughly enjoyed our discussions and sincerely appreciated your support.

Many thanks to researchers in PML, who helped me on board, in the labs and answered all my questions from basics to the most complicated. Thank you being competitive colleagues and close friends all in once.

I have been blessed with so many brilliant and nice people around me. You each and all proved to be such amazing friends. The list is so long that I cannot possibly fit all of you in here. Without you I wouldn't be the person I am today. Most of you happen

to be very good scientists who helped me with my studies as well as providing me the drinks after a long day in the lab. I thank you all.

A special thanks to my family. Words cannot express how grateful I am to my family for all of the sacrifices that you've made on my behalf.

ABBREVIATIONS AND CHEMICAL SYMBOLS

ADCP: Acoustic Doppler Current Profiler.

AVHRR: The Advanced Very High Resolution Radiometer.

BCD: Bacterial carbon demand.

BGE: Bacterial growth efficiency.

BODC: The British Oceanographic Data Centre.

BP: Bacterial production.

BR: Bacterial respiration.

Chl *a*: Chlorophyll *a.*

CR: Community respiration.

CTD: Conductivity, Temperature, and Density, refers to the instrument that measure these properties of the water.

DNA: Deoxyribonucleic acid.

dNTP: Deoxyribonucleotide triphosphate.

DOC: Dissolved organic carbon.

DOM: Dissolved organic matter.

DTT: Dithiothreitol.

EDTA: Ethylenediaminetetraacetic acid.

GMT: Greenwich Mean Time.

GOLD: Genomes On-line Database.

GPP: Gross Primary Production.

H_2O: Water.

H_2SO_4: Sulphuric acid.

HCl: Hydrochloric acid.

I^-: Iodide ion.

I_2: Iodine.

I_3^-: Triiodide ion.

ICON: The Impact of Coastal Upwelling on the Air-Sea Exchange of Climatically Important Gases.

IO_3: Iodate.

JGOFS: Joint Global Ocean Flux Study.

KIO_3: Potassium iodate.

LDPE: Low Density Polyethylene.

MBA: Marine Biological Association.

MDS: Multi-dimensional scaling.

MG-RAST: Metagenomic Rapid Annotations using Subsystems Technology.

MID: Multiplex Identifier.

Milli Q (water): Ultrapure water (a trademark of Millipore).

M_{KIO_3}: The molarity of KIO_3.

Mn(II): Manganese oxidation state +2.

Mn(III): Manganese oxidation state +3.

$Mn(OH)_2$: Manganese hydroxide.

Mn^{++}: Manganese ion.

MNO(OH): Manganese oxide-hydroxide.

$MnO(OH)_2$: Di-hydroxido manganite.

$MnSO_4 . H_2O$: Manganous sulphate tetrahydrate.

$MnSO_4$: Manganous sulphate.

MODIS-Aqua: The Moderate-resolution Imaging Spectroradiometer on board Aqua satellite.

$Na_2S_2O_3 . 5H_2O$: Sodium thiosulphate.

NACW: North Atlantic Central Water.

NaI: Sodium iodide.

NaOH: Sodium hydroxide.

NCBI: National Centre for Biotechnology Information.

NCP: Net Community Production.

NEODAAS: The Natural Environment Research Council Earth Observation Data Acquisition and Analysis Service.

NERC: The Natural Environment Research Council.

NH_3: Ammonia.

NH_4^+: Ammonium ion.

$NH_4\text{-}COO^-$: Ammonium acetate.

NO_2: Nitrite.

NO_3: Nitrate.

O_2: Oxygen.

OTU: Operational Taxonomic Unit.

OTE: Ocean Test Equipment, SeaBird sampling bottles.

PCR: Polymerase Chain Reaction.

PML: Plymouth Marine Laboratory.

PO_4: Phosphate.

POC: Particulate organic carbon.

POM: Particulate organic matter.

Proteinase K:	Tritirachium alkaline proteinase
QIIME:	Quantitative Insights into Microbial Ecology.
rDNA:	Ribosomal DNA.
RDP:	Ribosomal Database Project.
RNA:	Ribonucleic acid.
RNase:	Ribonuclease
rRNA:	Ribozomal RNA.
RRS:	Royal Research Ship
RT-PCR:	Reverse-Transcription Polymerase Chain Reaction
$S_2O_3^{--}$:	Thiosulphate ion
$S_4O_6^{--}$:	Tetrathionate ion
SACW:	South Atlantic Central Water.
SDS:	Sodium Dodecyl Sulphate.
SET (buffer):	Mixture of: SDS, EDTA, and Tris buffer.
SF_6:	Sulphur hexafluoride.
Si:	Silicate.
SST:	Sea surface temperature.
SSU rRNA:	Small sub-unit ribozomal RNA.

Tris: Tris (hydroxymethyl) aminomethane

UOR: Undulating Oceanographic Recorder.

V_{blank}: The volume of the blank, used in the formula to calculate the dissolved oxygen content of the given water sample.

V_{bottle}: The volume of the bottle at 20 °C, used in the formula to calculate the dissolved oxygen content of the given water sample.

V_{ch}: The volume of the reagents added, used in the formula to calculate the dissolved oxygen content of the given water sample.

V_{KIO_3}: The volume of KIO_3, used in the formula to calculate the dissolved oxygen content of the given water sample.

V_{std}: The average volume of the titrations, used in the formula to calculate the dissolved oxygen content of the given water sample.

V_{Thio}: The volume of sodium thiosulphate added, used in the formula to calculate the dissolved oxygen content of the given water sample.

WECO: Western English Channel Observatory.

γ: The glass expansion coefficient, used in the formula to calculate the dissolved oxygen content of the given water sample.

ρ_{fix}: The density of the seawater at the fixing temperature,

ρ_{is}: The density of the seawater at in situ temperature, used in the formula to calculate the dissolved oxygen content of the given water sample.

1 INTRODUCTION

1.1 MARINE MICROORGANISMS AND THEIR ECOLOGICAL IMPORTANCE

Microorganisms dominate life in the oceans, both in terms of overall biomass and metabolic activity, shaping life on Earth (Karl, 2007). Their metabolic processes are essential to the functioning of ocean ecosystems and global climate (Falkowski et al., 2008; Bowler et al., 2009; Fuhrman, 2009; Karsenti et al., 2011). They are also considered to be the most genetically diverse group of organisms on the planet (Fuhrman, 2009). Although it is known that they are abundant and responsible for crucial ecosystem functions, even with the latest technology, the scientific community has only relatively recently begun to understand the basics of the dynamics of microbial processes and their variability (Falkowski et al., 2008; Hewson et al., 2009; Bowler et al., 2009; Rusch et al., 2010; Fuhrman, 2012).

Marine microorganisms are abundant in a wide range of habitats and are diverse in their nature, spanning all three domains of life: Bacteria, Archaea and Eukarya, as well as viruses. Although the traditional classification of life clusters these three domains distantly to each other, recent studies using DNA fingerprinting and whole genome sequencing showed that the interaction between organisms is more complex than previously assumed (Figure 1.1), (Brown, 2003; Doolittle & Papke, 2006). In particular, bacteria and archaea have the capacity to gain and retain new traits by horizontal gene transfer (also called lateral gene transfer), genetic recombination and

mutations (McDaniel et al., 2010; Stewart, 2013). Together with their large numbers, high division rates and long evolutionary history, microbes host a vast genotypic and phenotypic diversity (Sogin et al., 2006).

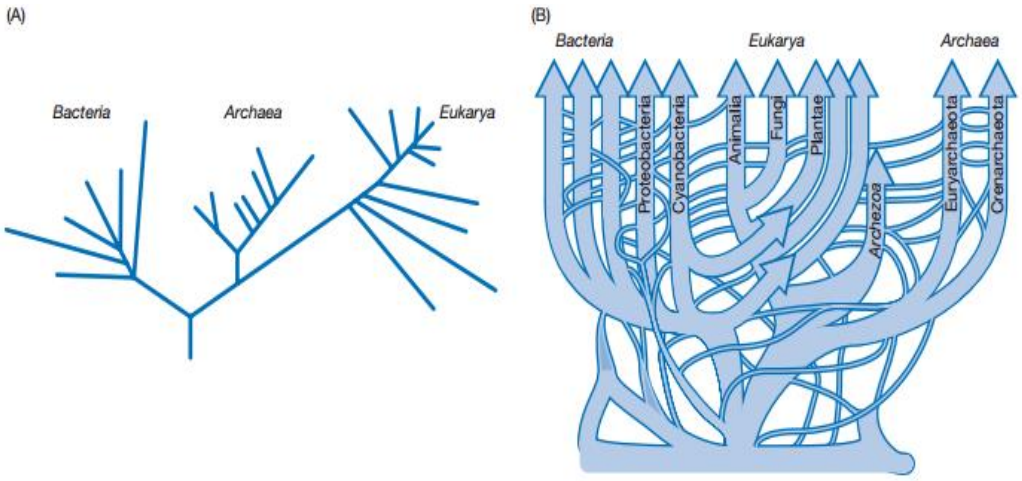

Figure 1.1. The three domains of life. (A) Phylogenetic tree based on ribosomal RNA sequences of Bacteria, Archaea and Eukarya. The root of this tree is based on a hypothetical common ancestor. (B) Phylogenetic tree representation of the three-domain tree, taking into account likely horizontal gene transfer. (Munn, 2011).

The capacity to exchange genes is important in studies of the diversity and activity of the microbial community. Identifying the presence or absence of a particular gene can reveal information about microbial processes and diversity. Hence scientists are using molecular biology techniques to categorize microorganisms in terms of operational taxonomic units (OTUs), instead of defining them as biological species. OTUs are the taxonomic level, with a threshold of ca 97% similarity in the microorganisms' genetic makeup of the small subunit (SSU) ribosomal DNA (rDNA) (Blaxter et al., 2005; Wooley et al., 2010).

With the advancement in scientific tools and methodologies, from microscopy to next generation sequencing, it has been shown that the oceans harbour a vast diversity of marine microorganisms (Venter et al., 2004; Sogin et al., 2006). Recently discovered microbes, genes and metabolic pathways have changed our understanding of their role

in geochemical cycles and our understanding of life on Earth (Gilbert & Dupont, 2011).

In this study, the term ‘microorganism’ (or ‘microbe’) is used to define the microscopic organisms from all three domains of life, both photosynthetic and heterotrophic; i.e. phytoplankton, protozoa, bacteria, and archaea. However, because archaea are not abundant in the surface ocean and it is impossible to differentiate archaeal respiration from bacterial respiration, the term ‘bacteria’ will be used here to encompass both heterotrophic bacteria and archaea.

1.1.1 The Microbial Loop

Marine microorganisms are responsible for the utilization of the particulate and dissolved organic matter lost from the planktonic food web via metabolic processes (Figure 1.2), (Pomeroy, 1974; Azam et al., 1983; Pomeroy et al., 2007). These processes and the interaction between the microorganisms were given the name the ‘microbial loop’, by Azam et al. (1983).

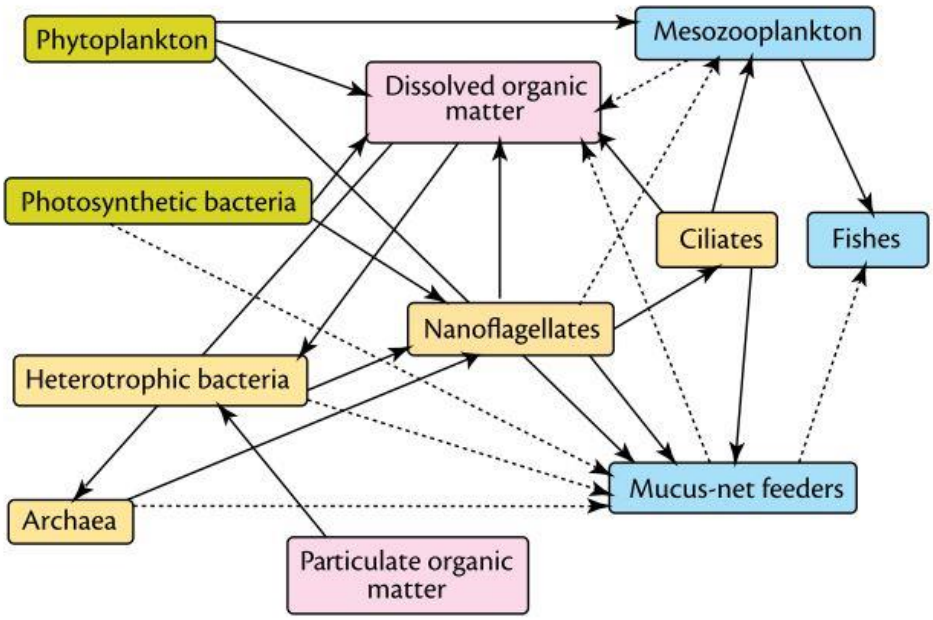

Figure 1.2**.** Simplified representation of the microbial loop and its relation with the rest of the food web in the ocean. The green (photosynthetic) and yellow (heterotrophic) boxes are the organisms making up the microbial loop, and the blue boxes are the rest of the organisms of the ocean's food web that are in immediate contact with microbes. Straight lines represent the major fluxes of energy and carbon, while the dotted lines represent less dominant ones. (Image from Pomeroy et al., 2007).

In the microbial loop, primary production is carried out by the phytoplankton, together with the photosynthetic and chemosynthetic bacteria. Heterotrophic bacteria are responsible for cycling of the organic and inorganic substances and are considered as the engines of the microbial loop (Falkowski et al., 2008; Delong, 2009). Heterotrophic microorganisms play a vital role in nutrient cycling, consuming between 30% and 60% of the primary production in the pelagic zone (Del Giorgio et al., 1997; Azam & Worden, 2004) and respiring most of the organic matter available in the oceans (Williams & Del Giorgio, 2005). Bacteria recycle the organic matter into inorganic substances which can be used by phytoplankton. Their numbers and biomass are, therefore, significantly important to the large scale ecosystem functioning and determine the efficiency of the microbial loop (Karl, 2007; Falkowski et al., 2008).

1.1.2 MARINE BACTERIA

The oceans contain between 10^{28} and 10^{29} bacterial cells (Whitman et al., 1998). Pomeroy et al. (2007) calculated a combined biomass of 50 mg C m^{-3} for plankton and estimated that the combined biomass of autotrophic and heterotrophic bacteria alone makes up ca 35% of the total plankton biomass.

Marine bacteria inhabit all habitats across the ocean, from surface waters to the abyss. They are the most diverse group genetically in the microbial community and their ecological roles are extremely important to our understanding of the ecosystem services, such as remineralisation of organic matter (Giovannoni & Stingl, 2005; Carlson et al., 2007). Bacteria dominate the metabolic activity in marine ecosystems (Hobbie et al., 1977; Chisholm et al., 1992; Fukuda et al., 1998; Pomeroy et al., 2007; Azam & Malfatti, 2007).

At a given time, bacterial communities are typically dominated by one or two phyla, with the remainder of the community represented by smaller numbers of other groups sometimes referred to as the rare biosphere (Sogin et al., 2006; Pedrós-Alió, 2012). For example, among the 10 most abundant phyla which contributed 99.4% of the relative abundance, the surface waters of the western English Channel were dominated by Protobacteria, more specifically only three subphyla; *Alphaproteobacteria* (ca 35 - 50%), *Gammaproteobacteria* (ca 15 – 25%) and *Bacteroidetes* (ca 20 – 45%), making up ca 70 – 90% of the relative abundance at a given time (Gilbert et al., 2009). While the bacteria from dominant phyla are responsible for most of the biomass and carbon cycling, the members of the rare biosphere are thought to serve as seed banks helping the bacterial community to recover through environmental changes (Caporaso et al., 2012). On average, 99.75% ± 0.06 (mean ± sd) of OTUs were observed both in shallow

and deep ribosomal RNA (rRNA) gene sequences, suggesting the majority of the rare taxa persist during environmental changes (Caporaso et al., 2012).

Although bacteria have small cell sizes (ca 0.055 pm^3 for inactive bacteria and 0.12 pm^3 for active bacteria, on average (Gasol et al., 1995)), they contribute >50% of the total calculated surface area for plankton in the oceans, reflecting their high surface area to volume (SA/V) ratios (Pomeroy et al., 2007). A higher SA/V ratio increases the efficiency of nutrient uptake, with the added advantage that smaller cells require little energy for their maintenance (Munn, 2011). Therefore bacteria can grow and multiply rapidly when conditions are suitable, increasing their competitive advantage and chances for survival in nutrient limited environments, as exist in most oceans (Pomeroy et al., 2007).

In order to elucidate the ecological niches of the different bacterial groups, it is important to study their abundance, diversity and function in the context of community structure and environmental conditions (Ducklow et al., 2000; Fuhrman, 2009). There are different theories about the distribution of bacterial groups in terms of where they exist in the oceans. The first is the 'everything is everywhere, but environment selects' theory proposed by Baas-Becking (1934), which suggests the uniform distribution of bacteria across oceans (Staley & Gosink, 1999). However, although it is almost impossible to prove the absence of a microorganism, recent studies have shown that different groups of bacteria are found in different water masses and depths through the water column (Pommier et al., 2005; Agogué et al., 2011; Sul et al., 2013), indicating a varying heterogenic distribution of bacteria in global oceans (Figure 1.3), (Wietz et al., 2010).

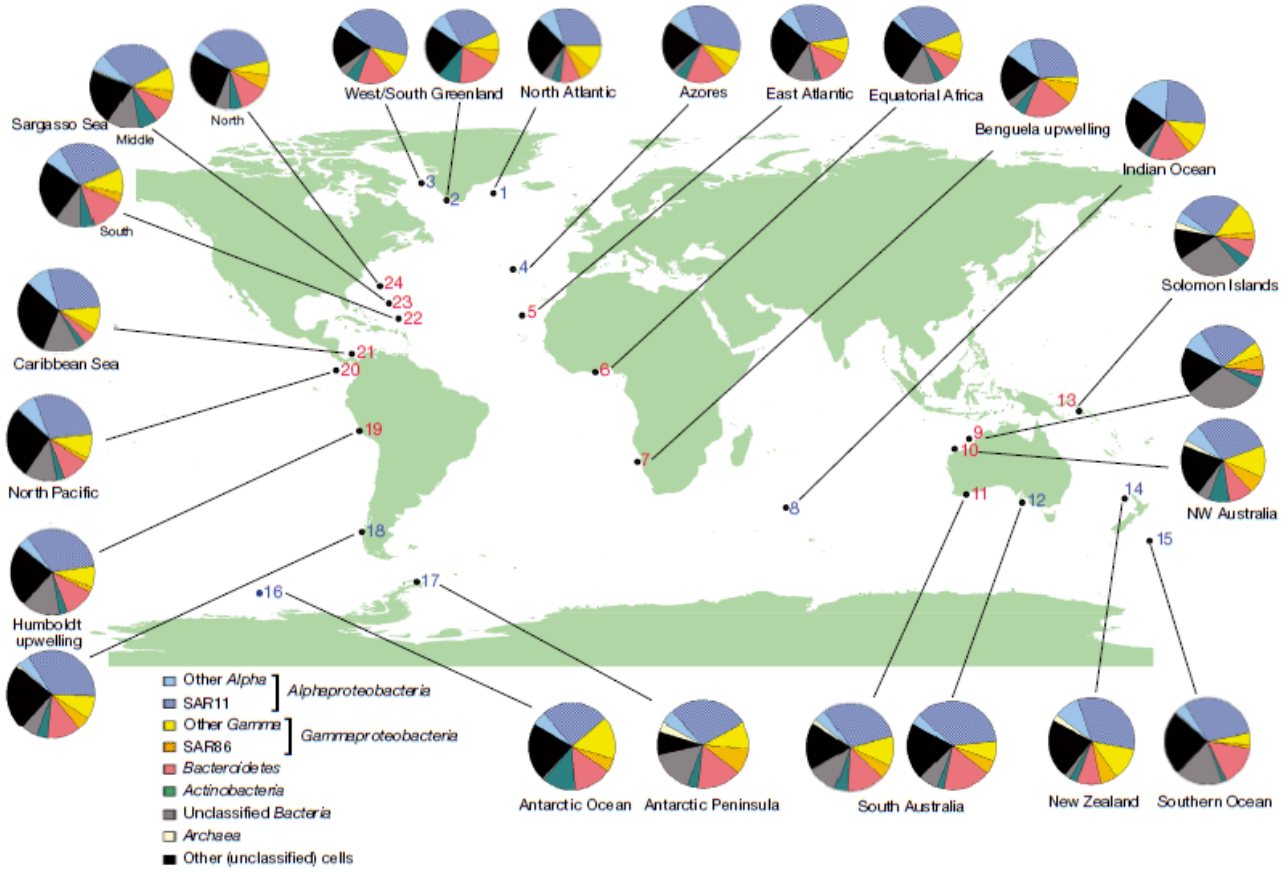

Figure 1.3. Relative abundances of different groups of bacteria (in %DAPI) at 24 stations around the world. Red numbers indicate the stations between 0 to 35° N and blue numbers indicate the higher latitudes (>35°). (Image from Wietz et al., 2010).

The distribution, abundance, biomass and metabolic rate of bacteria are limited by environmental conditions (Martiny et al., 2006; Agogué et al., 2011; Friedline et al., 2012; Sul et al., 2013; Müller et al., 2014). Predation by heterotrophic nanoflagellates and viral infections are the main factors controlling their abundance (Sherr & Sherr, 2002; Giovannoni & Stingl, 2005). Müller et al. (2014) showed that the non-uniform dispersal of bacterial groups mostly depends on ocean circulation and the connectivity of the water masses. In the eastern Atlantic Ocean, next generation sequencing data of rRNA genes showed that different water layers are occupied by different bacterial communities, characterized by variations in temperature, salinity and nutrient content (Friedline et al., 2012).

At the micro-scale that bacteria inhabit, the ocean environment is heterogeneous and made up of several different nano- and pico-habitats (Azam, 1998). Even though some bacteria are motile and use chemotaxis, because of their physiology and the fluid dynamics of the micro-environment in which they live, their growth is dependent on the nutrient availability of their immediate environment (Pomeroy et al., 2007; Stocker & Seymour, 2012).

Marine bacteria metabolize both particulate organic matter (POM) and dissolved organic matter (DOM). In surface waters of the oceans, the primary source of carbon for bacteria is labile DOM arising initially from primary production and subsequent activities such as excretion, cell lysis and sloppy feeding by predators. However, POM serves both as a food source and a physical structure on which microorganisms can accumulate. Particles or aggregates host a diverse microbial community which thrive on the nutrient rich surface (Giovannoni & Stingl, 2005). From dissolved to particulate form, organic matter varies in size (ranging from $< 10^{-4}$ to $> 10^{0}$ m) and structure; it is

made up of polymers, colloids, gels and fibres of suspended and sinking particles (Figure 1.4), (Azam, 1998; Robinson et al., 2010). The physical and chemical nature of POM changes with its decomposition, opening up new micro-niches and providing an environmental gradient for functionally and genetically diverse bacteria (Stewart, 2013), making POM a 'hotspot' of microbial activity (Azam, 1998). Bacterial activity on marine snow can affect sedimentation and primary productivity.

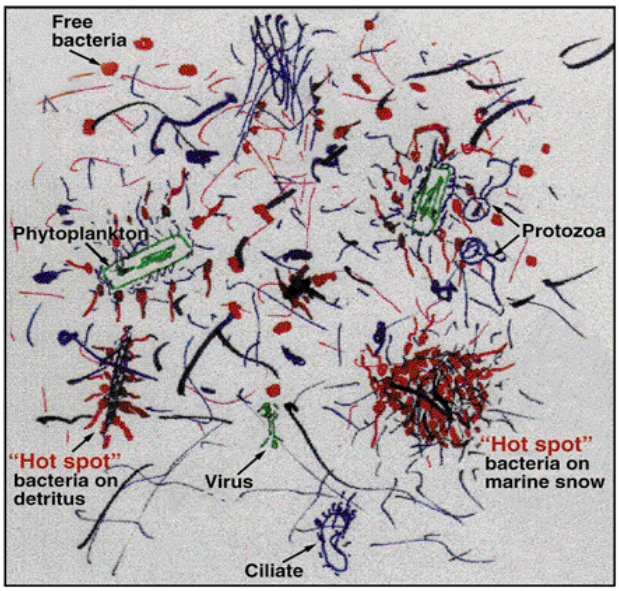

Figure 1.4. Representation of organic matter in seawater in micro scale, made up of polymers, fibrils and particles (all black) with bacteria (red) and algae (green), creating microniches, or "hot spots" of microbial activity. (Image from Azam, 1998).

Due to its complex physical structure, harbouring different groups of bacteria, POM is also found to be a hot spot for horizontal gene flow (Falkowski et al., 2008; Stewart, 2013). It provides a nutrient rich environment for numerous bacteria to rapidly grow and when in close contact they can also exchange genetic information. Although it is not well established how widely horizontal gene flow occurs in nature, there is strong evidence that most major metabolic pathways, i.e. photosynthesis and respiration, require genes which were exchanged between bacteria, archaea and eukaryotes ca 3

billion years ago, and that microorganisms attached to POM have a better chance to encounter other microorganisms and exchange genes (Stewart, 2013).

Bacteria living and feeding on particulate matter in the oceans produce exoenzymes to assimilate the breakdown products of POM as DOM (Fenchel, 2001; Robinson et al., 2010). The bacterial community composition varies depending on the source and the composition of the DOM (Kirchman et al., 2004). Moreover, the quality and availability of DOM affect the diversity of bacteria and their function (Eiler et al., 2003). In a recent study, Landa et al. (2013) showed that increased concentrations of DOM could support a higher diversity in bacterial communities. For their study, a natural bacterial community was grown in a continuous culture for several generations with natural seawater amended with diatom-derived DOM. Both in the control and DOM amended cultures, Gammaproteobacteria dominated the bacterial communities (between 87 and 99% of the 16S rRNA sequences). Alphaproteobacteria, Bacteroidetes, and Verrucomicrobia, were found in higher relative abundance in the cultures with the additional diatom derived DOM (ca 14% of gene sequences) in comparison to the control (< 5% of the sequences) (Landa et al., 2013).

Although it is difficult to measure the carbon flux from primary producers to the heterotrophic organisms in the microbial loop, the utilization of DOM by bacteria varies, depending on changes in the physiological state of the cell, community structure and environmental conditions (Pinhassi et al., 1999). DOM is composed of many different compounds such as amino acids, sugars and humics (Hansell & Carlson, 2001). One important component of DOM is dissolved organic carbon (DOC). The concentration of DOC is very low (ca 34 to >70 µmol C kg^{-1}) and the turnover time varies from hours to days for labile DOC and weeks to months for semi-

labile DOC to be consumed (Hansell et al., 2012). The composition of the bacterial community affects the turnover time depending on the environmental conditions. Large opportunistic bacteria alone may disproportionately utilize carbon and affect the ecosystem functioning (Pedler et al., 2014). In a series of experiments, they revealed that *Alteromonas* sp. strain Scripps Institution of Oceanography (AltSIO, ≥ 40 fg C $cell^{-1}$) can outgrow the native free-living bacteria and consume the entire pool of labile DOC, retaining its large size and never decreasing below 1% of the total bacterial abundance.

Although the community dynamics of heterotrophic bacteria in the ecosystem is not clearly understood, their metabolic processes during recycling of organic and inorganic matter are vital to the functioning of the biological carbon pump (Karl, 2007; Herndl et al., 2008).

The biological carbon pump is the process of photosynthetic fixation of atmospheric CO_2 and transport of the resultant organic carbon from the surface to the interior ocean. POM is transported by passive gravitational sinking and active transport via zooplankton migrational activity and/or mixing of water whereas, DOM is transported to deeper parts of the oceans by physical processes, such as subduction. The production and respiration of heterotrophic bacteria play an important role in sequestering the carbon in the oceans (Azam & Malfatti, 2007). Phytoplankton excretion, zooplankton excretion, egestion and sloppy feeding, heterotrophic bacterial utilization of POM and cell lysis due to virus infection produce DOM that is only accessible by heterotrophic bacteria (Azam & Malfatti, 2007; Yokokawa & Nagata, 2010). Different bacteria utilize organic matter from various sources (Landa et al., 2013). Hence the community structure of the bacterial community plays a crucial role

in the utilization of organic matter and its viability. Changes in the heterotrophic bacterial community structure and their activity can alter the pathways and the efficiency of the carbon pump (Azam & Malfatti, 2007), therefore it is important to monitor bacterial community structure and their activity.

1.2 BACTERIAL RESPIRATION IN THE MARINE ENVIRONMENT

Respiration is the transfer of electrons from reduced organic substrates to an electron acceptor to release energy for metabolic purposes. In aerobic respiration, the oxygen molecule is used as the terminal electron acceptor, while in anaerobic respiration; various inorganic compounds, such as iron, manganese and sulphur, are used as electron acceptors.

Measuring aerobic respiration in the marine environment is important to understand and explain the carbon cycle in the global ocean (Robinson & Williams, 2005; Robinson, 2008). Respiration measurements are arguably a better indicator of an ecosystem's productivity than primary production (Williams & Del Giorgio, 2005). Together with bacterial production (BP), respiration measurements are used to calculate the bacterial carbon demand (BCD, is the total amount of carbon needed for both bacterial respiration (BR) and BP: BCD = BP + BR) and bacterial growth efficiency (BGE, is the ratio of the BCD to BP: BGE = BP/BCD), which are required to determine the carbon flow through bacteria (Robinson, 2008). To be able to ascertain the bacterial contribution to the carbon flux, it is necessary to measure total community respiration (CR) and bacterial respiration (BR) separately. CR is the

respiration rate of all bacteria, phytoplankton and microzooplankton combined, in a non-prefiltered water sample (Robinson, 2008). To measure BR, the water sample needs to be filtered to remove all organisms larger than a certain size, eg. > 0.8 µm. However, fractionation may not isolate only heterotrophic bacteria. Some autotrophic bacteria and small phytoplankton may pass into the filtered water sample. In addition, some large or particle-attached bacteria may be excluded from filtered samples due to the small pore size or clogged pores of the filters used. Moreover, isolation of the bacteria from the rest of the community prior to measurement may cause either under- or over- estimation of respiration rates due to the exclusion of primary producers and predation pressure on bacteria (Robinson, 2008). To minimise these problems, various filtration units and pore-sized filters have been used in studies for size fractionation of water samples, varying from 0.6 to 1.2 µm. Heterotrophic bacterial respiration is one of the most important variables in marine carbon budget calculations; constituting 50 to 90% of community respiration (Rivkin & Legendre, 2001; Morán et al., 2010; Martínez-García et al., 2013).

1.2.1 Factors Affecting Bacterial Respiration

Ambient temperature is a main contributor to changes in BR because it directly affects the metabolic rate of bacteria. Changes in the temperature affect also the solubility properties of different gases, organic and inorganic material in sea water. In a review where 286 data points from different studies were analysed, Robinson (2008) showed that ca. 30% of the variability in bacterial respiration can be explained by the changes in *in situ* temperature. Bacterial respiration tends to be higher at lower latitudes than

at higher latitudes potentially due to the sea surface temperature (SST) (Rivkin & Legendre, 2001). Carlson et al. (2007) found that the relationship between temperature and respiration rates is weak in cold waters, i.e. < 10°C. Morán et al., (2010), suggested an indirect role for temperature in the changes in bacterial growth. Based on their study in the Bay of Biscay, they found that variations in bacterial activity are affected by the substrates supplied by phytoplankton only in cool waters (< 16°C). They concluded that in cool waters either the primary production is too low or the quality of DOM produced is low in nutrient content, failing to provide enough substrates for bacteria.

Nutrient limitation directly affects bacterial activity and hence bacterial respiration rates. However, different studies suggest various effects of inorganic nutrients, in different parts of the oceans. One study in the NW Mediterranean Sea found that bacterial respiration was not related to nitrate (NO_3) or phosphate (PO_4) concentrations in water (Lemée et al., 2002). Another study in the Sargasso Sea found bacterial respiration to be PO_4 limited (Obernosterer et al., 2003). Carlson et al. (2007) suggested that bacteria use multiple sources of organic and inorganic nutrients. Sebastian and Gasol (2013) found that different groups of bacteria respond differently to nutrient limitation; *Gammaproteobacteria* was the most susceptible to phosphorous (P) limitation, *Roseobacter* was limited by both PO_4 and nitrogen (N), *Bacteroidetes* by P, N and organic carbon, and SAR11 activity seemed unaffected by nutrient concentrations.

Bacterial metabolism depends on several factors both biotic and abiotic. They have a flexible physiology and a complex set of interactions with the environment they live in. Hence cell-specific bacterial respiration rates are not constant. Although bacterial abundance in a 0.8 µm filtrate could be 60 to 90% of that in the unfiltered sample,

their abundance explains only ca 27% of the variability in respiration rates (Figure 1.5, Robinson, 2008).

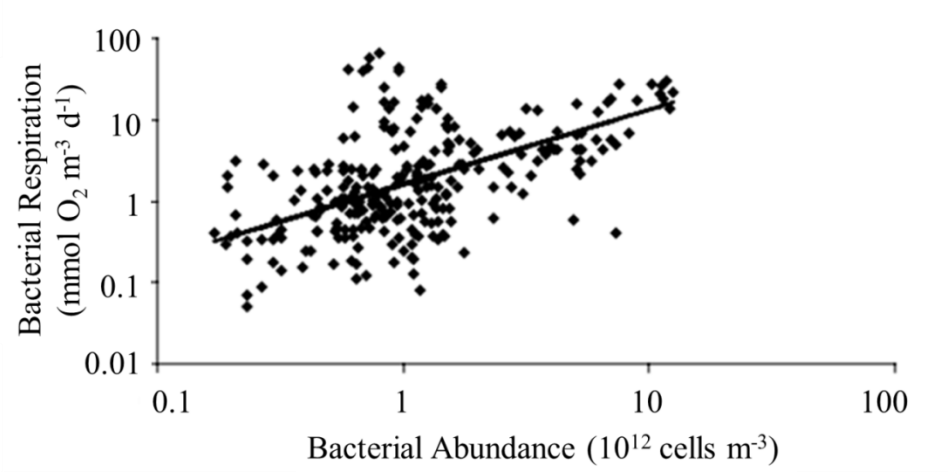

Figure 1.5. Relationship between bacterial respiration (BR) and abundance (BA). ($BR=1.62BA^{0.81}$, n=260, p<0.001, r^2=0.27, Robinson, 2008).

The composition of the bacterial community can affect ecosystem functioning and influence the rates of microbial processes. Evidence suggests that bacterial respiration and the richness of the active bacterial community are negatively correlated (Reinthaler et al., 2005; Obernosterer et al., 2010).

1.3 BACTERIAL COMMUNITY STRUCTURE

Until a few decades ago, research on bacteria was dependent upon pure cultures with relatively few isolated species. Although pure cultures provided detailed information on the physiology of the species in question, these types of experiments are unable to differentiate the ecological role of the microorganisms and their interactions within the community (Stahl et al., 2013). It wasn't until after the discovery of the epifluorescent microscope that scientists realized that pure strains in culture

collections represented less than 1% of marine microorganisms (Hobbie et al., 1977; Karl, 2007). Following the discoveries of dominant groups of cyanobacteria such as *Synechococcus* spp. (by epifluorescent microscopy, Waterbury et al., 1979) and *Prochlorococcus* spp., (by flow cytometry, Chisholm et al., 1992), the number of cultivation independent studies increased. These studies led to the development of ribosomal RNA (rRNA) sequencing (Olsen et al., 1986) and fluorescence *in situ* hybridization (FISH) (Amann et al., 1990) as well as new applications of the polymerase chain reaction (PCR) in microbial oceanography (Giovannoni et al., 1990; DeLong, 1992). Fingerprinting techniques such as denaturing gel gradient electrophoresis (DGGE) and terminal-restriction fragment length polymorphism (TRFLP) have been used to investigate microbial diversity. Although they have certain disadvantages (i.e. allowing only a limited number of samples to be analysed at one time), they were ground breaking techniques at the time for investigating community composition.

As sequencing became less expensive, it became possible to analyse collective genomes in a given environmental sample. Metagenomics is the analysis of the genetic material obtained from a community where the total DNA is extracted from the sample, sequenced and analysed altogether (Fuhrman, 2012). Next generation sequencing is widely used for metagenomics in microbial oceanography. The technique targets the specific genes, i.e. small subunit ribosomal RNA (ssu rRNA), to identify the presence of organisms within the sample (Thomas et al., 2012). For prokaryotes, 16S rRNA genes are used for sequencing due to both their conservative and highly variable structure.

The secondary structure of 16S rRNA and the hypervariable regions on it are shown in Figure 1.6. Modern phylogenetic systematics of bacteria and archaea are based on the comparative analysis of the conservative genes within these regions.

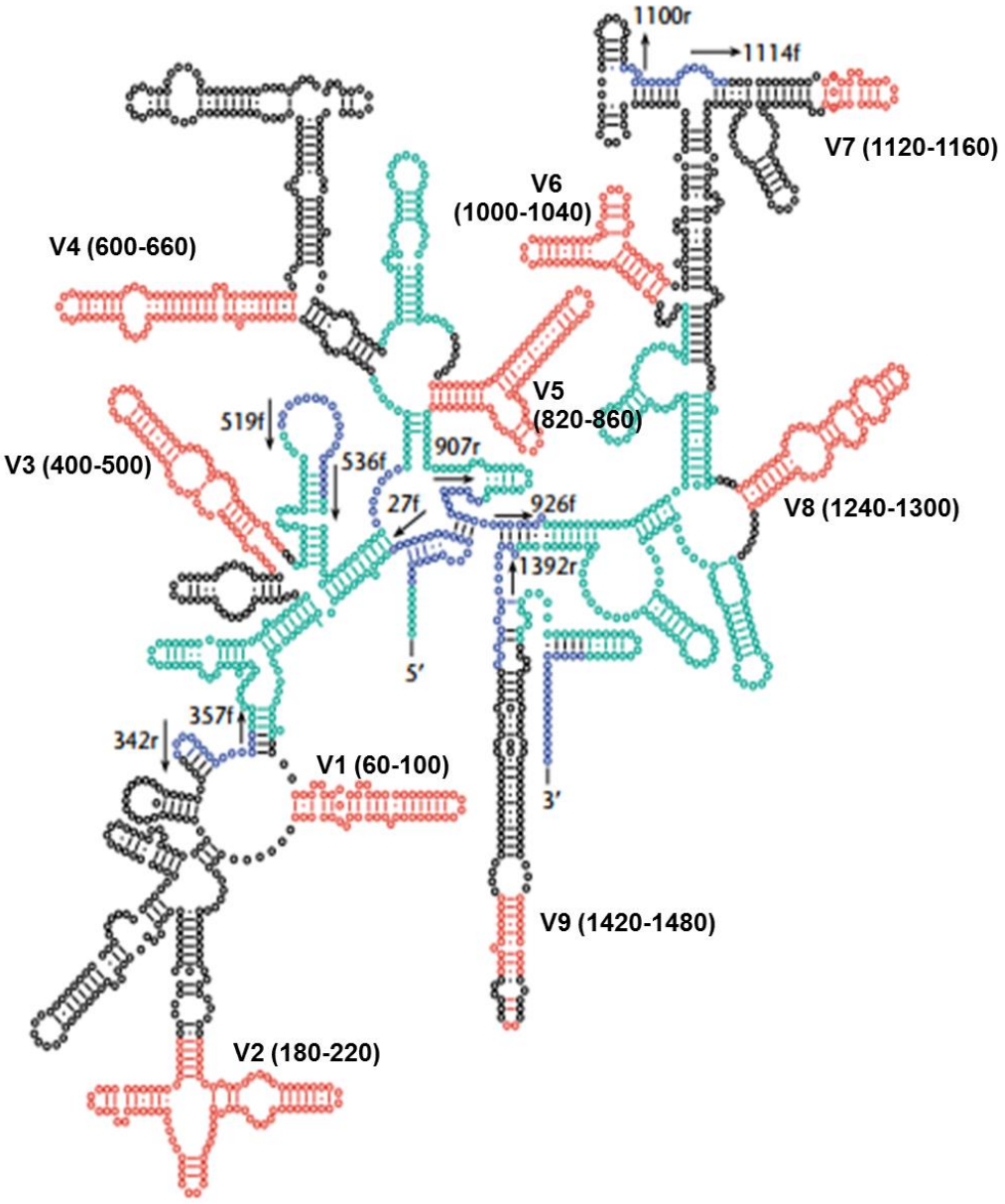

Figure 1.6. Secondary structure of a 16S rRNA based on *E. coli*. Highly variable regions are drawn red and labelled with their names. Highly conservative regions are shown in green and the binding sites of primers used in PCR amplification of the rRNA gene are shown in blue. Arrows indicate the directions of amplification. The rest of the nucleotides are drawn black. (Adapted from Stackebrandt et al., (2001); available in the public domain Ribosomal Database Project).

Metagenomics is a powerful tool to analyse the diversity of bacteria, without the need to culture. In the last decade, whole genome shotgun sequencing and next generation sequencing revealed millions of new genes and previously unknown metabolic pathways in the marine microbial loop (Karl, 2007; Gilbert & Dupont, 2011).

Venter et al. (2004) used shotgun sequencing, for the first time, in metagenomic investigations of marine microbes from the Bermuda Atlantic Time-series (BATS), in the Sargasso Sea. They revealed ca 1.2 million previously unknown genes from 148 novel phylotypes, just from the surface waters. After the unexpected scale of the discovery, they extended the study to different regions around the world. The global ocean sampling (GOS) expeditions, the first between 2003 and 2006 and the second from 2008 to 2010, (Rusch et al., 2007; Yooseph et al., 2010).

In a similar ocean circumnavigation expedition, scientists not only sampled the water for genes, they also collected samples for environmental parameters, such as temperature, salinity and nutrients, in an attempt to explain the observed patterns in the genetic and functional diversity (Karsenti et al., 2011). In this holistic approach, researchers further investigate biogeochemical cycles in relation to the changing interactions within the community, from viruses to bacteria to planktonic metazoans.

Metagenomics data have been used to reassemble genomes and model complete metabolic pathways of uncultured bacteria (Tyson et al., 2004). Sogin et al. (2006) used parallel tag sequencing in deep sea samples, discovering an extensive and a very diverse marine microbial community. Most of the identified organisms were present in low abundance, called the rare biosphere, with an extensive genetic diversity. Although the abundance of bacterial cells is a vital parameter to measure, the number

of the bacterial cells in the environment is not enough to ascertain the metabolic state of the bacterial community. There is growing evidence from the analysis of the sequences from 16S rDNA and rRNA (cDNA) libraries that the rare bacteria can show high metabolic activity in open oceans (Campbell et al., 2011; Pedrós-Alió, 2012; Hunt et al., 2013).

Metagenomic data collected during time series studies such as the Hawaii Ocean Time-series (HOT), Bermuda Atlantic Time-series Study (BATS) and Western English Channel Observatory (WECO) reveal the community dynamics over changing environmental conditions and the seasonality in bacterial communities. These studies suggest that environmental conditions, such as temperature, nutrient availability and day light are the main factors defining the seasonality in bacterial diversity (Treusch et al., 2009; Gilbert et al., 2009, 2012; Giovannoni & Vergin, 2012).

1.3.1 Factors Affecting Bacterial Diversity

Many studies from different parts of the oceans showed that temperature is one of the main drivers shaping bacterial community structure in surface waters (Fuhrman et al., 2006; Treusch et al., 2009; Gilbert et al., 2009, 2012; Hunt et al., 2013; Swan et al., 2013). Fuhrman et al., (2008) collected 103 samples from 57 near-surface, open ocean and coastal locations around the world, from all seasons over several years. They concluded that the richness of bacterial communities is primarily driven by temperature but not correlated with chlorophyll or primary production measurements.

Gilbert et al. (2009) showed that bacterial diversity was correlated to a combination of temperature and inorganic nutrient availability, such as phosphate and silicate, over an 11-month sampling period at station L4, WECO. In another study at the same station, the most abundant taxa could be predicted from nutrient concentrations, such as phosphate, ammonia and total organic nitrogen (Gilbert et al., 2012). Other studies, under varying culture and *in situ* conditions, showed that changes in DOM composition can significantly alter the community composition of bacterial diversity (Hansell & Carlson, 2001; Gómez-Consarnau et al., 2012).

In a recent study at station L4, analysis of samples extending over a 6 year period showed that the annual change in day length was the most significant factor to affect bacterial diversity, explaining ca 65% of the variation (Gilbert et al., 2012). Their results also suggested that there is a resilient seasonal pattern among the bacterial community.

1.4 OBJECTIVES OF THE STUDY

The central goal of the present study is to further the understanding of the factors affecting the temporal dynamics and spatial distribution of heterotrophic bacteria and the underlying processes causing differences in community structure, composition and their respiration.

For that reason, we design two sets of sampling; the annual time series and the Lagrangian study. Data collected during the study were analysed to find out which bacterial groups were present in surface waters, what the dynamics within the microbial community were and how they were affected by the changing environment..

2. METHODOLOGY

This chapter describes the sampling strategies and data analyses used throughout the thesis. Two sampling strategies, a time series study and Lagrangian sampling, were designed to sample the surface waters of two different regions with different characteristics. The time series study was carried out at station L4 of the WECO, in the English Channel, and Lagrangian sampling took place at an upwelling plume off the Mauritanian coast. The environmental and biological variables which were determined are summarized in Table 2.1.

Table 2.1. The environmental data shown in this chapter, sampled during the time series and the Lagrangian sampling

	L4: Time Series		**ICON: Lagrangian Study**	
Data Collected	**Analysed by**	**Instrument**	**Analysed by**	**Instrument**
Temperature & Salinity	James Fishwick, Tim Smyth	SeaBird SBE19 CTD	BODC	SeaBird SBE 911plus/917plus CTD
Inorganic Nutrients	Malcolm Woodward	Technicon AAI Flow Autoanalyser	Malcolm Woodward	Technicon AAI Flow Autoanalyser
Chlorophyll *a*	Dennise Cummings	Trilogy Turner Fluorometer	Claire Widdicombe	Trilogy Turner Fluorometer
Cell Abundance	Cansu Bayindirli, Glen Tarran	BD FAC Sort Flowcytometer	Glen Tarran	BD FAC Sort Flowcytometer
Bacterial Production	N/A	N/A	Polly Hill	Tri-Carb Liquid Scintillation Counter
Dissolved Oxygen and Respiration rates	Cansu Bayindirli	Automated Winkler Titration System	Pablo Serret, Vassilis Kitidis	Automated Winkler Titration System
Gene sequences	Cansu Bayindirli, Sarah Owens	Illumina HiSeq2000	Cansu Bayindirli, Sarah Owens, Simon Thomas	Illumina HiSeq2000
Bioinformatics	Argonne National Laboratories, Il, USA			

2. 1. STUDY SITES

2. 1. 1. TIME SERIES STUDY AT STATION L4

The present study was undertaken at station L4 of The Western Channel Observatory (WECO), as a part of the time series research. WECO is one of the longest time series in the world, conducted by Plymouth Marine Laboratory (PML) and the Marine Biological Association (MBA). Station L4 has been sampled continuously by scientists at PML, since its addition to the observatory in 1987. It is a coastal station, located 10 km southwest of Plymouth (50°15.00'N, 4°13.02'W), with a water depth of about 55 m (Figure 2.1).

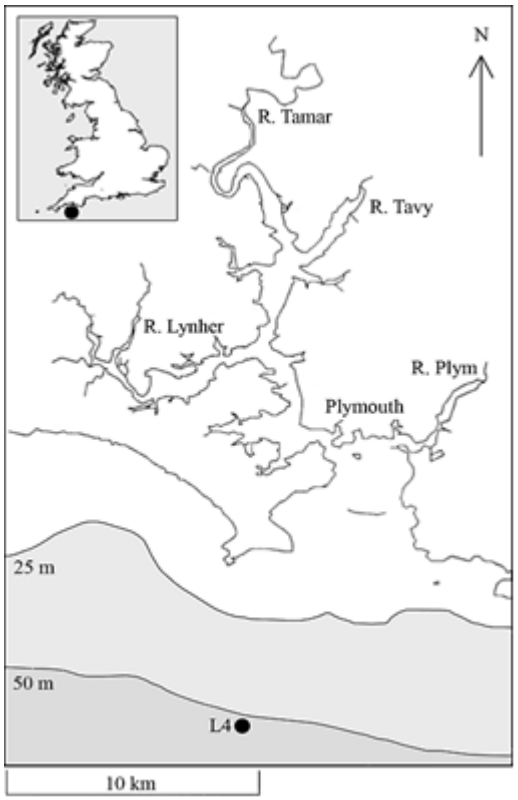

Figure 2.1. Location of the station L4 of Western Channel Observatory.

Station L4 is under the influence of both tides and the fresh water input from nearby rivers, the Tamar and the Plym, at varying magnitudes, throughout the year (Pingree & Griffiths, 1978; Rees et al., 2009; Smyth et al., 2009). Intense rainfall, strong winds and the tides increase the river input (Rees et al., 2009). Also tidal mixing plays a vital role in nutrient and light availability for photosynthesis and growth (Pingree & Griffiths, 1978).

Surface water samples were collected weekly from the time-series station, weather permitting, on Mondays at ca 10 am (local time). The sampling was carried out using the rosette bottle sampler onboard R/V *Quest* or R/V *Sepia*, over an annual cycle from 6th April 2009 to 26th April 2010. All samples were analysed at Plymouth Marine Laboratory (PML). The average time between sample collection and return to PML was about 2 hours.

2. 1. 2. Lagrangian Sampling at an Upwelling Plume off the Mauritanian Coast

As part of the NERC-funded "Impact of Coastal Upwellings on Air-Sea Exchange of Climatically Important Gases" (ICON) cruise, 20-200 km off the Mauritanian coast, in April and May 2009, water samples were collected on board RRS *Discovery*, to identify the bacterial community structure by next generation sequencing. The aim of the cruise was to understand the impact of upwelling on physical and microbial processes and their contribution to ocean-atmosphere gas exchange.

Satellite derived sea surface temperature (from AVHRR) and chlorophyll *a* (from MODIS-Aqua) data, together with the data collected with the instruments on-board, were used to identify the upwelling filaments. The inert tracer sulphur hexafluoride (SF_6) was deployed in a 2 km^2 surface patch together with five Argos buoys to 'label' the filament, one in the centre of the deployment and 4 on the corners. Using a combination of buoys, real time monitoring of SF_6 concentrations and remote sensing data (by NEODAAS), and measuring the currents with acoustic doppler current profilers (ADCP), the upwelled plume was tracked continuously on its way from the upwelling centre adjacent to the coast to a location ca 140 km off shore. Surface water concentrations of SF_6 were determined daily, whilst the ship carried out surveys around the buoys. The ship was relocated on a daily basis to the position of the highest concentration of SF_6 for collection of vertically resolved data during the day.

The data analysed for the present study were collected from the 55% light intensity depth (ca 8 m) of the 2nd filament between 15th and 22nd May 2009, at ca 04:00 GMT each day. Figure 2.2 shows the positions of the 8 'pre-dawn' stations on an AVHRR sea surface temperature image, on 20 May 2009. Table 2.2 shows the latitude and longitude of the stations, the sampling dates and the distance travelled between each station. Note that the distance travelled between each station varied from 14.3 to 25.4 km.

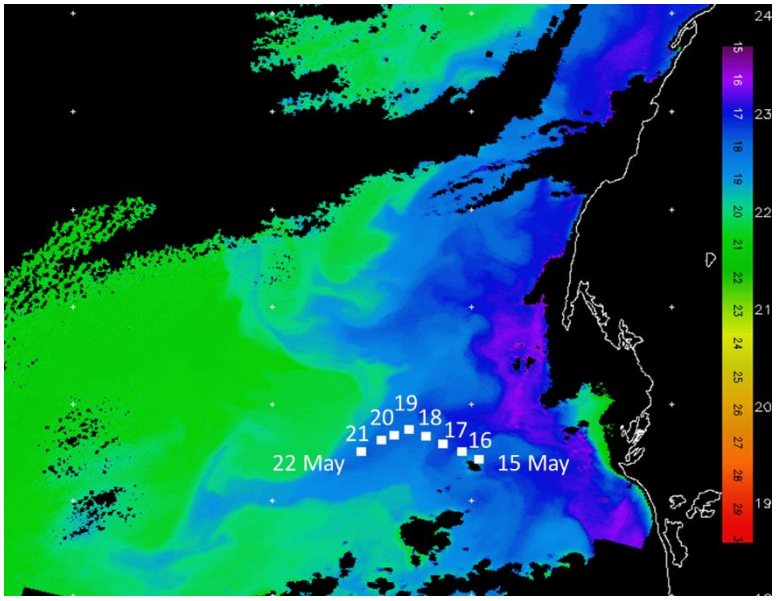

Figure 2.2. The study site and station locations, with dates of sampling marked on the map, overlaid on the sea surface temperature data taken on 20th May 2009. (Image courtesy of NEODAAS).

Table 2.2. The sampling dates, station coordinates and the distance between each station.

Date	Latitude	Longitude	Distance travelled (km)
15-May	19.4286	17.9313	
16-May	19.5147	18.1059	20.6424
17-May	19.592	18.2959	21.6698
18-May	19.6754	18.4662	20.0884
19-May	19.7401	18.6279	18.3796
20-May	19.6872	18.782	17.1579
21-May	19.6348	18.9069	14.3078
22-May	19.5163	19.1143	25.3942
Total distance (km):			137.64

2. 2. HYDROGRAPHIC MEASUREMENTS

Station L4 has hydrographic data dating from 1987. In this study, the data collected between 2000 and 2009 were used to describe the historic trends observed at the station prior to the present sampling period, which was between 6th April 2009 and 26th April 2010.

Changes in temperature and salinity at the station were measured using a Sea-Bird Electronics CTD probe. Prior to the SeaBird CTD probe which has been in use since 2002, Undulating Oceanographic Recorder (UOR) used for collecting samples for chlorophyll, particulate C and N, phytoplankton and zooplankton analysis, and a mercury-in-glass thermometer were used for temperature measurements at L4 (Southward et al., 2004). The salinity and the fluorometer data have been collected since the introduction of a modern CTD probe in 2002. Smyth et al. (2009) did a qualitative error analysis and found that the error margin for the mercury-in-glass thermometer is ± 0.18 °C. The SeaBird SBE 19+ CTD probe measurements are accurate to ± 0.0018 °C for temperature and ± 0.01 for salinity.

Water samples were collected with a stainless steel rosette of 24 x 20 dm^3 OTE sampling bottles fitted with a Seabird 911+ CTD and a Chelsea Instruments Aquatracker 3 fluorometer.

2. 3. INORGANIC NUTRIENTS

The temporal changes in key inorganic nutrient concentrations, both at station L4 and off the Mauritanian coast, were measured using a five-channel Technicon AAII segmented flow autoanalyser. Water samples were collected directly from the Niskin bottle into clean sample bottles. The concentrations of nitrate, nitrite, ammonium, silicate and phosphate were determined. The detection limit for the analysis is 2 nmol dm^{-3}.

The nitrite concentration has to be subtracted from the concentration of total nitrate and nitrite ions, in order to obtain the nitrate concentration. The concentration of the total of nitrate and nitrite ions was determined according to Brewer & Riley, (1965): The nitrate concentrations were determined following a modified protocol described in Grasshoff, Kremling, & Ehrhardt (1976). The reaction is based on the reduction of nitrate to nitrite, using a copper/cadmium column, in an ammonium chloride solution (pH = 8.5), which was then measured by a chemi-luminescence analysis. The method was modified by decreasing the concentration of ammonium chloride solution.

A nanomolar analysis system, using gas permeation and fluorescence detection, was used for the detection of ammonium concentrations as described in Mantoura & Woodward, (1983). The analysis runs at an optimum pH of 10.6 at 55°C and is based on the production of the indophenol-blue complex.

Silicate was determined according to Kirkwood, (1989), This method relies on the reaction of silicate with ammonium molybdate which is reduced by ascorbic acid to form a silico-molybdenum blue complex. Oxalic acid is added to prevent any competitive reaction from phosphates.

Phosphate was determined as described in Zhang & Chi, (2002) and is based on the production of the phospho-molybdenum-blue complex by reaction with molybdate and ascorbic acid. The pH was kept below 1 to avoid a competitive reaction with silicate.

2. 4. CHLOROPHYLL *α* AND PRIMARY PRODUCTION

Chlorophyll *α* concentrations were determined according to the JGOFS protocol, (1994), during both the time series and the Lagrangian sampling. At station L4, samples were collected from the Niskin bottles into 500 ml acid washed glass bottles. They were then immediately prefiltered through 10 µm and 5 µm Nucleopore membrane filters, by using peristaltic pumps, followed by a filtration onto Whatman GF/F glass fibre filters, whilst on board R/V Quest (vacuum pressure <1 bar). During the Lagrangian sampling, chlorophyll α samples were collected pre-dawn from 6 depths corresponding to between 97% and 1% surface irradiance using 20 L Niskin bottles, into 250 ml bottles. They were immediately sequentially filtered through 2 µm and 0.2 µm polycarbonate filters (vacuum pressure 0.25 bar). The filters were frozen until fluorometric analysis with a Turner 1000R fluorometer after extraction in 90% acetone overnight. Once thawed, the filters were placed in polypropylene centrifuge tubes, submerged in 86% acetone and kept in the dark at -20 °C for extraction of chlorophyll *α*, e.g. if using 15 ml centrifuge tube, add ca 10 ml acetone to cover the filter. The samples were then centrifuged at ca 2400 rpm for 20 minutes to separate the pigments from the rest of the biological material. The extract was placed in cuvettes mixed with 90% acetone, enough to fill the cuvette, to get fluorometer

readings. The chlorophyll *α* concentration was calculated as described by Environmental Protection Agency (EPA) (Arar & Collins, 1997).

During the Lagrangian sampling, phytoplankton primary production was measured using the ^{14}C method as described in Tilstone et al. (2009). Samples were collected from the same 6 depths as chlorophyll α samples were collected. Triplicate 75 ml subsamples were spiked with between 185 and 740 kBq (5–20 mCi) $NaH^{14}CO_3$ and incubated on-deck for 24 hours. Incubations were terminated by sequential filtration through 2 µm and 0.2 µm polycarbonate filters (vacuum pressure 0.25 bar) and ^{14}C disintegration was measured onboard using TriCarb liquid scintillation counter.

2. 5. ABUNDANCE BY FLOW CYTOMETRY

Phytoplankton, bacteria and nanoflagellate cell abundance was determined using analytical flow cytometry in both the time series and Lagrangian sampling. Seawater samples were collected from the Niskin bottles into 0.25 L square polycarbonate bottles.

During the time series study, the bottles were kept in a cool-box and transported back to the laboratory for analysis. The phytoplankton and *Synechococcus* samples were analysed on the day of sampling, as soon as possible after the samples were returned to the laboratory. The samples for heterotrophic bacteria and heterotrophic nanoflagellate counts were preserved in 50% glutaraldehyde solution at -20 °C, and analysed within 10 days.

Samples collected during the Lagrangian sampling for phytoplankton cell counts were stored at 4˚C in the dark and analysed on board within 2 hours. Bacterial samples were fixed with paraformaldehyde (1% final concentration), left at 4˚C in the dark for 24-hour, and frozen at -80˚C until post-cruise analysis.

All analyses were carried out using a Becton Dickinson FACSort^{TM} flow cytometer equipped with an air-cooled laser providing blue light at 488 nm. Besides counting the cells, the flow cytometer also measured chlorophyll fluorescence (>650 nm), phycoerythrin fluorescence (585 nm ±21 nm), green fluorescence (530 ±15) nm and side scatter (light scattered at ninety degrees to the laser beam). Data acquisition was triggered on chlorophyll fluorescence. The flow rate of the flow cytometer was calibrated before each analysis using Beckman Coulter Flowset fluorospheres of known concentration. Measurements of light scatter and fluorescence were made using CellQuest software (Becton Dickinson, Oxford) with log amplification on a four-decade scale with 1024 channel resolution. Bivariate scatter plots of phycoerythrin against chlorophyll fluorescence were used to discriminate *Synechococcus* sp. from the other phytoplankton, based on their phycoerythrin fluorescence. Picophytoplankton were discriminated based on a combination of side scatter and chlorophyll fluorescence. Samples for heterotrophic bacteria and nanoflagellates were stained with Sybr® Green-I DNA stain (1 % of commercial concentration) and potassium citrate (300 mM) in the ratio of 100:1:9 (water sample:Sybr® Green-I:potassium citrate) for 1 hour at room temperature, in the dark. Bacterial samples were analysed on the flow cytometer for 1 minute at a flow rate of approximately 40 µl min^{-1} whereas the heterotrophic nanoflagellates were analysed

for 7 - 10 min at a flow rate of 150µl min^{-1}. They were enumerated using a combination of side scatter and green fluorescence from the Sybr® Green-I.

2. 6. RADIOACTIVELY LABELLED AMINO ACID DILUTION BIOASSAYS

Bacterial activity during the Lagrangian study was determined by measuring the leucine, methionine and tyrosine uptake rates on untreated samples. The turnover rates of amino acids, together with the ambient concentrations, were estimated using a radiotracer bioassay technique (Wright & Hobbie, 1966).

The following protocol, as described in Mary et al., (2008) and Zubkov et al., (2008) was used for the bioassays. L-[4,5-^{3}H]leucine (specific activity 4-6 TBq $mmol^{-1}$) was added in a series of 0.2 - 2.0 nM concentrations. The L-[3,5-^{3}H]tyrosine (specific activity 2 TBq $mmol^{-1}$) was added in the range 0.1 - 2.0 nM. The L-[^{35}S]methionine (specific activity >37 TBq $mmol^{-1}$) was added at a standard concentration of 0.05 nM and diluted with unlabelled methionine in the range 0.1 - 2.0 nM. Triplicate samples (1.6 mL) for each amino acid and at each concentration were incubated in 2 mL polypropylene screw cap vials at in situ temperature. One sample from each concentration was fixed at 10, 20 and 30 min by the addition of 20% paraformalydehyde (1% v/w final concentration). Due to the short incubation times, it was not possible to work in the dark; however, incubations were kept in dim indirect light. Fixed cells were filtered onto 0.2 µm polycarbonate membrane filters soaked in the corresponding non-labelled amino acid solution to reduce adsorption of tracer.

Filtered samples were washed twice with 4 mL deionised water. Radioactivity of samples was measured as disintegrations per minute (DPM) by liquid scintillation counting (Tri-Carb 3100TR or 2900TR, Perkin Elmer).

Amino acid uptake rates were calculated at each addition concentration as the gradient of the linear regression of community assimilated radioactivity against incubation time. The time it would have taken the community to assimilate all the added amino acid was then plotted against added concentration; ambient uptake rate was determined from the slope of its linear regression. Ambient concentration was estimated as the intercept on the x-axis (at which turnover time is equal to zero). The ambient turnover time is thus derived as the uptake rate divided by ambient concentration; that is, the turnover time when addition concentration is equal to zero.

2. 7. DISSOLVED OXYGEN CONTENT OF THE WATER

Although modified for sea water samples (Carpenter, 1965; Carrit & Carpenter, 1966, Blight et al., 1995), the titration method originally developed by Winkler (1888) is still considered to be one of the most accurate ways of measuring dissolved oxygen in aqueous environments. The principle is simple, but needs very careful handling in order to avoid loss or introduction of dissolved oxygen.

In order to measure the dissolved oxygen content of the seawater at L4, duplicate sea surface water samples were carefully collected into gravimetrically calibrated borosilicate glass bottles (ca. 60 ml), directly from the Niskin bottles using acid washed silicon tubing, avoiding the formation of bubbles. The temperature of the

samples was measured with a Digitron T208 thermometer with a probe (precision 0.1°C). Samples were then fixed with 0.5 ml of 3 M manganous sulphate tetrahydrate ($MnSO_4.4H_2O$) and 0.5 ml of alkaline sodium iodide (4 M NaI + 8 M NaOH) solution, with Nichiryo 8100 repetitive pipettes. The sample bottles were kept under water until analysis (within 24 hours).

Winkler titration was used to determine the dissolved oxygen as described by Williams and Jenkinson (1982), with the modifications by Carpenter (1965), as described in section 2. 7. 1, on page 57 and 58. 0.5 ml of 10 N sulphuric acid (H_2SO_4, Fisher Scientific) solution is added to each sample prior to titration with sodium thiosulphate ($Na_2S_2O_3 \cdot 5H_2O$). The sodium thiosulphate solution (prepared to 0.1 N, Sigma Aldrich) was calibrated with 0.1 N potassium iodate (KIO_3, Sigma Aldrich) standard each analysis day.

2. 7. 1. Sampling and Automated Titration Apparatus

- **Bottles:** 60 ml borosilicate bottles with ground glass stoppers were used for the dissolved oxygen measurements. Each bottle-stopper pair was hand-made to order and calibrated in the lab for the determination of the precise volume. For the calibration, the volume of each bottle with its stopper is measured gravimetrically by weighing with Milli-Q water. The bottles were cleaned with Milli-Q water after each titration.
- **Thermometer:** The temperature of the samples was measured with a Digitron T208 digital thermometer with a probe (precision 0.1°C). Calibration of the instrument was done by the manufacturer.

- **Reagent dispensers:** Three repetitive pipettes (Nichiryo 8100) and their syringe tips were separately labelled for the use of 3 M manganous sulphate tetrahydrate ($MnSO_4.4H_2O$), alkaline sodium iodide (4 M NaI + 8 M NaOH) solution and 10 N sulphuric acid (H_2SO_4). The tips were cleaned with Milli-Q water after each use, bagged and kept separately. The accuracy of the 15 ml syringe tip is ±0.8% (4 µl for 500 ml dispense). The pipettes were routinely calibrated by the manufacturer.
- **Silicone tubing:** White silicone tubing that is narrow enough to fit onto the Niskin bottle petcock, cut to a length just enough to reach to the bottom of either the borosilicate bottle or the aspirator, was used for drawing the water sample from the Niskin bottle. The silicone tubing was acid washed and rinsed with Milli-Q before and after each sampling.
- **Automated Winkler titration:** The system comprises a Dosimat (765 Dosimat, Metrohm) with a 1 ml piston burette (2 µl precision dispenser), a custom-made photometric end-point detector with magnetic stirrer, a computer with custom-made software for the analysis and a printer (Blight et al., 1995; Robinson et al., 1999).

2. 7. 2. PREPARATION OF THE REAGENTS

The reagents used to carry out the Winkler titration were prepared as 1L stock solutions routinely over the sampling period. The concentrations of the reagents were optimised to achieve good precision in dissolved oxygen measurements.

- **Manganous Sulphate Tetrahydrate (3 M,** $MnSO_4 \cdot 4H_2O$, Sigma Aldrich): 453 g Manganese sulphate was dissolved in Milli-Q water to a final volume of 1 litre. The stock solution was kept in a brown safe-break glass bottle; aliquots (in 250 ml low-density polyethylene (LDPE) bottles) were used for the sampling and analysis.
- **Sodium Iodide (4 M,** NaI, Sigma Aldrich) **and Sodium Hydroxide (8M,** NaOH, Sigma Aldrich): 320 g of NaOH was dissolved in 500 ml of Milli-Q water, with constant mixing, in a volumetric flask placed in a cool water bath. 600 g of NaI was slowly added with constant mixing followed by the addition of Milli-Q water to a volume of 1 L. The stock solution was kept in a brown, safe-break glass bottle; aliquots (in 250 ml low density polyethylene (LDPE) bottles) were used for the sampling and analysis.
- **Sulphuric Acid (10 N,** H_2SO_4, Fisher Scientific): 280 ml concentrated H_2SO_4 was mixed into ca. 500 ml of distilled water, with constant mixing. The solution was then transferred into a volumetric flask and Milli-Q water was added to a final volume of 1 L. The preparation of the solution was carried out in a cool water bath in a fume hood, owing to its exothermic nature.
- **Sodium Thiosulphate (ca. 0.11 M,** $Na_2S_2O_3 \cdot 5H_2O$, Sigma Aldrich): Sodium thiosulphate (ca. 17 g) was dissolved in 1 L Milli-Q water in a volumetric flask. The solution was kept in an amber glass bottle, at room temperature, until use.
- **Potassium Iodate (0.1 N,** KIO_3, Sigma Aldrich): KIO_3 was dried at 180°C overnight, and then 0.3567 g of the dried KIO_3 was dissolved in 1 L Milli-Q water in a volumetric flask. It was stored in an amber glass bottle, at room temperature, until use.

2. 7. 3. CALIBRATION OF SODIUM THIOSULPHATE AND CALCULATION OF THE DISSOLVED OXYGEN

Sodium thiosulphate solution has an unstable concentration at room temperature and therefore needs standardization by calibrating with a standard solution. Standardization is based on the co-proportionation reaction of iodide with iodate. In this study, potassium iodate (KIO_3) was used as the standard solution, which reacts with the excess iodide (I^-), forming three moles of triiodide (I_3^-) per iodate in the reaction. Since one mole of iodine reacts with two moles of thiosulphate, the precise concentration of the sodium thiosulphate can be calculated by titrating potassium iodate addition of sulphuric acid (H_2SO_4), sodium iodide (NaOH-NaI), and manganous hydroxide ($Mn(OH)_2$) (Carpenter, 1965). The stoichiometric equations for the standardization of thiosulphate are as follows:

$$IO_3^- + 8I^- + 6H^+ \longrightarrow 3I_3^- + 3H_2O \qquad (1)$$

$$I_3^- + 2S_2O_3^{--} \longrightarrow 3I^- + S_4O_6^{--} \qquad \text{reduction of } I_3\text{- to } I^- \qquad (2)$$

In order to be able measure the dissolved oxygen content of the water, the dissolved oxygen is fixed by the addition of $Mn(OH)_2$ and NaOH-NaI respectively. $Mn(OH)_2$ reacts with the dissolved oxygen forming a brown precipitate of a hydrated tetravalent oxide of manganese ($MnO(OH)_2$).

$$Mn^{++} + 2OH^- \longrightarrow Mn(OH)_2 \qquad (3)$$

$2Mn(OH)_2 + O_2 \longrightarrow 2MnO(OH)_2$ oxidation of Mn(II) to Mn(III) *(4)*

To dissolve the precipitate, 10 N sulphuric acid (H_2SO_4) is added, prior to the titration, causing the released Mn(III) ions to oxidize iodide ions (I^-) to iodine.

$MnO(OH)_2 + 4H^+ + 2\ I^- \longrightarrow Mn^{++} + I_2 + 3H_2O$ oxidation of I^- to I_2 *(5)*

The iodine, equivalent to the amount of dissolved oxygen in the water, is reduced to iodide by titration with freshly calibrated thiosulphate

$I_2 + 2S_2O_3^{--} \longrightarrow 2I^- + S_4O_6^{--}$ reduction of I_2 to I^- *(6)*

The endpoint is determined by the photometric endpoint detector and the titration is ended automatically by the computer. The amount of oxygen was then calculated from the amount of thiosulphate titrated, 4 mole of thiosulphate is used to titrate each mole of dissolved oxygen in the water sample (Benson & Krause, 1984). The formula used to calculate the dissolved oxygen, is as follows:

$$c(O_2) = \left(\left(\frac{(V_{thio} - V_{blank}) \times V_{KIO_3} \times M_{KIO_3}}{V_{std} - V_{blank}} \times 4 \right) - 0.0355 \right) \times \left(\frac{\rho_{is}}{\rho_{fix} \times (\gamma V_{bottle} - V_{ch})} \right) \quad (7)$$

where:

$\boldsymbol{V_{Thio}}$ is the volume of sodium thiosulphate added,

$\boldsymbol{V_{blank}}$ is the volume of the blank,

$\boldsymbol{V_{KIO_3}}$ is the volume of KIO_3 added for the standardization of the sodium thiosulphate,

M_{KIO_3} is the molarity of KIO_3, which was 0.1 M,

V_{std} is the average volume of the titrations,

ρ_{is} is the density of the seawater at in situ temperature,

ρ_{fix} is the density of the seawater at the fixing temperature,

γ is the glass expansion coefficient,

V_{bottle} is the volume of the bottle at 20 °C,

V_{ch} is the volume of the reagents added, which was 1 ml, and

$0.0355\ \mu mol$ is the dissolved oxygen content of the added reagents for 60 ml flasks (Carpenter, 1965).

Blank determination is important for the accuracy of the analysis. To calculate the blank volume, Milli-Q water is titrated to the endpoint with the addition of KIO_3, H_2SO_4, NaOH-NaI and $Mn(OH)_2$, respectively. After the first titration, 0.5 ml of KIO_3 is added and the solution is titrated again. The volume of the blank is equal to the difference between the two volumes of thiosulphate needed for the consecutive titrations. The blank may be either positive or negative.

2. 8. RESPIRATION RATE MEASUREMENTS

The changes in dissolved oxygen due to microbial respiration were measured using the automated Winkler titration method described above. The respiration rates were measured in two different groups of samples: the bacterial community, where the water sample was pre-filtered and the total community, where the sample water was directly incubated. In order to fractionate the bacteria from the rest of the community, the water samples were gravimetrically filtered through 0.8 µm membrane filters

(Boyd et al., 1995; Robinson et al., 1999). The bottle incubations, both total community and the <0.8 µm fraction, were carried out in the temperature-controlled laboratory at PML, where the temperature was adjusted to the in situ sea surface temperature at the time of sampling, on the day.

In order to measure the respiration of the total community, surface seawater from a 10 L aspirator was siphoned into 12 replicate acid-washed and gravimetrically calibrated borosilicate bottles (ca. 60 ml). After measuring the sample temperatures, six bottles were fixed with 0.5 ml of 3 M $MnSO_4$ and 0.5 ml 4 M NaI + 8M NaOH using calibrated repetitive pipettes for time zero (T_0) concentrations. These were stored underwater until analysis. The remaining six bottles were incubated underwater at in situ temperature, in the dark, for 24h. At the end of the incubation, the sample temperatures were recorded and the samples (T_{24}) were fixed and stored underwater prior to analysis. T_0 and T_{24} samples were analysed together within 2 hours of the end of the incubation.

In order to separate the heterotrophic bacteria from the rest of the plankton community, the remainder of the ca. 8 L surface water sample was filtered through a pre-washed 0.8 µm polycarbonate membrane filter, using a reverse flow gravity fed fractionator (Blight et al., 1995; Boyd et al., 1995; Robinson et al., 1999). The size-fractionated water was then carefully siphoned into twelve 60 ml borosilicate glass bottles using acid washed silicon tubing. Six bottles were fixed at time zero and six bottles were incubated at in situ temperature, underwater, in the dark for 24h. Sample analysis was as described above. The respiration rates of both the total community and the <0.8 µm fraction were calculated as the difference between the means of the T_0 replicates and the T_{24} replicates, and reported with the standard error.

2. 9. MICROBIAL COMMUNITY STRUCTURE

2. 9. 1. SAMPLE COLLECTION, FILTERING AND STORAGE

For the time series study, water samples for bacterial community structure were collected weekly (at ca 10 am, weather dependent), at Station L4, for over a year. During the Lagrangian sampling, samples were collected from the transect following the progression of the upwelling filament, on 8 occasions at 'pre-dawn'.

For the time series study, two 20 L samples of surface water were collected into two separate clean carboys directly from the Niskin bottle. They were stored in the dark in a cool box until return to the laboratory. One of the 20 L samples was filtered directly through 0.22 µm Sterivex® filter (Millipore) in duplicate, whereas the other one was first prefiltered through a 0.8 µm polycarbonate filter and then through the 0.22 µm Sterivex® filter in duplicate, via a peristaltic pump. The reason for two different treatments was to see the difference in the particle attached and the free-living bacterial groups. The filters were plugged at both ends, wrapped in parafilm and stored at -80°C until further analysis, within 9 months.

During the Lagrangian sampling, 5 L of seawater from the 55% light depth was filtered through a 0.22 µm Sterivex® filter in duplicate, 1.8 ml of RNALater® (Qiagen) was then added to each Sterivex® in order to prevent mRNA degradation. The filters were then plugged at both ends and kept at 4°C overnight. The RNALater® was then removed; they were wrapped in parafilm and stored at -80°C on board until further

analysis. The workflow from the filtration to the statistical analysis is shown in Figure 2.3.

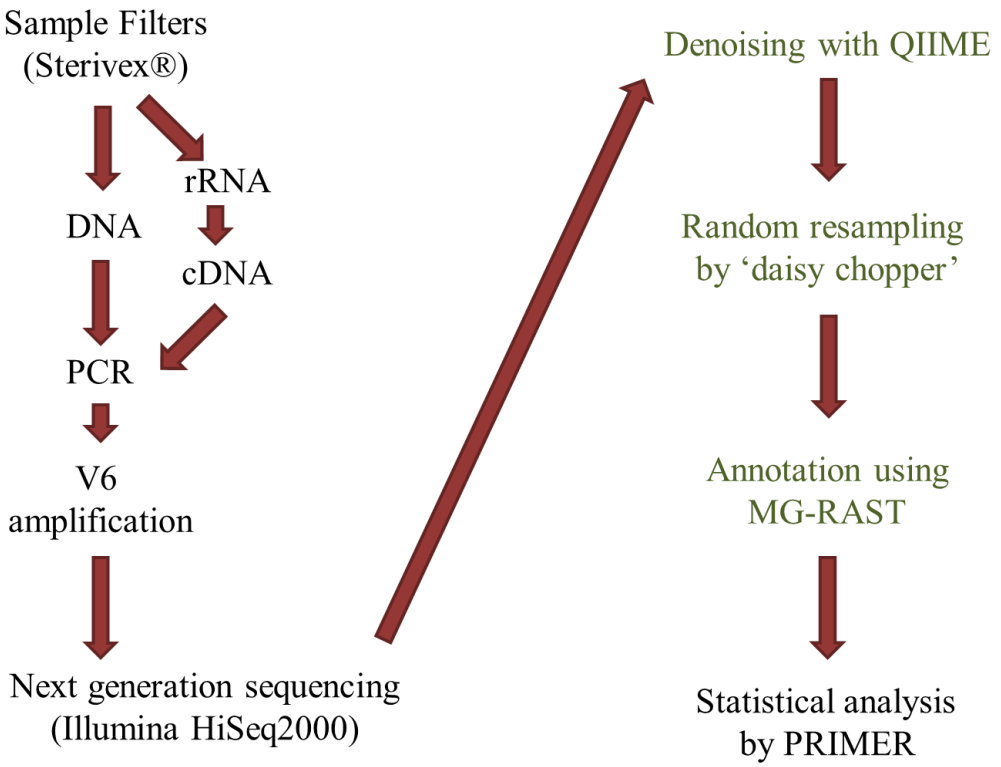

Figure 2.3. Workflow for the metagenome sequencing.

2. 9. 2. NUCLEIC ACID EXTRACTION

The nucleic acid content of the sample was extracted from the Sterivex filters by a modification of the protocol described by Neufeld et al., (2007). The filters were first thawed on ice. Then 1.4 ml of SET lysis buffer was added directly into the Sterivex® filters, followed by 180 µl of lysozyme, 14 µl of mercapto-ethanol, 200 µl of 10% SDS and 55 µl of 20 mg/ml freshly prepared proteinase K. The filters were incubated at 37°C for 30 minutes with rotation in a hybaid oven. The lysate, from each filter, was withdrawn with a 5 ml syringe. 1 ml SET buffer was added to each Sterivex ® filter

to rinse, which was then withdrawn into the same syringe. The lysate was transferred into a 15 ml Maxtract® tube (QIAGEN). Two rounds of 3 ml of phenol:chloroform:isoamyl alcohol (25:24:1) extraction was carried out, at 1500 x g for 5 minutes, at 4°C. 3 ml of chloroform:isoamyl alcohol (24:1) was added to each tube, which were then centrifuged at 1500 x g for 5 minutes, at 4°C. The supernatant was transferred into a clean centrifuge tube. 1.5 ml of 7.5 M ammonium acetate (NH_4-COO^-) and 7.5 ml of 100% ethanol were added to the tubes, mixing gently. They were left at -20°C for 30 minutes, followed by a centrifugation at 10000 x g for 35 minutes, at 4°C. The pellet was washed twice with 80% ethanol and left to dry at room temperature, for ca 15 minutes. It was then suspended in 500 µl of RNase free water. The solution was left on ice for ca 20 minutes to dissolve. The nucleic acid extract was then divided into two Eppendorf tubes, one for DNA, the other for RNA sequencing. The DNA samples were stored at -20°C until further analysis. 25 µl of 125 mM EDTA was added to the RNA samples, which were stored at -80°C, until further analysis.

2. 9. 2. 1. **List of the Chemicals Used during Nucleic Acid Extraction**

SET buffer: Stored at room temperature

- 40 mM EDTA
- 50 mM Tris-HCl (pH 8.0)
- 0.75 M sucrose

Lysozyme: Freshly prepared for each extraction and stored on ice.

- 990 µl sterile water
- 9 mg lysozyme
- 9 µl 1 M Tris-HCl (pH 8.0)

Proteinase K: Freshly prepared for each extraction.

- 950 µl sterile water
- 50 µl Tris-HCl (pH 8.0)
- 20 mg proteinase K

The quantity of the extracted DNA from each sample was measured using a NanoDrop 2000c spectrophotometer (Thermo Scientific), with instrument's software.

2. 9. 3. RNA PURIFICATION

RNA was purified using the TURBO DNA-free™ kit (Ambion®, Life Technologies) followed by RNAeasy® plus mini kit (Qiagen), according to the manufacturer's instructions (Appendix A), in a fume cupboard, cleaned with RNaseZap® (Life Technologies). The total RNA quality of each sample was assessed using the Agilent 2100 Bioanalyser with the RNA 6000 Nano kit (Agilent Technologies). The samples were prepared as described in the manufacturer's protocol, by using specified ladder and the chips (Appendix A).

2. 9. 4. REVERSE TRANSCRIPTION POLYMERASE CHAIN REACTION (RT-PCR) AND POLYMERASE CHAIN REACTION (PCR)

RT-PCR is used to qualitatively detect gene expression. Complementary DNA (cDNA) copies were transcribed from the extracted and purified RNA copies for each sample. RNA was reverse transcribed using the Superscript III kit (Invitrogen) and random hexamer primers (Invitrogen) to produce cDNA. The kit contains

SuperScript™ III RT (200 U/µl), 5X First-Strand Buffer (made up of 250 mM Tris-HCl (pH 8.3), 375 mM KCl, 15 mM $MgCl_2$) and 0.1 M Dithiothreitol (DTT). Random Primers are short oligodeoxyribonucleotides of random sequence. They were used to prepare cDNA from RNA templates. To start the reaction, 11.5 µl RNA, 0.5 µl of the random primers and 1 µl of 10 mM dNTP were mixed in a 200 µl Eppendorf tube. The sample mixture was heated at 65°C for 5 minutes and cooled at 4°C for 3 minutes. It was then put on ice for 1 minute, followed by an addition of 7 µl of the RT-master mix (MM-I). MM-I was prepared by mixing 4 µl of 5X first strand buffer, 1 µl of DTT, 1 µl RNase-out, and 1 µl of Superscript™ III RT for each sample. After the addition of the MM-I to the sample mixture, it was incubated first at 25°C for 5 minutes, then at 50°C for 1 hour and at 70°C for 15 minutes. The reaction products, cDNA, were stored at -80°C until further amplification by PCR.

For both DNA and cDNA samples, PCR reaction was carried out by adding the master mix (MM-II), to the samples, using a primer pool. MM-II was prepared by adding 6 µl of 5X buffer, 3 µl of 2 mM dNTP, 2.4 µl of $MgCl_2$, 0.3 µl of Taq polymerase and 17.1 µl of nuclease free water, with 1.2 µl of the primer pool, for each 1 µl of sample. The amplification conditions were 94°C for 3 minutes, followed by 30 steps of 94°C for 30 seconds, 57°C for 45 seconds and 72°C for 1 minute, followed by a final extension step of 72°C for 1 minute. The reactions were run in triplicates, on an ABI Prism 7000 (ABI) RT-Machine. The PCR product was visualized by gel electrophoresis, after ethidium bromide staining, making sure that is was between 100 and 115 bp.

For each sample 5 forward and 4 reverse primers were needed to cover the variability in the V4 region of the 16S rRNA. These primers were identified according to the

Silva and RDP databases. cDNA and DNA were used as a template for V4 region of 16S rRNA amplification. Each amplicon was labelled with a unique multiplex identifier (MID) sequence, used in the primer pools, to enable it to be differentiated from the rest of the samples.

The PCR products were cleaned by using SureClean Plus (Bioline). The protocol requires an equal volume of Sureclean addition to the volume of the amplicon. After incubating the mixture at room temperature for 10 minutes, it was centrifuged at maximum speed for 10 minutes. The supernatant was discarded and the pellet was dissolved in double the volume of the original PCR product. It was then centrifuged again at maximum speed for 10 minutes. The supernatant was discarded and the sample was air dried on ice. The pellet was resuspended in ca 20 µl DNA water.

All sample amplicon product pools were sequenced on the Illumina HiSeq 2000 platform. All sequences have been submitted to the National Centre for Biotechnology Information (NCBI) short reads archive and registered with the Genomes On-line Database (GOLD). The sequencing was performed at the Argonne National Laboratories (Chicago, Il, USA)

2. 9. 5. Sequence Clean-up, Annotation and Statistical Analysis

Sequences were then cleaned using the Quantitative Insights into Microbial Ecology (QIIME) pipeline at Argonne National Laboratory (Chicago, Il, USA), randomly resampled with Daisy chopper (daisychopper.pl) and annotated using the Metagenomic Rapid Annotations using Subsystems Technology (MG-RAST) bioinformatics server (Caporaso et al., 2010).

The statistical analysis of the environmental parameters, respiration and the annotated sequences were performed using SigmaPlot (Systat Software, Inc., 2011) and PRIMER v6 multivariate statistics package (PRIMER-E, 2009). The data were first checked for normality. Square root transformation was carried out where necessary. In order to understand the relationships between bacterial respiration and other biological and environmental variables, cluster and multi-dimensional scaling (MDS) analysis, by using the Bray-Curtis similarity coefficient, were performed on the data set.

3. ANNUAL TIME-SERIES STUDY ON THE BACTERIAL DIVERSITY AND ACTIVITY

In this chapter, the variation of the diversity and the activity of the bacterial community in the surface waters will be discussed in relation to physical, chemical and biological factors, over a 12-month period, at station L4 of the WECO.

3. 1. SEA SURFACE TEMPERATURE AND SALINITY

Between the beginning of 2000 and the end of the present study on 26th April 2009, surface temperature (SST) varied between 7.37°C (in February and March 2001) and 18.39°C (September 2004) and the mean monthly averaged surface temperatures ranged from 8.7°C in March to 16.4°C in August during the same period (Figure 3.1).

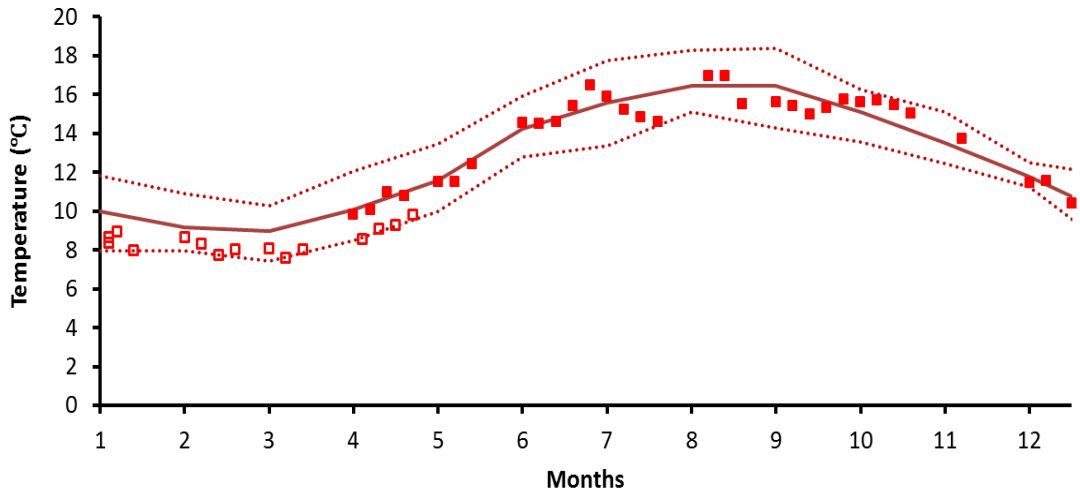

Figure 3.1. The mean SST (—), maximum and minimum values (·····) recorded between 2000 and 2008, and the SST data recorded during the present study, from April 2009 to April 2010, shown in red squares. Solid square is used (■) for data collected in 2009 and empty square (□) for data collected in 2010.

The SST measurements recorded during this study (2009-2010) are shown together with the historical data (2000-2009) in Figure 3.1. The surface temperatures ranged

from 7.59ºC (March 2010) to 16.97ºC (August 2009) during the 12 months of sampling. The SST was consistently below the historical average in 2010, but around the mean in 2009.

The station has been reported to be well mixed during the autumn and winter months followed by a weak stratification during spring and summer (Smyth et al., 2009). Our data shows a similar trend in winter months with a mixed water column (Figure 3.2). However, the thermocline did not form until June 2009, regardless of the increasing water temperatures. The stratification persisted only until late summer. It gradually disappeared from the beginning of September 2009. The water column stayed mixed for the rest of the study period, except for a weak reappearance in January 2010 for two weeks.

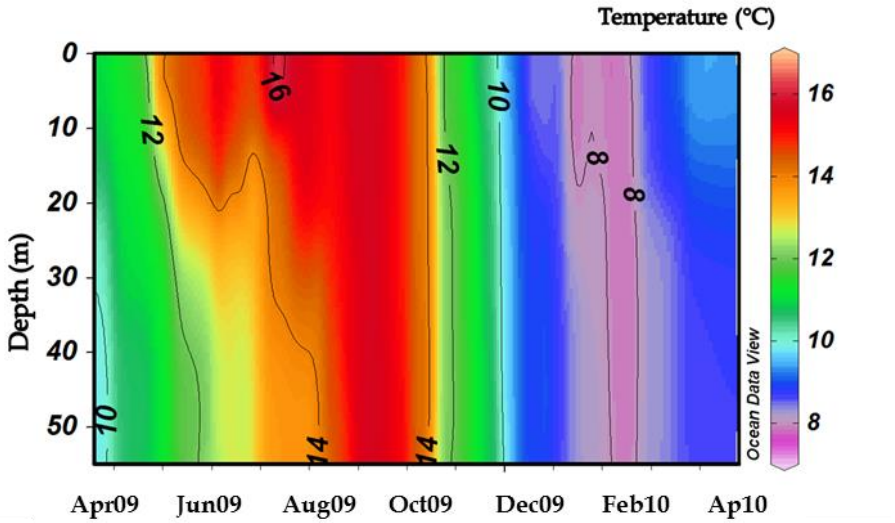

Figure 3.2. The temperature depth profile during the study period.

The stratification and mixing at L4 was described as wind driven by Smyth et al. (2009). The prevailing south-westerly winds in the western English Channel can be as

strong as 10 m s^{-1}, causing the water to mix (Smyth et al., 2009). It has also been shown that tidal mixing may play an important role in the coastal regions in the English Channel (Pingree & Griffiths, 1978). The mixing conditions that produce the frontal systems largely determine the availability of light and nutrients necessary for phytoplankton growth.

Salinity measurements began in 2002 at station L4, with the arrival of the SeaBird SBE19 CTD. The minimum salinity recorded was 33.91 in July 2008 and the maximum was 35.86 in June 2009 (Figure 3.3). The average salinity at L4 was 35.05 ± 0.27 (mean ± SD). The station receives fresh water input from the nearby rivers especially after heavy rainfall (Rees et al., 2009).

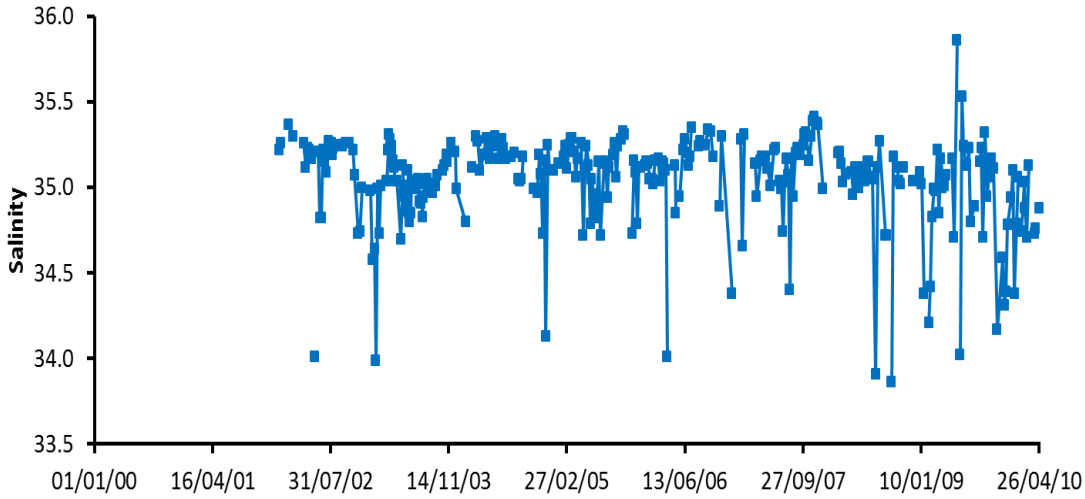

Figure 3.3. The salinity measurements (—■—) at L4, from 07th January 2002 to 26th April 2010.

The average salinity during the present study period was 34.9 with a standard deviation of 0.35. The maximum salinity observed was 35.86 on 2nd June 2009, which also is

the maximum measured since January 2000. The minimum-recorded salinity of the study period was 34.02, on 15th June 2009, only two weeks after the maximum recorded salinity.

3. 2. INORGANIC NUTRIENTS

The chemistry of the station L4 is under a strong influence of riverine input (Rees et al., 2009). The intense rainfall, strong winds and the tides increase the river run off, resulting in pulses of inorganic nutrient input to the system (Smyth et al., 2009). Despite the riverine input, Station L4 is characterized by inorganic nutrient depletion during summer months (Rees et al., 2009; Smyth et al., 2009). However, sudden increases in inorganic nutrient concentrations, especially in summer months, were correlated with heavy rain falls and river run offs (Rees et al., 2009).

The maximum and the mean values for different inorganic nutrients, from January 2000 to the end of April 2010, are shown together with the measured values during the study period in Figure 3.4 to Figure 3.8. Especially during the summer months, the inorganic nutrient concentrations in some samples were below the detection limits of the instrument used; those sample points were plotted as '0' to show that the sample was collected for that date in the study period.

Historically, the average nitrate concentrations were ca 8 µmol L^{-1}, more than 10-fold higher than summer values, gradually decreasing in spring (Figure 3.4). The nitrate concentrations gradually decrease towards the summer, and by late spring and early summer, they are below the detection limit. This change in nitrate concentration is correlated with the stratification and mixing (Pingree & Griffiths, 1978; Smyth et al.,

2009). The average concentration for nitrate at L4, since the beginning of the record in 2000, is 3.11 µmol L^{-1} (± 3.46). The maximum concentration of nitrate in the surface waters of station L4 was 14.61 µmol L^{-1} in December 2004. During the present study, in autumn 2009, the nitrate values were below the average concentrations, however, in December 2009, it reached ca 8.5 µmol L^{-1} exceeding the monthly averages. The maximum value for nitrate was observed in January 2010 as 11.90 µmol L^{-1}. The average winter concentrations in the present study were ca 9 µmol L^{-1} and persisted at that average until the end of April 2010. Although a decrease to ca 5 µmol L^{-1} at the beginning of March was observed, the concentrations quickly increased to 10.95 µmol L^{-1} in April 2010. This unusual increase also set the record as the highest nitrate concentration observed in April since the beginning of the inorganic nutrient analysis at L4, in 2000. However, the concentrations decreased to average values within a few weeks.

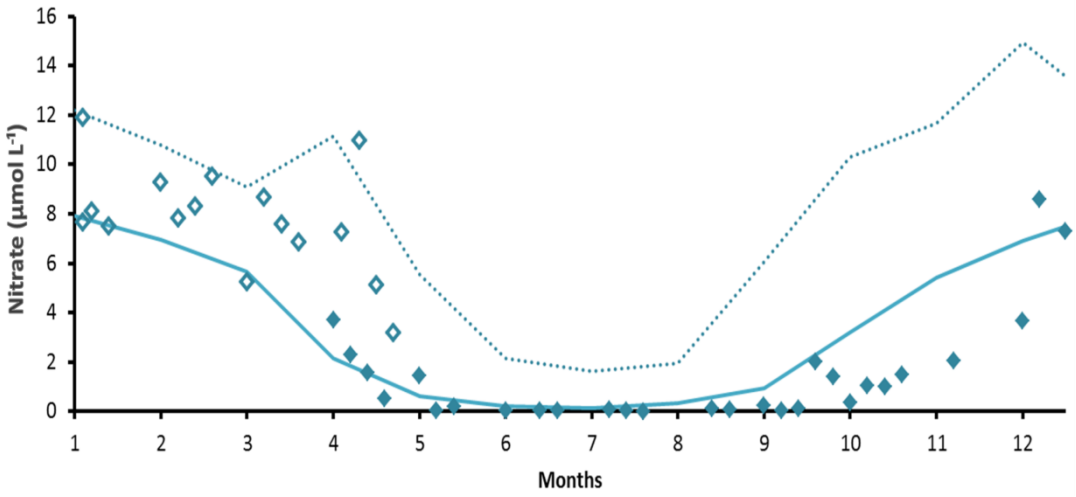

Figure 3.4. The mean (——) and the maximum (·····) nitrate concentrations recorded between 2000 and 2009, with the concentrations recorded during the present study, in 2009 (♦) and 2010 (◇).

The nitrite concentrations were lower during the winter months, but higher in the autumn (Figure 3.5). The maximum ever-recorded concentration for nitrite is

1.25 µmol L^{-1} in October 2006. These high concentrations were related to microbial nitrification, following the breakdown of the late summer blooms (Smyth et al., 2009). The average winter and spring concentrations were at ca 0.2 µmol L^{-1}, the maximum winter-spring value was 0.55 µmol L^{-1} in February 2004. During the study period, the nitrite values were mostly at average values of the historic data. Following below detection limit values of the summer months, the concentrations increased to high values in autumn, reaching a maximum of 0.67 µmol L^{-1}, in October 2009. Although this increase came a little later than expected, the values stayed high longer than usual. Some of the highest nitrite concentrations of the record were observed during the last week of December 2009 and the beginning of January 2010. However, the nitrite concentrations then dropped to average values and remained at average values until the end of the study period.

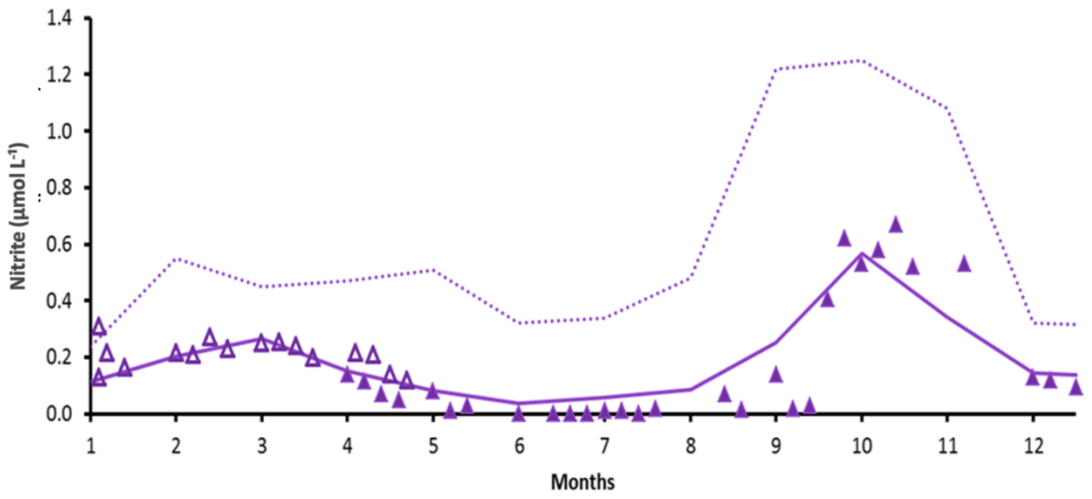

Figure 3.5. The mean (—) and the maximum (·····) nitrite concentrations recorded from 2000 to 2009, with the concentrations recorded during the present study, in 2009 (▲) and 2010 (▲).

Station L4 is characterized by low average ammonia concentrations throughout the year (Figure 3.6). The yearly average for ammonia was 0.31 ± 0.37 µmol L^{-1} (mean ±

SD). It was previously observed to peak in the spring and late summer-early autumn periods. The spring and autumn maximum values recorded for ammonia were 1.55µmol L^{-1} in March 2009 and 2.95 µmol L^{-1}, in September 2006, respectively. During the study period, the spring and summer concentrations for ammonia were below the average most of the time and below the detection limit occasionally. The concentrations reached a maximum of 1.56 µmol L^{-1} on 17th August 2009. This then decreased to average concentrations, possibly due to depletion by the late summer algal bloom. Following the bloom, the ammonia concentrations again increased in late September 2009, only to be depleted in two weeks, returning to below average values by October 2009. In the winter, ammonia concentrations were similar to the historic averages, except for the sudden peak and fall in January 2010. In the beginning of April 2010, the ammonia concentration once again increased to 0.87 µmol L^{-1}, twice the historic mean for that time of the year, which was 0.43 µmol L^{-1}.

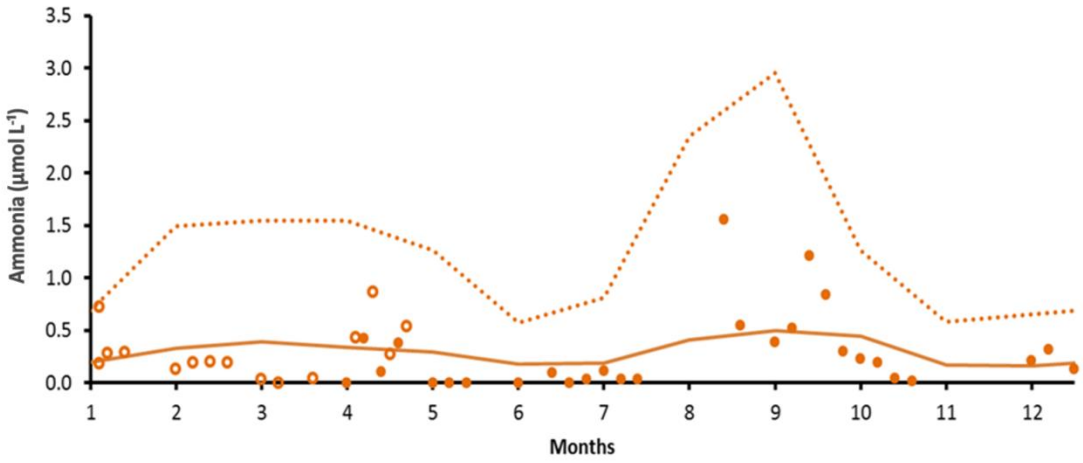

Figure 3.6. The mean (——) and the maximum (·····) ammonia concentrations recorded from 2000 to 2009, with the concentrations recorded during the present study, in 2009 (●) and 2010 (○).

The average silicate concentration at station L4 is relatively high in winter months, decreasing in summer (Figure 3.7). The highest mean values for silicate observed at ca 5 µmol L^{-1}, gradually depleted to minimum concentrations in July. However,

historically silicate peaked at different times throughout the year, in every season. Smyth et al. (2009) suggested that the source of silicate at L4 most likely is the Tamar River. During the study period, the silicate values followed the historical pattern of high winter-low summer concentrations. The concentrations reached a maximum of 6.4 µmol L^{-1} in January 2010, and were below the detection limit (of 2 nmol L^{-1}) in July 2009.

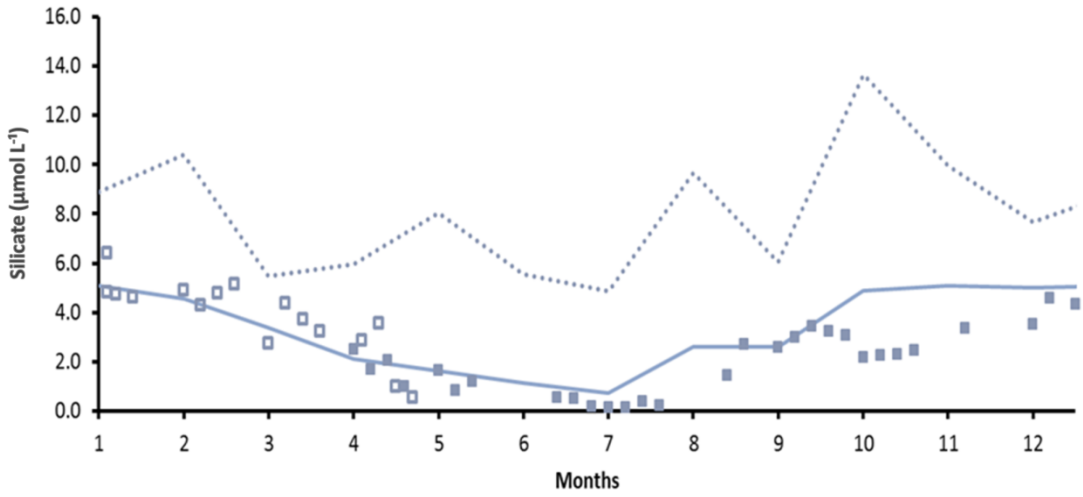

Figure 3.7. The mean (——) and the maximum (·····) silicate concentrations recorded from 2000 to 2009, with the concentrations recorded during the present study, in 2009 (■) and 2010 (□).

The concentrations of phosphate follow a similar pattern to that of nitrate and silicate; higher concentrations in winter followed by lower values in summer. In the past, phosphate concentrations at L4 reached their highest mean concentrations of 0.5 µmol L^{-1} in late autumn, gradually decreasing through winter and spring. The maximum value for phosphate recorded was 1.11 µmol L^{-1} in October 2005. The lowest mean values observed at L4 were ca 0.1 µmol L^{-1}, in April-May time, followed by an increase through the summer months, reaching high concentrations in autumn. During the present study period, the pattern lagged the annual means by about 2-3 months. The lowest phosphate concentrations were observed during July, August

and September 2009. The highest concentrations during the sampling period were in winter and early spring, setting some of the highest records in the historical time-series data for March and April. The average phosphate value from December 2009 to April 2010 was ca 0.6 ± 0.05 µmol L^{-1}.

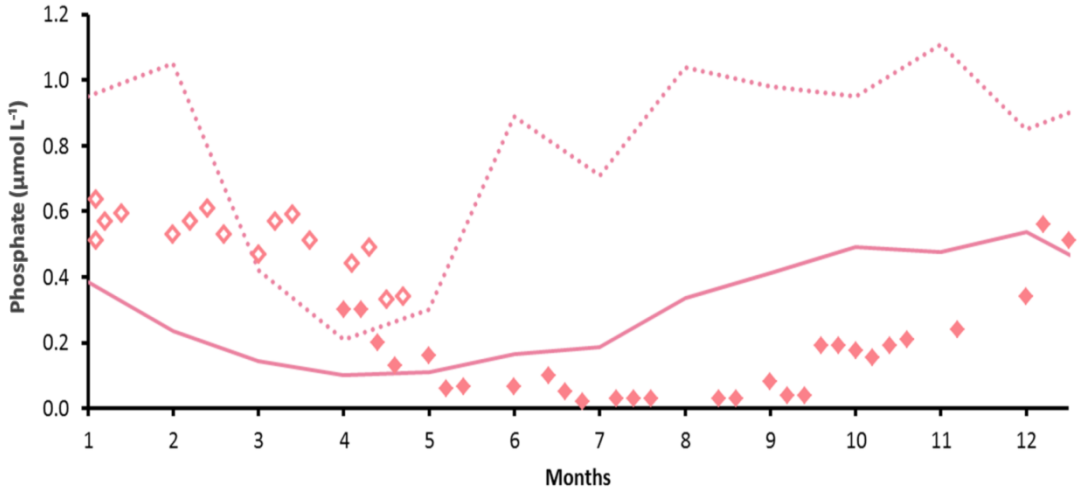

Figure 3.8. The mean (——) and the maximum (·····) phosphate concentrations from 2000 to 2009, with the concentrations recorded during the present study, in 2009 (◆) and 2010 (◇).

Figure 3.21 on page 92 shows the changes in the inorganic nutrient concentrations, throughout the study period. The inorganic nutrient concentrations had been in a decreasing trend at the beginning of the sampling period, except ammonia peaking in the second and fourth week of April 2009, just before and after the spring bloom. From mid-May to mid-August, the concentrations of all of the inorganic nutrients were at their minimum. Occasionally, the concentrations were below the detection limit during this time of the year. The first to increase to its maximum concentration was ammonia (1.56 µmol L^{-1}), on 17th August 2009, followed by the peak in the chlorophyll *a* measurements in the following week, 24th August (Figure 3.20, page 92). The ammonia concentration then was depleted to ca 0.4 µmol L^{-1}, but increased again to 1.21 µmol L^{-1} in the following two weeks, possibly due to the breakdown of the algae,

following the bloom. The nitrite was the second inorganic nutrient to reach its maximum (0.67 µmol L^{-1} on 19th October 2009), after a gradual increase in its concentrations from mid-September. This may be caused by the remineralisation following the post bloom conditions at L4. As winter arrived to the station L4, the nitrate, phosphate and silicate concentrations started to increase. The increase in the nitrate concentrations at L4 was previously shown to be correlated with riverine input following heavy rainfall (Rees et al., 2009). The silicate concentrations follow a very similar pattern to nitrate during winter months, which might suggest that the source for silicate at L4 possibly is the Tamar River, as previously argued by Smyth et al. (2009). Both nitrate and silicate reached their maximum concentrations on 26th January 2010 (11.9 and 6.4 µmol L^{-1}, respectively). Their values both stayed above average almost until the end of the sampling period. Phosphate had higher concentrations in winter, than the rest of the study period. However, unlike the other inorganic nutrients, the concentrations of phosphate showed gradual increasing and decreasing patterns from autumn 2009 towards spring 2010, rather than pulses of increased concentrations.

3. 3. DISSOLVED OXYGEN

The changes in the dissolved oxygen concentrations at surface waters at station L4 are shown in Figure 3.9.

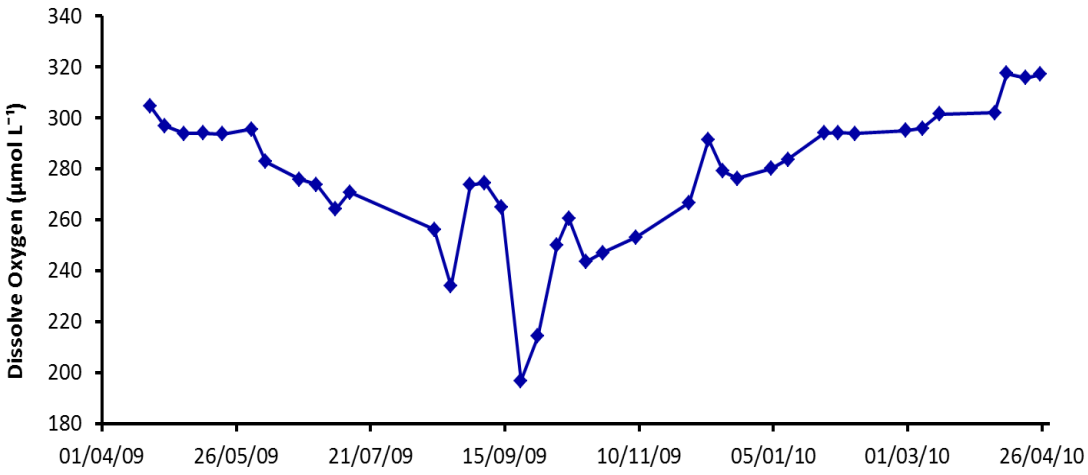

Figure 3.9. The dissolved oxygen content (—◆—) of the surface waters at station L4.

The dissolved oxygen concentration was 304.6 µmol L^{-1} on 21st April 2009, the beginning of the study period. It gradually decreased throughout the spring with an average concentration of ca 298 µmol L^{-1} until the beginning of June 2009. With the sea surface temperatures increasing above 14ºC, the decline in the oxygen concentrations accelerated. It dropped to 233.9 µmol L^{-1} on 24th August, where the chlorophyll *a* reached its maximum (Figure 3.22, page 93). The dissolved oxygen concentration decreased even further in the following month, reaching a minimum of 196.77 µmol L^{-1} on 22nd September 2009, in the post bloom conditions at L4. The average oxygen content of the water between June and November 2009, where the SST was above 14ºC, was 257.2 µmol L^{-1}. The dissolved oxygen concentrations increased during winter and spring 2010, reaching maximum concentration of 317.4 µmol L^{-1} on 12th April 2010.

3. 4. CHLOROPHYLL *α*

Chlorophyll *a* measurements have been carried out by PML scientists, since 1992, using a Turner Fluorometer. Figure 3.10 shows the average concentrations of chlorophyll *a* with minimum and maximum values observed from the beginning of 2000 to the beginning of 2009. The data collected during the study period are plotted on the same graph for comparison reasons. Although the chlorophyll *a* time-series shows a large degree of annual and inter-annual variability (Figure 3.10), the station L4 is characterized by two distinct blooms, one in spring and the other in the late summer (Figure 3.11). In the past, the spring bloom was found to be dominated by diatom species and the surface chlorophyll *a* concentrations ranged from 0.77 to 9.12 mg m^{-3} between 2000 and 2009 (Figure 3.11). The annual spring bloom concentration averaged 2.5 mg m^{-3}, peaking in April. The late summer bloom, on the other hand, has been dominated by dinoflagellate species (Widdicombe et al., 2010). The chlorophyll *a* concentrations ranged between 0.2 to 10.55 mg m^{-3}, however the maximum bloom concentration averaged 2.6 mg m^{-3} since 2000.

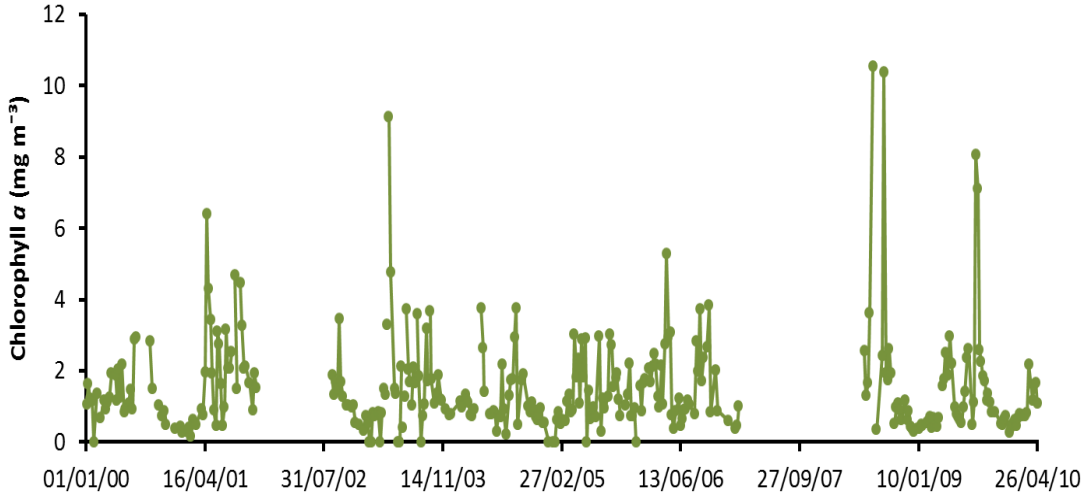

Figure 3.10. The chlorophyll *a* measurements (—●—) at station L4, from beginning of 2000 to end of April 2010.

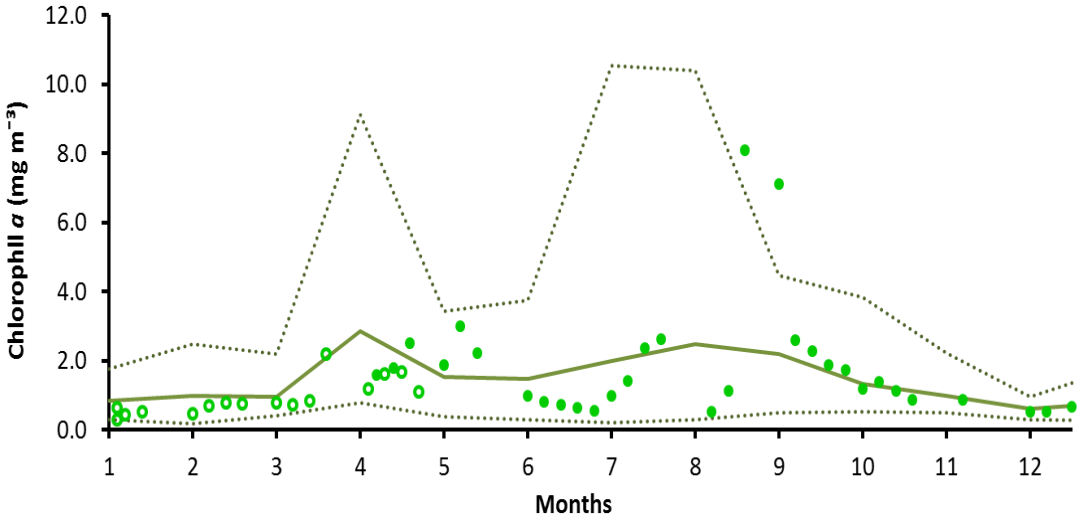

Figure 3.11. The mean chlorophyll *a* (——), the maximum and minimum values since 2000 (·····), and the chlorophyll *a* measurements recorded during the present study, samples from 2009 (●) and 2010 (○).

The chlorophyll *a* concentration in the surface waters at L4 increased throughout April and early May 2009, reaching 2.97 mg m^{-3} on 13th May 2009 (Figure 3.20, page 92). Towards the end of July 2009, the chlorophyll *a* concentration again increased to ca 2.6 mg m^{-3} but decreased to 0.5 mg m^{-3} at the beginning of August. Following this event, the chlorophyll *a* concentration peaked to its maximum value of 8.07 mg m^{-3} on 24th August 2009, increasing ca 10-fold in just a week. Barnes et al., (in press) reported that the bloom was dominated by *Karenia mikimotoi*, after a period of heavy rainfall creating a nutrient rich and less saline environment at station L4 (Barnes et al., 2014). The chlorophyll *a* concentrations persisted above the average values for two to three weeks.

3. 5. EUKARYOTIC AND BACTERIAL CELL ABUNDANCE

The abundance of phytoplankton, heterotrophic nanoeukaryotes and bacteria have been monitored at L4 since 2007 using automated flow cytometry. Samples for the present study were collected between April 2009 and May 2010.

Figure 3.12 shows the seasonal variability in abundance of phototrophic picoeukaryotes. Their abundance of ranged from 165 to 8.2 x 10^4 cells ml^{-1}, between 2007 and 2008. Cell numbers tend to be higher in spring and summer months. Although it was close to the average values at the beginning of the study period in spring 2009 (recorded as 2.7 x 10^4 cells ml^{-1} on 20th April 2009), the maximum abundance of the phototrophic picoeukaryotes observed during the study period was 6.3 x 10^4 cells ml^{-1}, on 20th July 2009 (Figure 3.24, page 94). This increase coincided with the increase in the chlorophyll *a* values on that date (Figure 3.20, page 92).

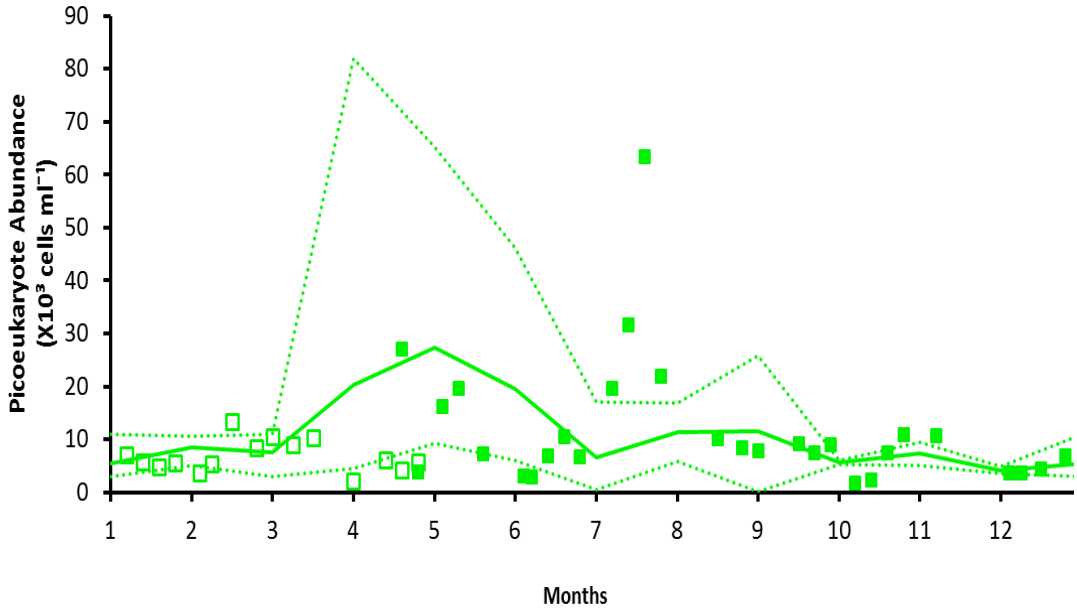

Figure 3.12. The mean (——), the maximum and the minimum (·····) cell counts for phototrophic picoeukaryotes, together with the abundances observed during the present study, samples from 2009 (■) and 2010 (□).

Figure 3.13 shows the seasonal fluctuation in phototrophic nanoeukaryote abundance. The abundance of the phototrophic nanoeukaryotes is characteristically high during spring and summer months (Figure 3.13). The minimum number of cells was 199 cells ml^{-1}, on 1st December 2009 and the maximum cell count was 6.8 x 10^3 cells ml^{-1} on 20th July 2009. The phototrophic nanoeukaryote abundance remained within the range of the three-year average during most of the year. However, during late spring and summer, their numbers fluctuated over a wider range than previously observed. Some of the lowest and highest phototrophic nanoeukaryote cell counts were recorded during that period. The increase in cell numbers was delayed by ca 6 weeks, in comparison to the previous years' data collected during the same time of the year. This increase in their abundance coincides with the increased chlorophyll *a* concentrations in spring and the summer of 2009. The maximum cell count for nanoeukaryotes during the study period was 6.7 x 10^3 cells ml^{-1}, on 20th July 2009 (Figure 3.24, page 94). Their numbers indicate that they dominated the spring bloom in 2009. The increase in the abundance of both phototrophic picoeukaryotes and the phototrophic nanoeukaryotes on 20th July 2009 also coincided with the chlorophyll *a* peak in that week.

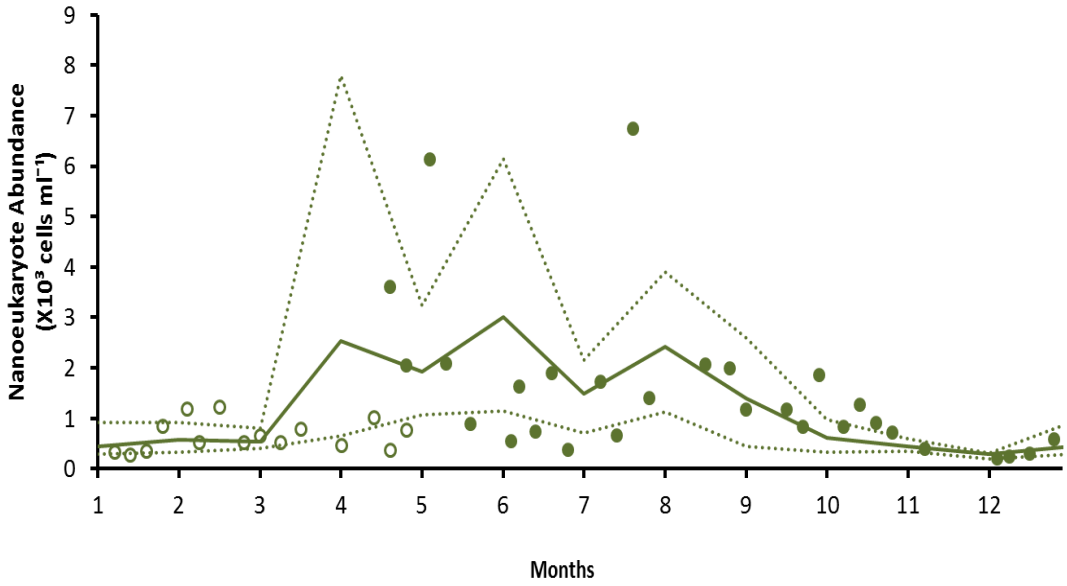

Figure 3.13. The mean (—), the maximum and the minimum (·····) cell counts for phototrophic nanoeukaryotes, together with the abundances observed during the present study, samples from 2009 (●) and 2010 (○).

The changes in coccolithophore abundance are shown in Figure 3.14. Prior to 2009, the highest coccolithophore abundance was recorded in spring, reaching ca 350 cells ml^{-1} in May, and lowest in June and July (ca 4 cells ml^{-1}, Figure 3.14). During the study period, the minimum coccolithophore abundance was 5 cells ml^{-1}, observed on 15th June 2009, and the maximum abundance was 416 cells ml^{-1}, on 1st March 2010 (Figure 3.14, below, and Figure 3.25, page 94). The coccolithophore abundance between September 2009 and April 2010 was generally higher than the average abundances of 2007-2008. The high coccolithophore abundance in March and April 2010 coincided with the increase in chlorophyll *a* concentration during the same period (Figure 3.20, page 92).

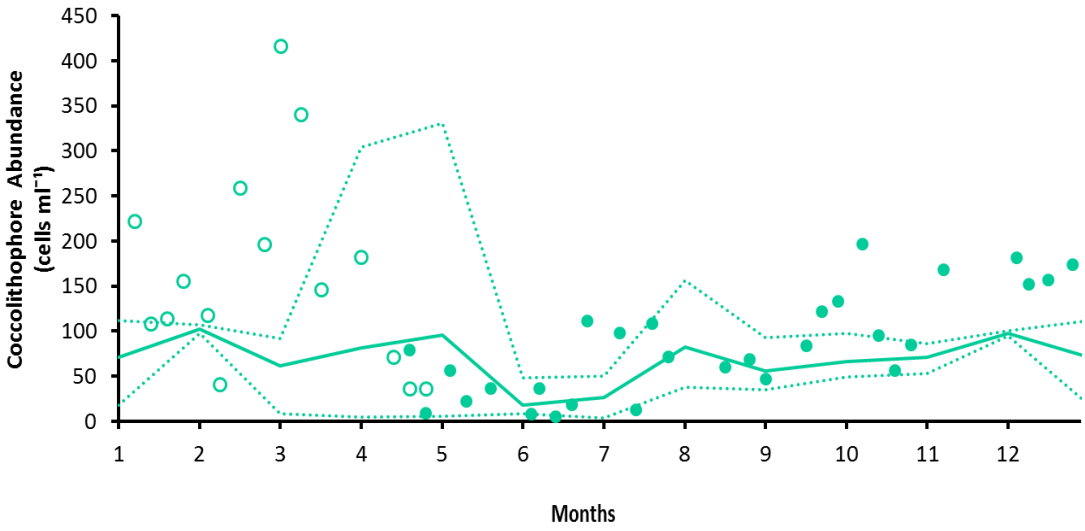

Figure 3.14. The mean (——), the maximum and the minimum (·····) coccolithophore cell counts with the abundances observed during the present study, samples from 2009 (●) and 2010 (○).

The heterotrophic nanoeukaryote abundance was highest from spring to autumn (Figure 3.15). In 2009, average heterotrophic nanoeukaryote cell numbers were below those previously recorded at L4. The increase in abundance followed the phytoplankton blooms, in April, May and July 2009 (Figure 3.25, page 94). During the study period, the maximum and the minimum cell counts for the heterotrophic nanoeukaryotes were 2.0 x 10^3 cells ml^{-1}, on 20th July 2009, and 92 cells ml^{-1}, on 26th April 2010, respectively.

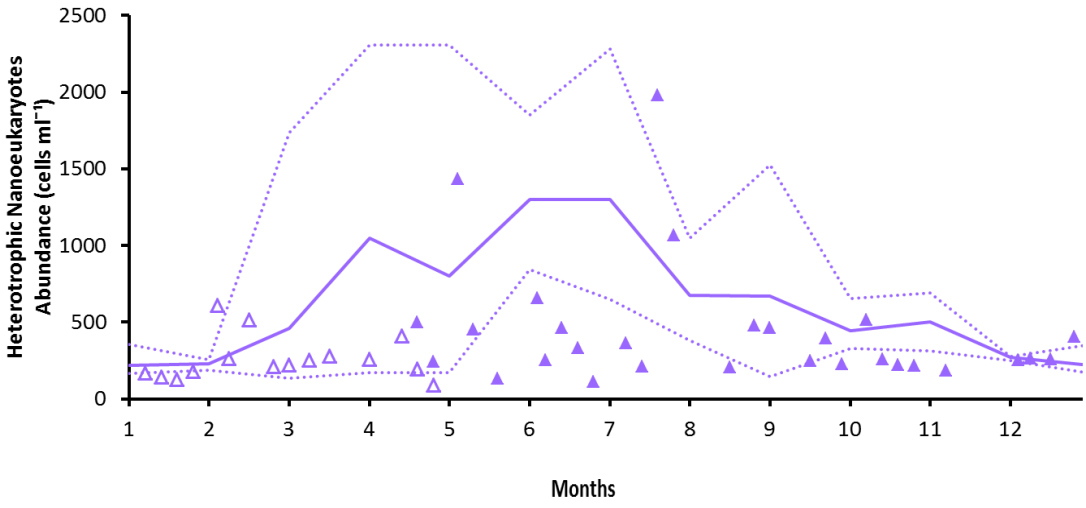

Figure 3.15. The mean (——), the maximum and the minimum (·····) heterotrophic nanoeukaryote cell counts with the abundances observed during the present study, samples from 2009 ( ) and 2010 ( ).

Between 2007 and 2008, the cryptophyta cell numbers increased in spring and autumn (Figure 3.16). Their cell numbers vary greatly, from a few thousands to more than half a million per millilitre. During the present study, their numbers were within the range of previous observations. Except for the increase in abundance which occurred in October and November 2009, ca a month later than observed in previous years. The high cryptophyta abundance in early spring 2009 and 2010 occurred just before the increase in the chlorophyll *a* concentration, on both occasions. The lowest abundance of cryptophytes was 17 x 10^3 cells ml^{-1}, on 29th June 2009, and the highest was 592 x 10^3 cells ml^{-1}, on 26th October 2009 (Figure 3.16 and Figure 3.26, page 95).

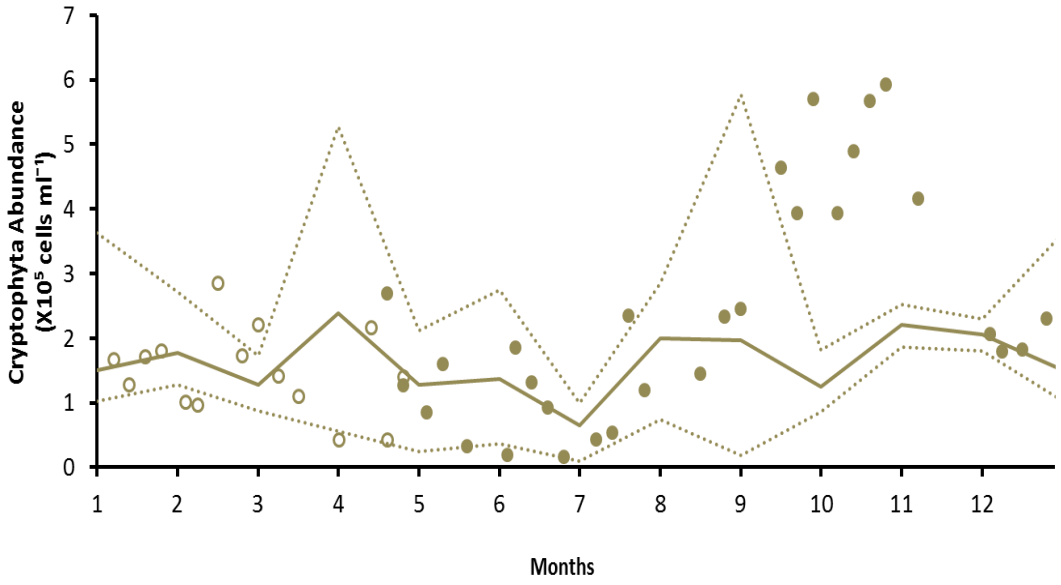

Figure 3.16. The mean (——), the maximum and the minimum (·····) cryptophyta cell counts with the abundances observed during the present study, samples from 2009 (●) and 2010 (○).

In 2007 and 2008, the average *Synechococcus* spp. abundance was below 10^4 cells ml^{-1} from October to July, with an average abundance of ca 8.5 x 10^3 cells ml^{-1} (Figure 3.17). However, their cell numbers increased in summer and early autumn. The highest abundance was 77.3 x 10^3 cells ml^{-1}, on 22nd September 2008. The lowest abundance

was 142 cells ml^{-1}, on 2nd June 2009, which also was the lowest abundance during the present study. During the sampling period, the maximum cell count for *Synechococcus* spp. was 51.2 x 10^3 cells ml^{-1}, recorded on 7th September 2009 (Figure 3.26, page 95). Their numbers remained above the seasonal average until December (Figure 3.17).

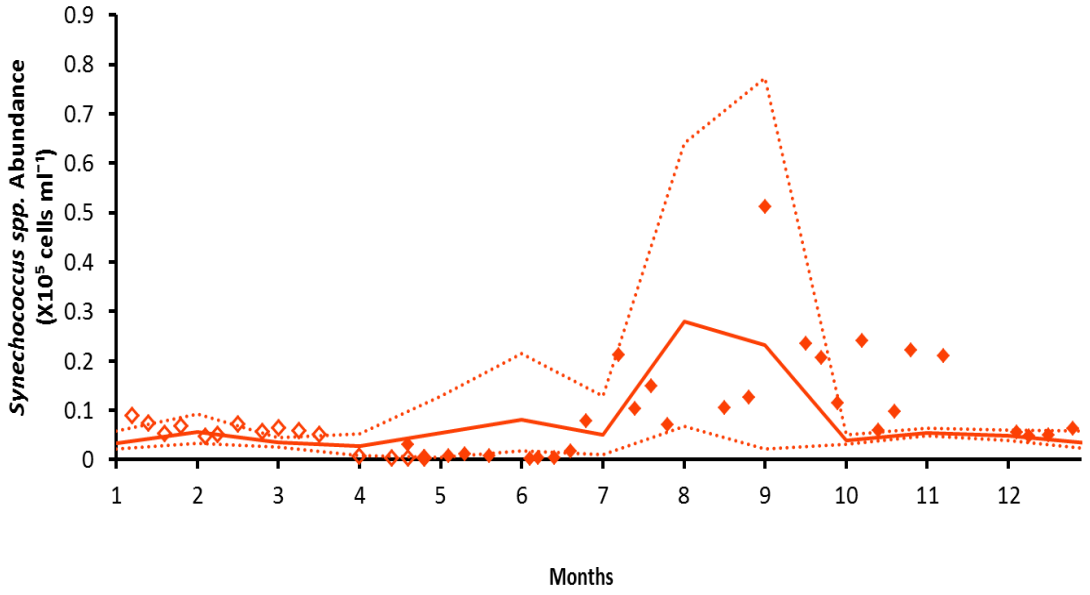

Figure 3.17. The mean (——), the maximum and the minimum (·····) *Synechococcus* spp. cell counts with the abundances observed during the present study, from 2009 (♦) and 2010 (◇).

Figure 3.18 shows the seasonal variability in abundance of heterotrophic bacteria at station L4. The average abundance for the heterotrophic bacteria was ca 9.4 x 10^5 cells ml^{-1} (± 0.5 x 10^5 cells ml^{-1}), since the beginning of 2007, with an increase from mid spring to early autumn (Figure 3.18). Prior to 2009, the maximum abundance was 2.2 x 10^6 cells ml^{-1} in June 2007. During the sampling period, the maximum abundance was 4 x 10^6 cells ml^{-1}, on 27th July 2009 (Figure 3.27, page 95), following the increase in phototrophic pico- and nanoeukaryote as well as the heterotrophic nanoeukaryote abundances. Their numbers remained above the average of 2007 and 2008 from July until almost the end of December. The abundance of heterotrophic bacteria increased to ca 1.5 and 2 x 10^6 cells ml^{-1}, on 7th July and

7th September, respectively, coinciding with the increases in the *Synechococcus* spp. cell numbers on the same dates (Figure 3.26 and Figure 3.27, both on page 95).

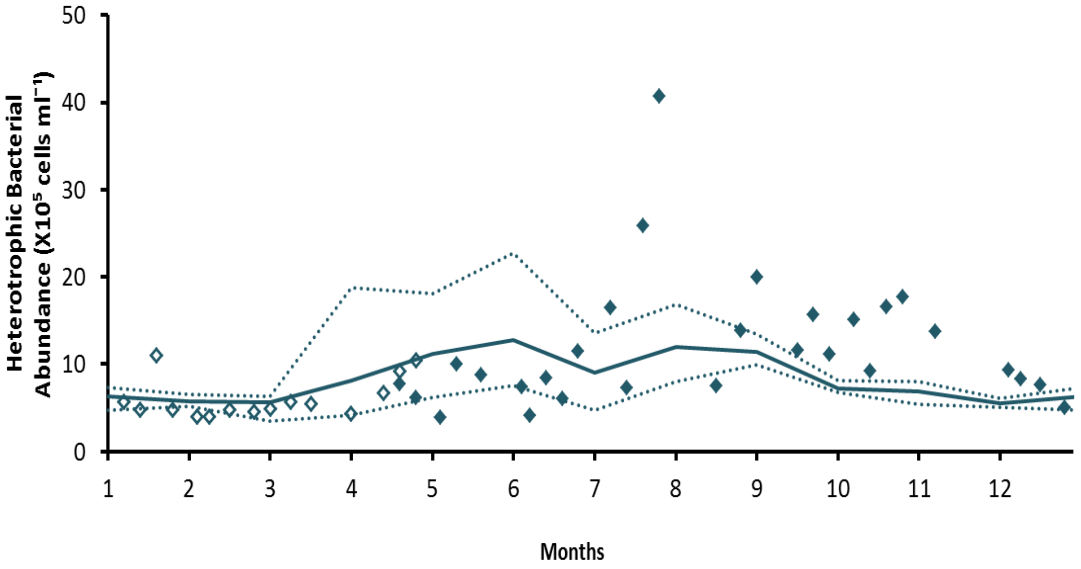

Figure 3.18. The mean (—), the maximum and the minimum (·····) cell counts for heterotrophic bacteria together with the abundances observed during the present study, from 2009 (♦) and 2010 (◊).

With the flow cytometer, heterotrophic bacteria can be differentiated according to the nucleic acid content within their cells; high nucleic acid (HNA, metabolically active cells) and low nucleic acid content (LNA, metabolically less active cells). By doing so, actively growing members of the bacterial community can be tracked in changing proportions between HNA and LNA bacteria (Gasol et al., 1999; Morán et al., 2010). Figure 3.19 shows the changes in the percent distribution of the HNA and LNA bacteria throughout the sampling period.

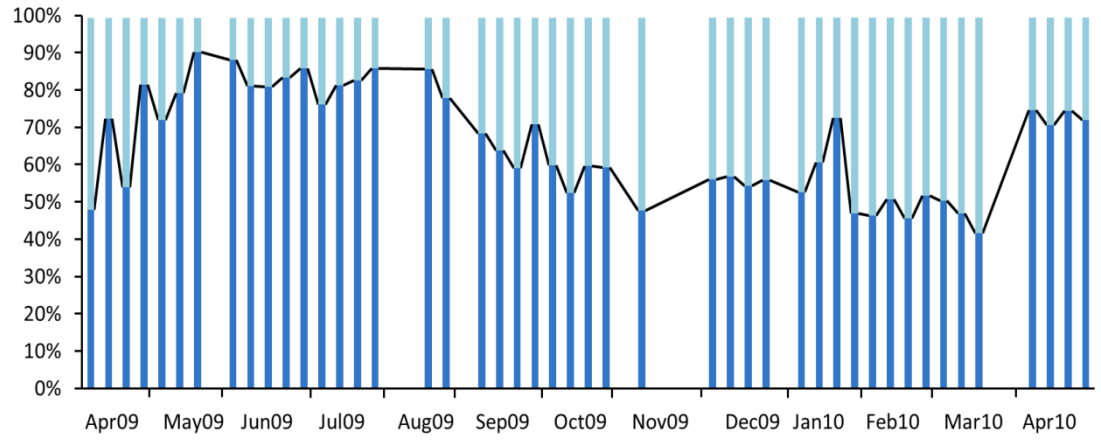

Figure 3.19. The changes in the percentages of the HNA (dark blue) vs LNA (light blue) heterotrophic bacteria during the sampling period.

The HNA heterotrophic bacteria contributed 80 to 90% to the total heterotrophic bacterial community from late spring to late summer. However, their dominance diminished to ca 50% in most weeks, from autumn to early spring. Although the hypothesis is that HNA bacteria are the most active members of the community, their abundance is an indicator of bulk activity only when the production in the community mainly depends on the phytoplankton substrates for growth (Morán et al., 2010). In their study, Morán et al., (2010), found that these conditions can be observed commonly in temperate waters, where the SST is above 16°C. During the present study, SST exceeded 16°C only twice, on 29th June and 11th August 2009. There is unfortunately no AFC data for 11th August, due to bad weather conditions. The abundance of HNA on 29th June is 85.8%. However, on 18th May and 2nd June, the HNA abundances as a percentage of the total abundance were higher than that of 29th June; 90.1 and 88.1 respectively.

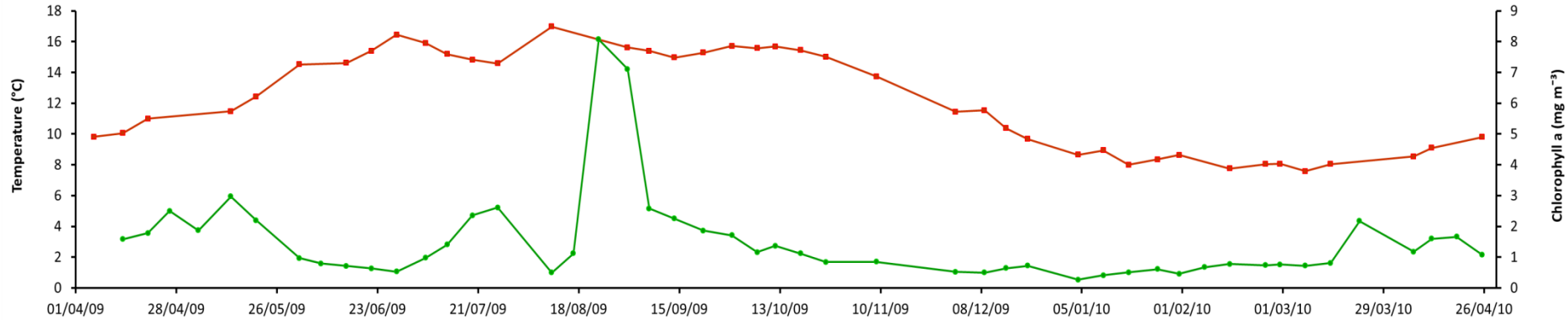

Figure 3.20. The sea surface temperature (—●—) and the chlorophyll *a* concentrations (—●—) throughout the sampling period.

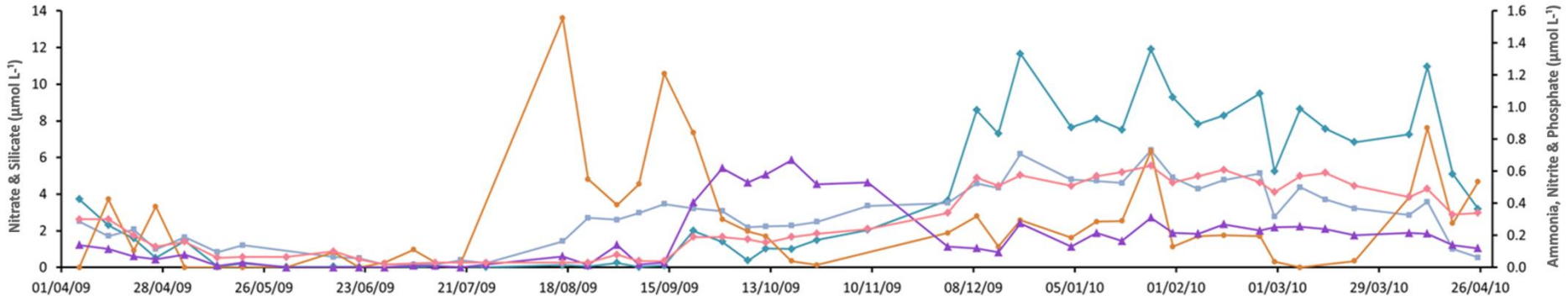

Figure 3.21. The ammonia (—●—), nitrate (—●—), nitrite (—●—), phosphate (—●—), and silicate (—●—) concentrations throughout the sampling period.

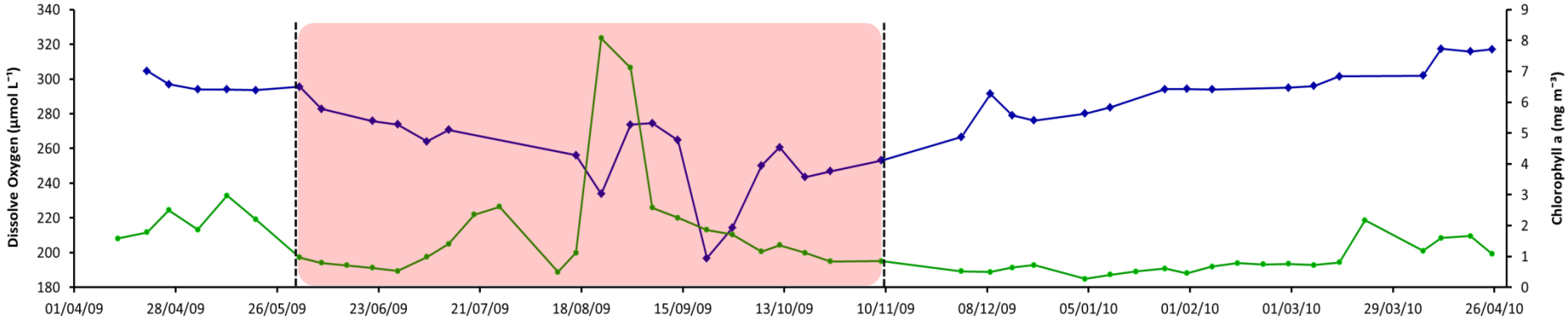

Figure 3.22. The dissolved oxygen (—◆—) and the chlorophyll *a* (—●—) concentrations at the surface waters at station L4. The shaded area between the dashed lines represents the period of SST above 14ºC.

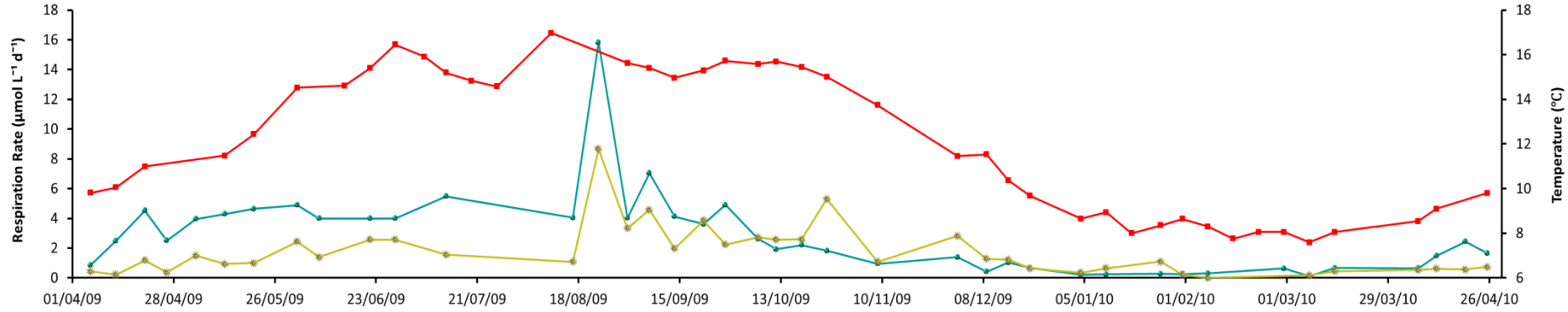

Figure 3.23. The changes in the respiration rates of the total (—●—) and the bacterial (—●—) community, with the SST (—■—), throughout the sampling period at station L4.

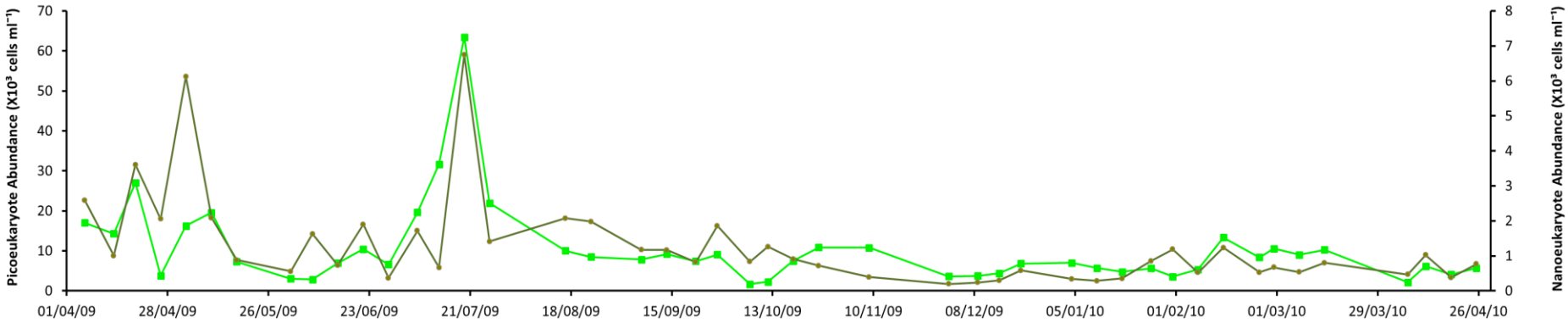

Figure 3.24. The picoeukaryote (-■-) and the nanoeukaryote (-●-) cell counts by flowcytometry during the sampling period.

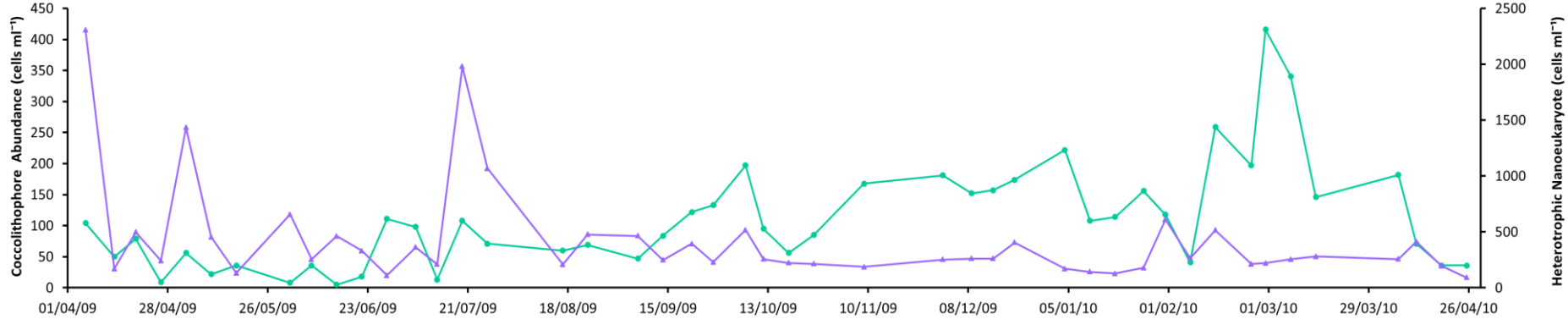

Figure 3.25. The coccolithophore (-●-) and the heterotrophic nanoeukaryote (-▲-) abundances during the sampling period.

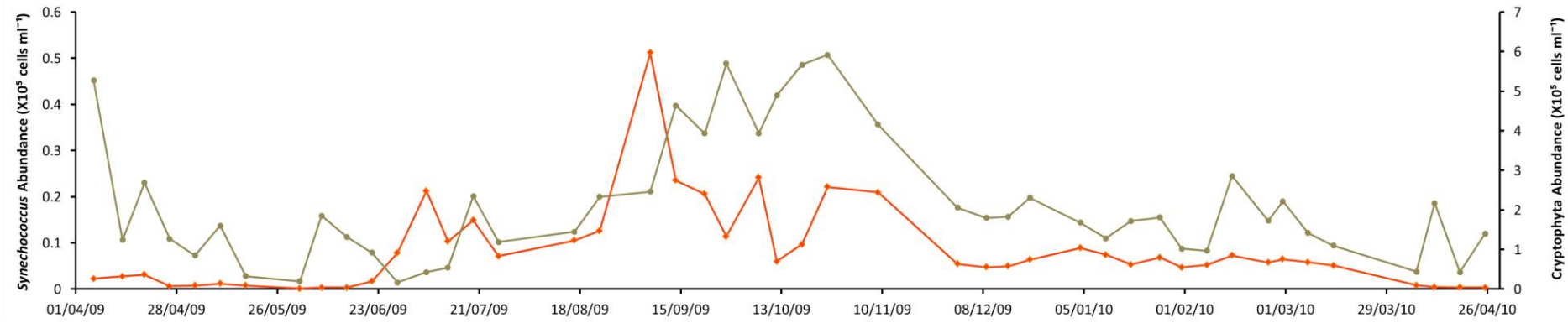

Figure 3.26. The *Synechococcus* spp. (—) and the cryptophyta (—) abundances during the sampling period.

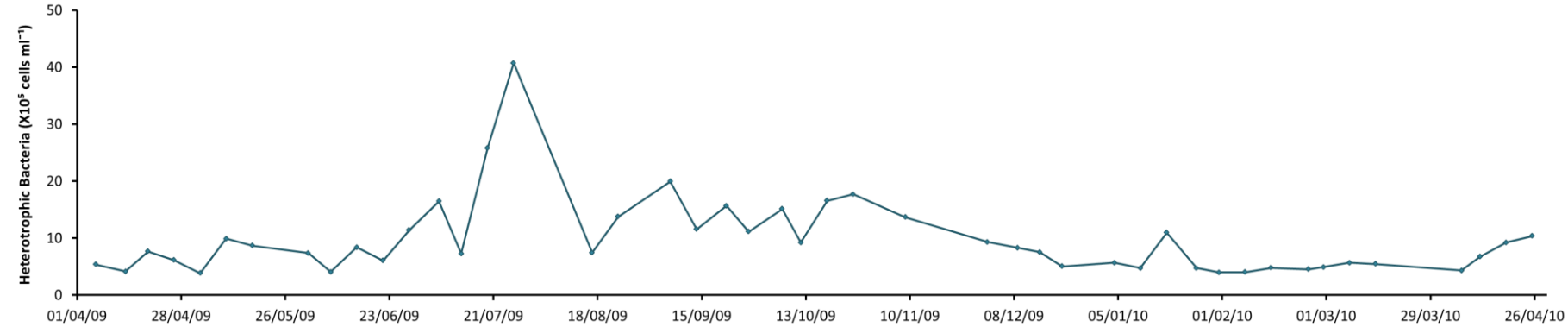

Figure 3.27. The change in the heterotrophic bacterial (—) abundance during the sampling period.

3. 6. RESPIRATION RATES

In this section, where the respiration rates of the microbial community will be discussed, the respiration rates of the unfiltered water samples will be referred to as the total community respiration (CR) and the respiration rates measured in the filtered fraction (<0.8 µm) will be referred to as the bacterial community respiration (or simply as the bacterial respiration, BR).

The changes in the respiration rates of the total and the bacterial community are shown in Figure 3.23, page 93. No respiration data was collected during four week period from mid-July to mid-August 2009, which could have been critical due to the summer phytoplankton bloom. The total community respiration rates were higher in spring and summer months, reaching a maximum of 15.82 µmol L^{-1} d^{-1}, in the late summer phytoplankton bloom, on 24th August 2009. The respiration rates for the total community were below 2.5 (± 0.22) µmol L^{-1} d^{-1} from mid-autumn to the following spring 2009, with a minimum value of 0.12 (± 0.08) µmol L^{-1} d^{-1}, on 8th March 2010. The bacterial respiration varied over the sampling period from 0.17 µmol L^{-1} d^{-1} (± 0.06) to 8.65 µmol L^{-1} d^{-1} (± 0.2), measured on 8th March 2010 and 24th August 2009, respectively.

Changes in in situ temperature directly affect the metabolic activities in microbial communities and can explain ca 30% of the variability in bacterial respiration (Fenchel, 2005, Robinson 2008). During the present study, it was found that 52% of the variation in BR and 31% of CR could be explained by SST alone (Figure 3.28). Both bacterial and community respiration are highly positively correlated with in situ temperature (Table 3.1).

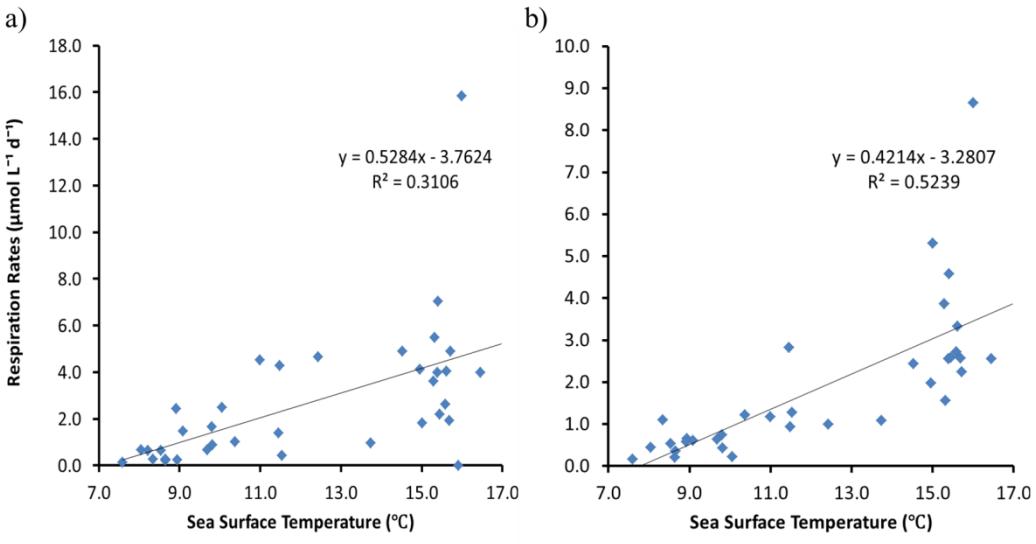

Figure 3.28. The relation between the total community (a) and bacterial respiration (b) with sea surface temperature, during the study period, at station L4.

The strongest correlation was between bacterial respiration and HNA abundance (r = 0.711, p<0.001, Table 3.1). HNA abundance explained 51% of the variability in bacterial respiration (Figure 3.29). LNA abundance on the other hand, could only explain less than 20% of the variability in BR.

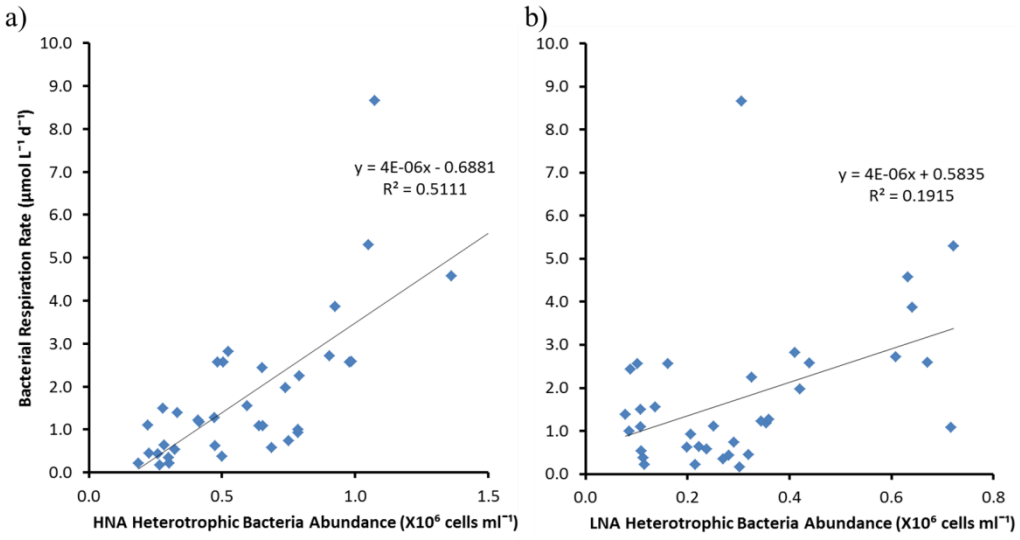

Figure 3.29. The relation between the bacterial respiration with HNA (a) and LNA (b) bacteria, during the study period, at station L4.

Both community and bacterial respiration were positively correlated to chlorophyll *a* (r = 0.752, p<0.001 and r = 0.609, p<0.001, respectively, Table 3.1). They were also both negatively correlated to the changes in nitrite concentrations (CR: r = -0.464, p<0.001 and BR: r = -0.614, p<0.001, Table 3.1).

Table 3.1. The Pearson correlations between the environmental parameters and the respiration rates. The significant correlations are marked ** p<0.001 (red). *p<0.05 (black). The negative correlations are highlighted blue.

		CR	BR	T (°C)	NO_2^-	NO_3^-	NH_3	Si	PO_4^{3-}	Chl α	spp	Peuk	Neuk	Cocco.	Crypto.	HNEuk	HNA	LNA
CR																		
BR	p	**.762****																
	N	37																
T (°C)	p	**.562****	**.676****															
	N	38	37															
NO_2^-	p	-0.157	0.221	0.006														
	N	38	37	46														
NO_3^-	p	**-.614****	**-.441****	**-.814****	0.183													
	N	37	36	45	45													
NH_3	p	0.124	0.22	0.12	-0.026	0.023												
	N	36	35	43	43	42												
Si	p	**-.418****	-0.072	**-.522****	**.393****	**.822****	0.18											
	N	38	37	46	46	45	43											
PO_4^{3-}	p	**-.646****	**-.464****	**-.847****	0.288	**.957****	-0.05	**.817****										
	N	38	37	46	46	45	43	46										
Chl α	p	**.752****	**.609****	**.316***	-0.123	**-.408****	0.15	-0.173	**-.413****									
	N	38	37	47	46	45	43	46	46									
Synec. spp	p	0.245	**.509****	**.462****	0.275	-0.242	**.537****	0.2	-0.214	0.17								
	N	35	35	39	38	37	35	38	38	39								
Peuk	p	0.249	-0.017	0.198	-0.269	-0.298	-0.257	**-.324***	**-.329***	0.197	0.124							
	N	35	35	39	38	37	35	38	38	39	39							
Neuk	p	0.315	0.07	0.168	-0.207	**-.382***	-0.142	**-.346***	**-.400***	**.319***	-0.019	**.703****						
	N	35	35	39	38	37	35	38	38	39	39	39						
Cocco.	p	**-.437****	-0.257	**-.463****	**.328***	**.675****	-0.02	**.651****	**.719****	-0.292	0.081	-0.106	-0.243					
	N	35	35	39	38	37	35	38	38	39	39	39	39					
Crypto.	p	0.169	**.490****	**.564****	**.679****	-0.322	0.092	0.144	-0.212	0.146	**.474****	0.02	0.071	-0.075				
	N	35	35	39	38	37	35	38	38	39	39	39	39	39				
HNEuk	p	0.24	0.122	0.126	-0.173	-0.214	-0.147	-0.238	-0.236	0.249	0.042	**.691****	**.813****	-0.133	-0.014			
	N	35	35	39	38	37	35	38	38	39	39	39	39	39	39			
HNA	p	**.573****	**.711****	**.489****	-0.009	**-.596****	0.273	**-.404***	**-.612****	**.358***	**.338***	**.488****	0.245	-0.243	0.19	**.497****		
	N	35	35	39	38	37	35	38	38	39	39	39	39	39	39	39		
LNA	p	-0.024	**.426***	0.307	**.605****	-0.055	0.219	**.328***	0.069	0.06	**.691****	0.116	-0.087	0.184	**.688****	0.076	**.456****	
	N	35	35	39	38	37	35	38	38	39	39	39	39	39	39	39	39	

In the first half of the sampling period, the bacterial respiration was lower than the total community respiration and showed similar patterns, as expected. However, after mid-September, the bacterial respiration rates were, occasionally, higher than the total community respiration rates. Figure 3.30 shows the respiration rates in the second half of the sampling period, where the bacterial respiration rates exceed the total community respiration. In fact, bacterial respiration was greater than that of the total community on 13 occasions (Figure 3.31).

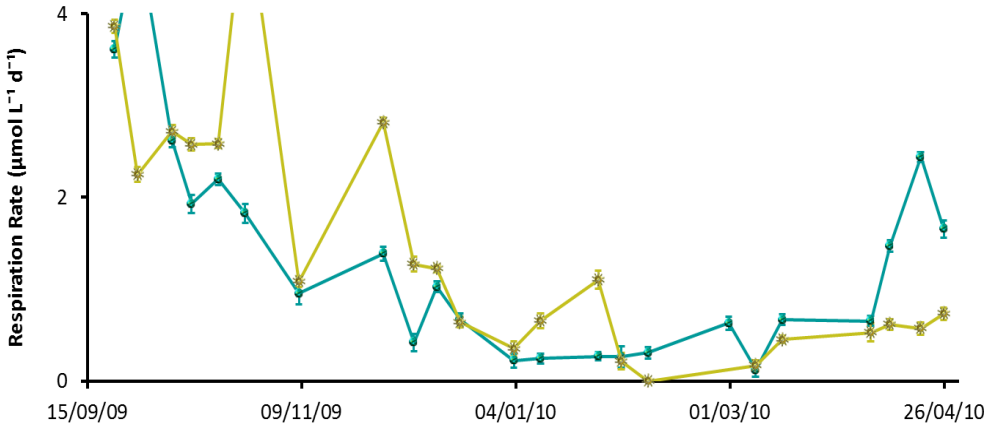

Figure 3.30. The changes in the respiration rates of the total (—●—) and the bacterial (—●—) community, from 22nd September to end of the sampling period. Please note the scale.

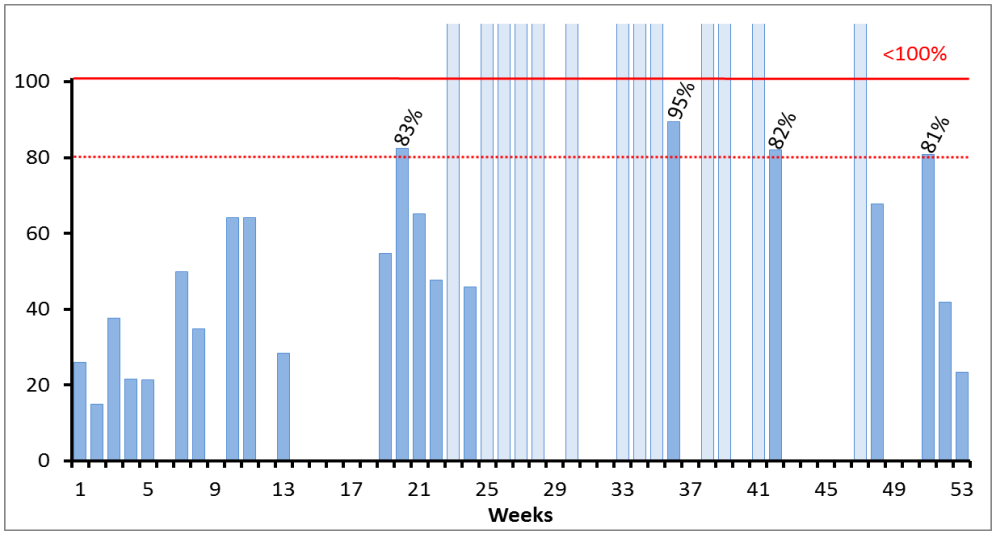

Figure 3.31. The percent bacterial respiration in relation to the community respiration.

Especially under oligotrophic conditions, when measured by Winkler titration method with 24h incubation and pre-filtration, bacterial respiration has been found to exceed community respiration (Del Giorgio et al., 1997; Lemée et al., 2002; González et al., 2003; Alonso-Sáez & Gasol, 2007; Aranguren-Gassis et al., 2012). Aranguren-Gassis et al., (2012), showed that under oligotrophic conditions, where pre-filtration and 24h incubation is required, %BR values may be up to 400%. It is known that the pre-filtration would eliminate grazing on the bacteria and might cause cell lysis (Gasol & Moran, 1999; Robinson, 2008; Teira et al., 2010). Due to that, there is the potential for an artificial increase in the bacterial numbers as well as their activity with the lack of predatory pressure from protists on the specific community within the sample bottle affecting their respiration rates (Blight et al., 1995). Additionally, because the respiration measurements with Winkler method requires long incubation times, any change in the sample chemistry due to cell lysis in the sample bottle could result in increased bacterial metabolic activity, hence the increase in the respiration rates (Aranguren-Gassis et al., 2012). On the other hand, González et al., (2003), found that if the water sample volume is less than 20 L, pre-filtration does not affect either the concentrations of DOC and nitrate or the abundance of bacteria in the samples. Baltar et al., (2012), investigated the effects of long-term incubation on bacterial community composition and their activity. They have found that during the first 24h, the bacterial community composition showed only minor changes. Moreover, oxygen consumption rates were stable for up to 10 to 23-day long incubations. They have concluded that as a result of changes in community structure, bacterial community is capable of maintaining their overall metabolic rate.

3. 7. BACTERIAL DIVERSITY AND THE ACTIVE GROUPS

In this section, the DNA and RNA sequences of the bacterial community will be investigated, in two different sample categories; the unfiltered samples (the total community) and the <0.8 μm fraction (bacterial fraction). The reason for this dual sampling is to be able to see the changes in the dynamics of the entire bacterial community (free living and attached, together) and the free-living bacteria, alone, over an annual cycle. The aim of analysing the sequence data against the environmental parameters and the respiration rates to better understand the driving forces behind the changes in the bacterial diversity and activity.

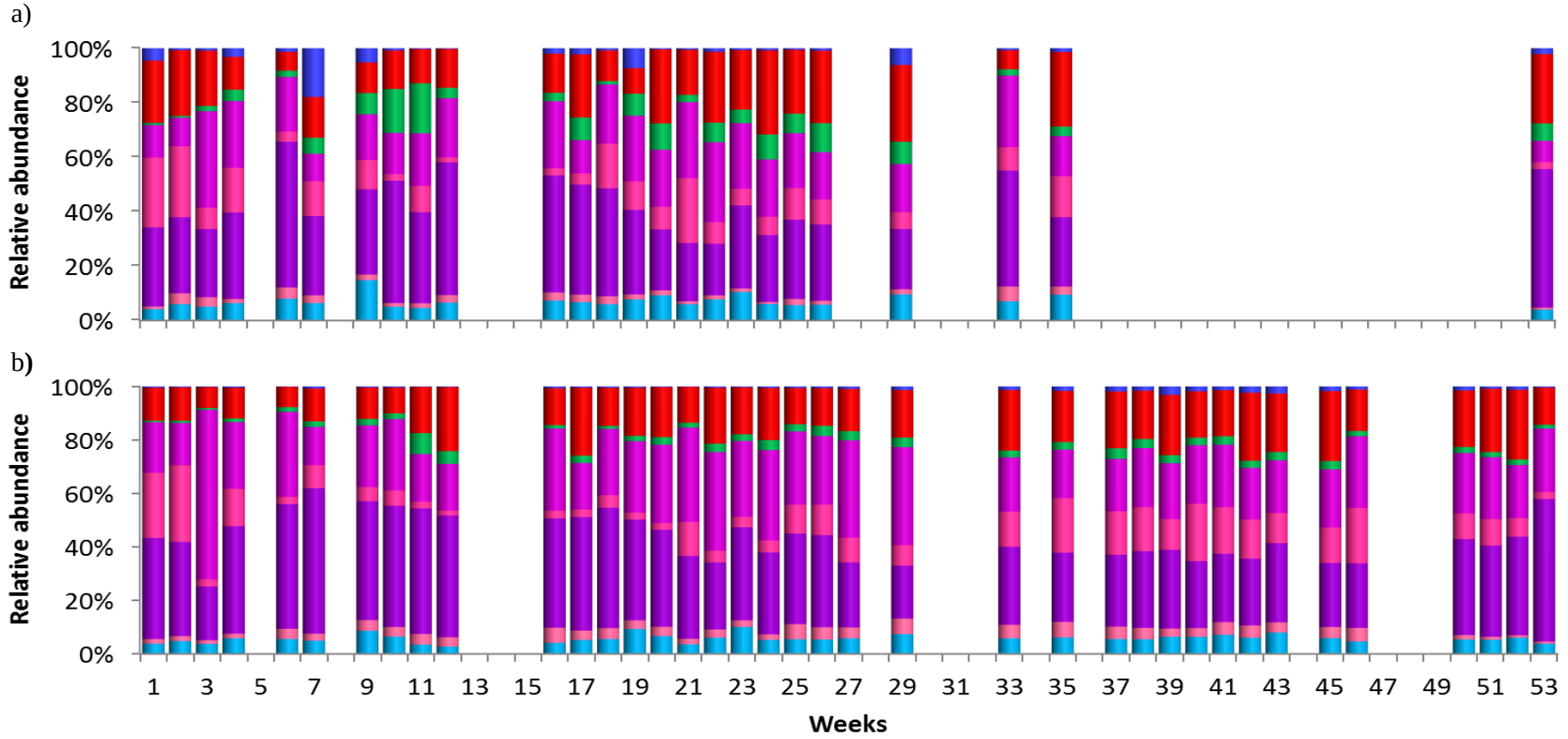

Figure 3.32. The relative abundance of actinobacteria (■), bacteriodetes (■), cyanobacteria (■), proteobacteria (alphaproteobacteria (■), betaproteobacteria (■), gammaproteobacteria (■), and other proteobacterial groups (■) and other bacteria (■) in the unfiltered water, from 6th April 2009 to 26th April 2010, a) 16S rDNA and b) rRNA (cDNA).

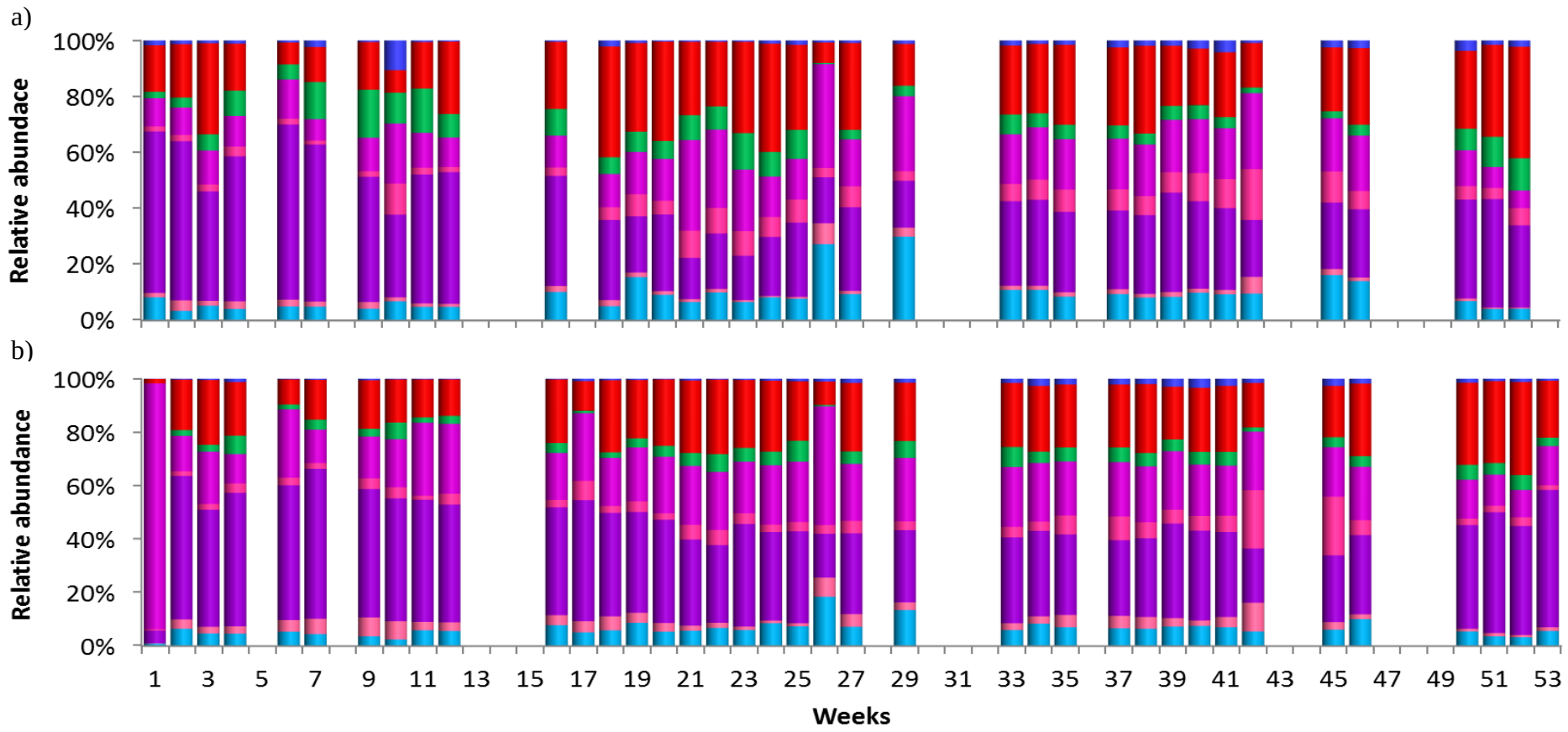

Figure 3.33. The relative abundance of actinobacteria (■), bacteriodetes (■), cyanobacteria (■), proteobacteria (alphaproteobacteria (■), betaproteobacteria (■), gammaproteobacteria (■), and other proteobacterial groups (■) and other bacteria (■) in the >0.8 µm size fraction, from 6th April 2009 to 26th April 2010, a), 16S rDNA and b) rRNA (cDNA).

Figure 3.32 and Figure 3.33 show the changes in the relative abundance of bacterial phyla over the year, from 6th April 2009 to 26th April 2010.

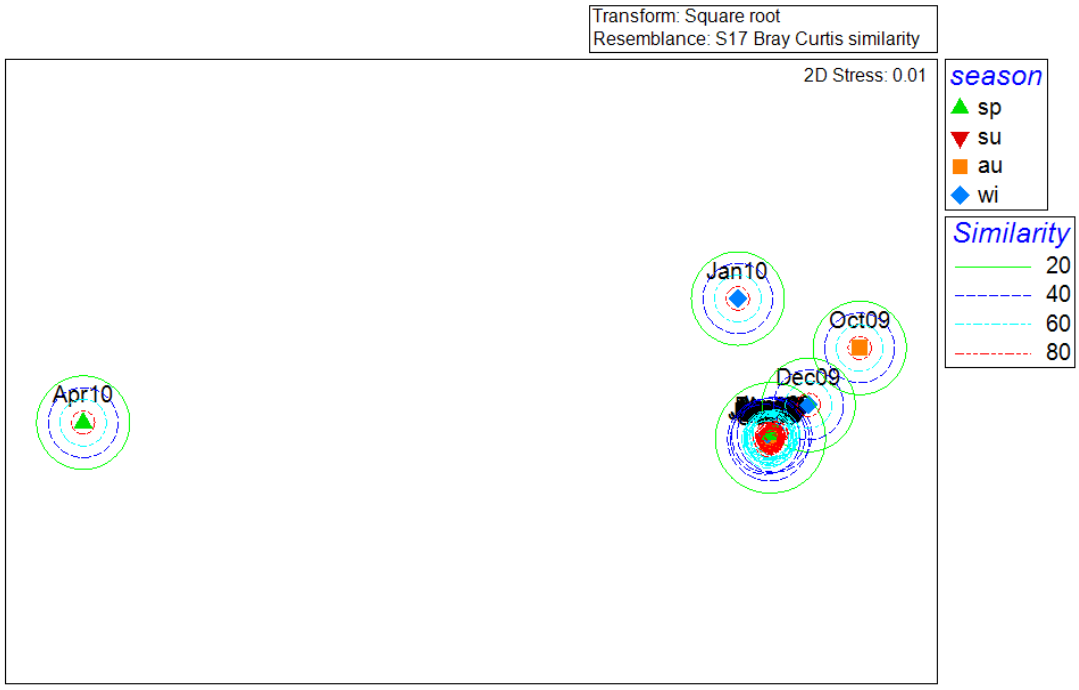

Figure 3.34. MDS plot for the DNA sequences of the unfiltered water. (Bacterial OTUs only).

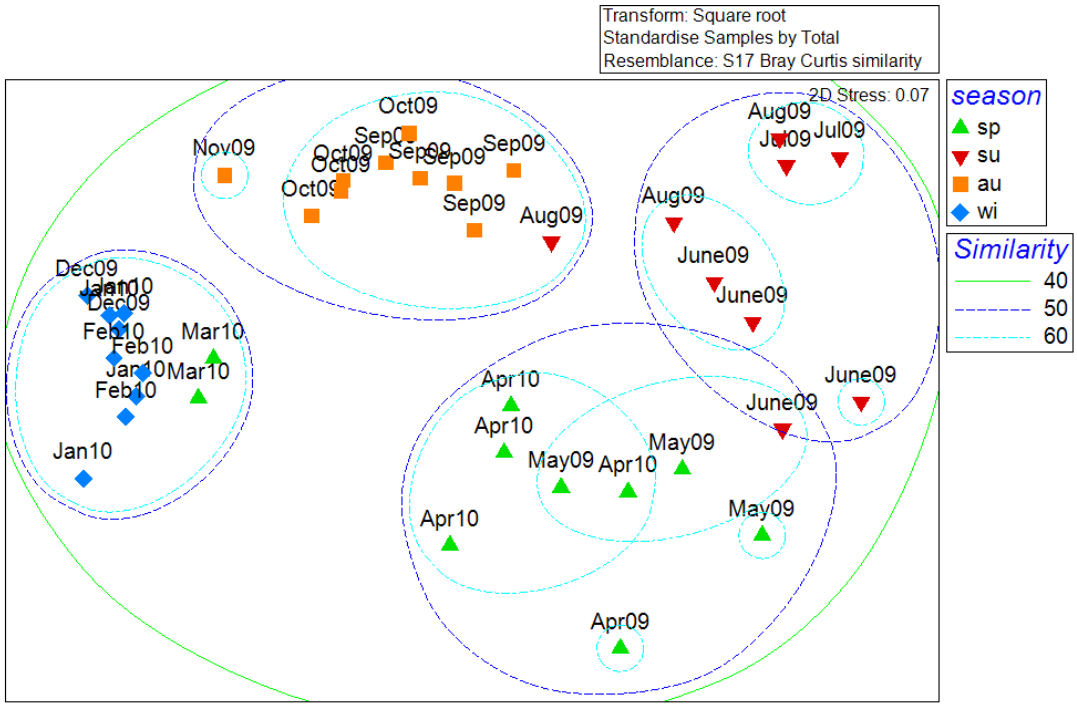

Figure 3.35. MDS plot for the RNA sequences of the unfiltered water. (Bacterial OTUs only).

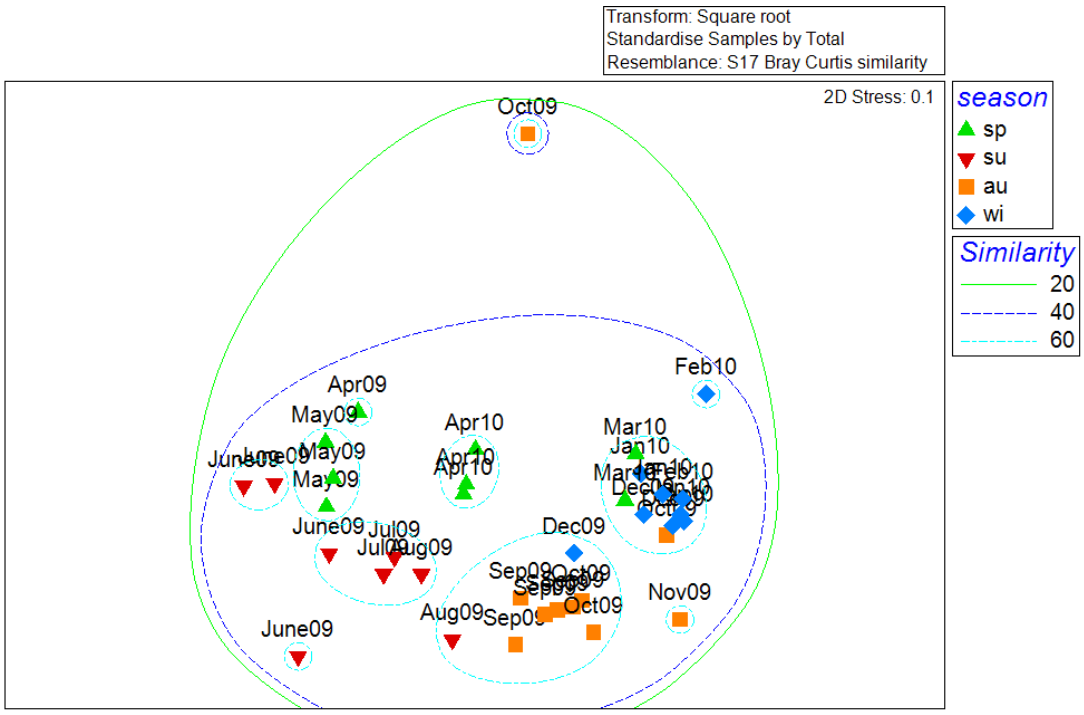

Figure 3.36. MDS plot for the DNA sequences of the <0.8 µm fraction. (Bacterial OTUs only).

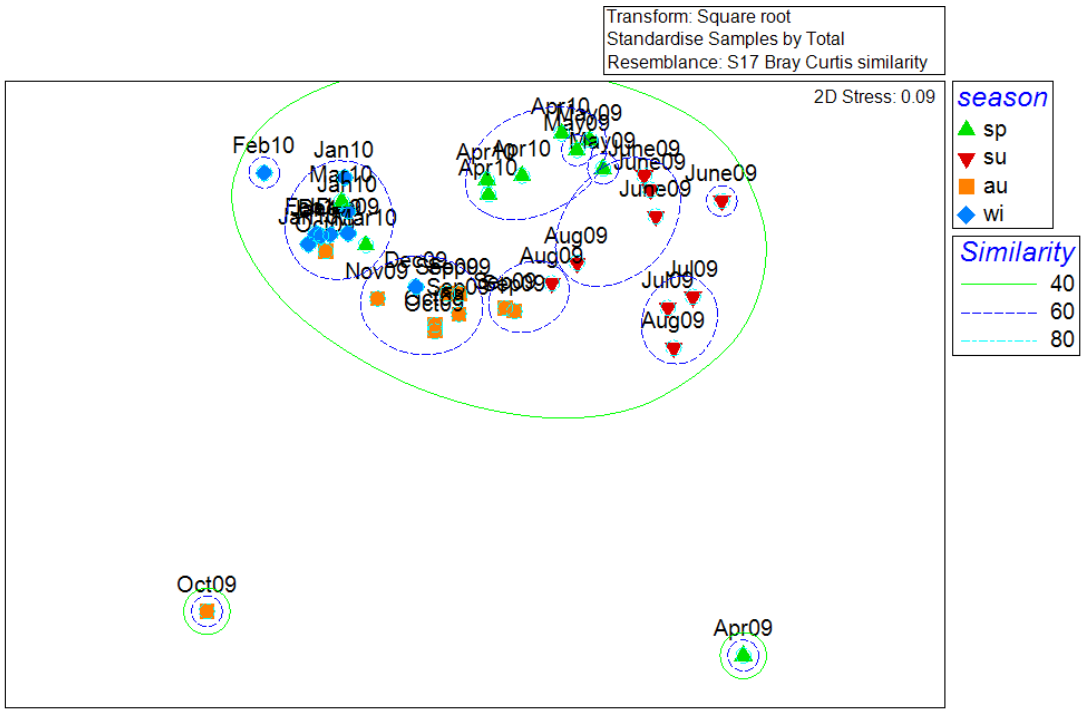

Figure 3.37. MDS plot for the RNA sequences of the <0.8 µm fraction. (Bacterial OTUs only).

4. MICROBIAL COMMUNITY STRUCTURE DURING AN UPWELLING EVENT OFF THE NORTH WEST AFRICAN COAST

The changes in bacterial diversity and respiration in relation to the environmental factors over 8 days following an upwelled filament of water will be discussed in this chapter. The samples were collected during the "Impact of coastal upwellings on the air-sea exchange of climatically important gases" (UK SOLAS ICON) cruise, off the Mauritanian coast, in April and May 2009. The data presented here are collected from the 2nd filament that was traced and sampled during the cruise.

4. 1. MAURITANIAN UPWELLING REGION

The Mauritanian upwelling system is one of the most productive eco systems in the world's oceans and is the driving force to the commercial fisheries in the region, yet it remains largely understudied (Rees et al., 2011; Loucaides et al., 2012). The upwelling is triggered by the strong winds alongshore, moving the surface water towards off shore, forcing deeper nutrient rich water from deep to move to the surface near the coast of Cap Blanc, Mauritania (Loucaides et al., 2012). Nutrient rich water triggers phytoplankton blooms, which in turn increases the production throughout the food web (Arístegui et al., 2003).

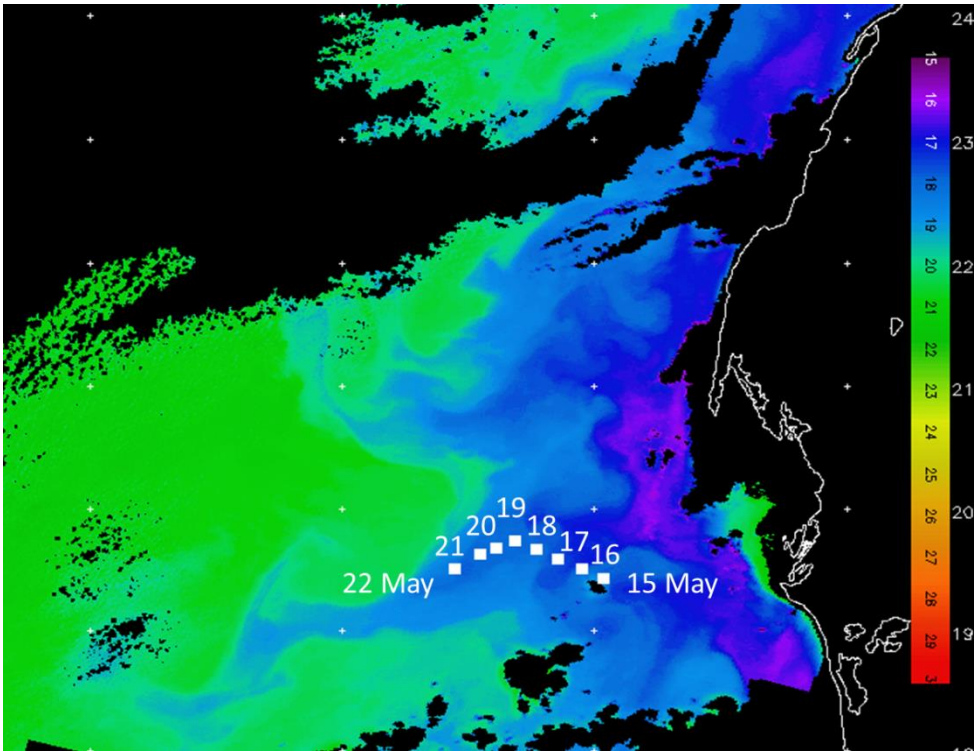

Figure 4.1. The study site and station locations, with dates of sampling marked on the map, overlaid on the sea surface temperature data taken on 20th May 2009. (Image courtesy of NEODAAS).

The study area, as well as being an upwelling region, is also the meeting point of two major water masses: South Atlantic Central Water (SACW) and North Atlantic Central Water (NACW). SACW is generally rich in nutrients and warmer relative to the nutrient-poor NACW (Minas et al., 1982). NACW, on the other hand, generally has higher dissolved oxygen content (Minas et al., 1982).

Rees et al., (2011), showed that for the first 3 days of the sampling (15th-17th May 2009, from 18°W to 18.4°W), SACW was dominant in the upper 500 m (Figure 4.2). On the last 3 days of the sampling, NACW was dominant in the upper 100 m (50–80%) (Rees et al., 2011).

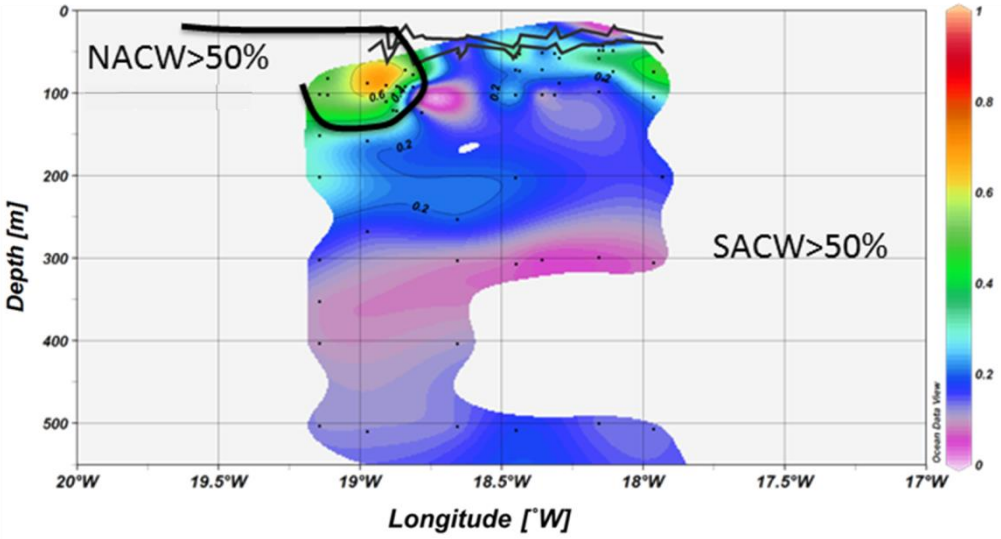

Figure 4.2. The wire-walker data showing the relative proportions of the two water masses. Warm colours indicate higher percentage of the NACW (max being 1 (red) is 100% NACW) and colder colours indicate higher percentage of the SACW. The thick black line indicates NACW front. The thin black line above is the euphotic layer, and the thin black line below is the mixing layer. (Image courtesy of Ricardo Torres).

During the ICON cruise, satellite data were used to identify the high production areas in the region as an indicator of upwelling and sulphur hexafluoride (SF_6) was used to label the newly upwelled water to be able to follow the upwelling plume. The samples analysed in this chapter were collected from the 2nd Lagrangian study of the ICON cruise. Figure 2.21 shows the satellite image taken on 20th May 2009, where the purple and blue colours represent low SST. From the colours on the map, the upwelling filament can clearly be seen. Figure also shows the geographical positions of each sampling station with the dates of sampling overlaid on the map, following the upwelled water. The distance travelled each day between the stations varied between 14.3 and 25.4 km during the 8 days of the Lagrangian study. The 2nd filament was estimated to be a 7-day old upwelling by 15th May, at the beginning of the sampling (Rees et al., 2011).

4. 2. SEA SURFACE TEMPERATURE

The sea surface temperature data were collected both with instruments on board the research vessel and via satellite imagery. Temperature profiles of the water column were measured by CTD profiler, and the data collected is shown in Figure 4.3. The samples analysed in this study are collected from ca 8 m depth, which showed only slight increase from 18.015 °C on 15th May to 18.748°C on 22nd May 2009.

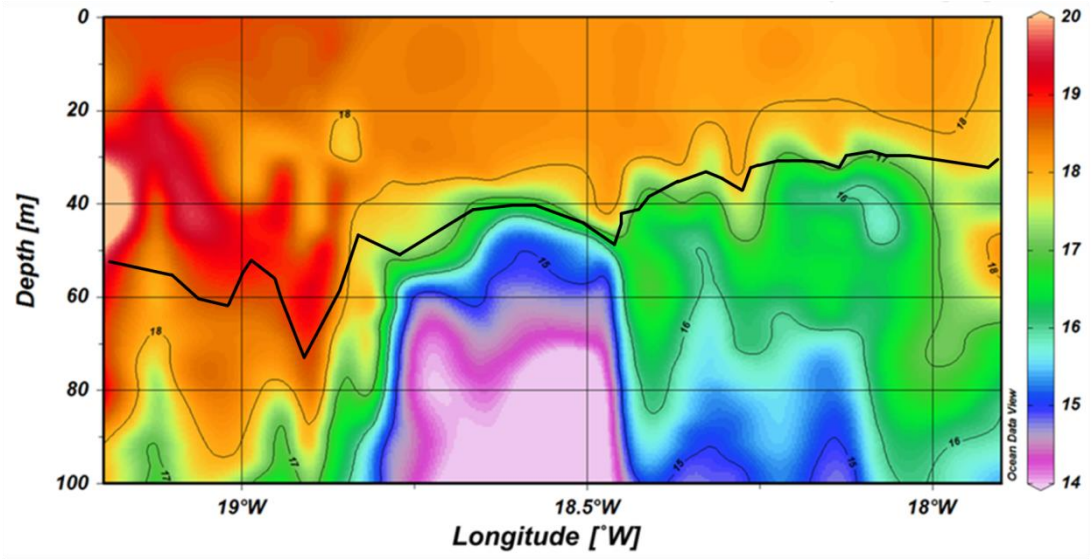

Figure 4.3. Vertical section of temperature (°C) from 15th May to 22nd May 2009. Black line represents the mixed layer depth. Please note the upwelled plume travelled from east (coast) to west (off shore); the direction of the transit is from east to west.

Although temperature data showed fluctuations and stratification in the water column, sea surface temperatures varied between ca 18°C and ca 19°C throughout the filament (Figure 4.3). Towards the end of the sampling, particularly to the west of 18.8°W, from 20th to 22nd May 2009, NAWC dominated the surface waters. The mixed layer depth increased from ca 30 m, at the beginning of the transect sampling,

to ca 50 – 70 m in the last two days of the sampling. On 18th May, below the mixed layer depth, a body of cold water was observed, reaching to 40 m up in the water column. The temperature difference was ca 4°C within 10 m of the mixed layer depth.

4. 3. INORGANIC NUTRIENTS

Figure 4.4 shows the variation in (a) combined nitrite-nitrate and (b) phosphate concentrations in the upper 500 m of the water column, though the Lagrangian transect.

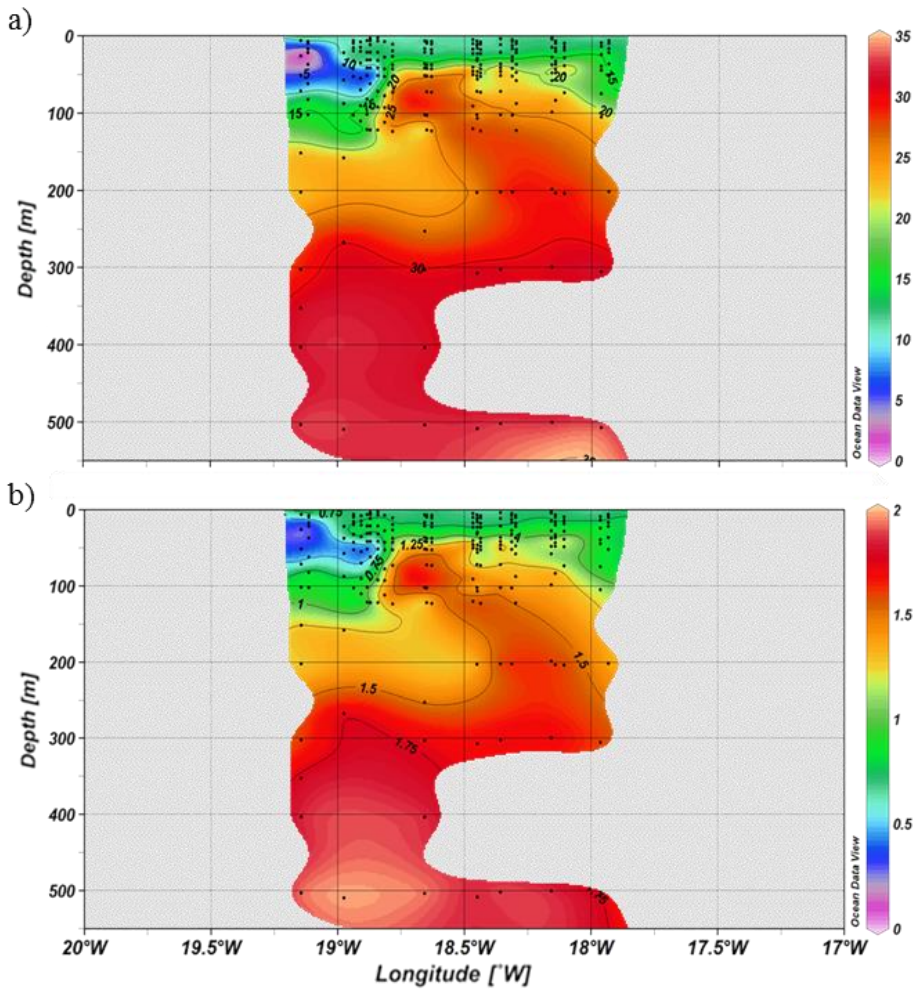

Figure 4.4. The distribution of the concentrations of (a) nitrate + nitrite and (b) phosphate in the upper 500 m of the transect. The unit of measurement is µmol L^{-1}. (Image courtesy of Ricardo Torres).

Below 200 m, combined nitrite and nitrate concentrations were ca 30 µmol L^{-1} on average, throughout the transect. The surface waters, however, showed a gradually decreasing trend, with an average of 11.34 µmol L^{-1} at the sampling depth (Figure 4.5 (a)). Phosphate concentrations also showed a similar pattern, averaging 0.71 µmol L^{-1} (Figure 4.5 (b)). Concentrations of nitrite and nitrate combined, as well as phosphate all decreased to their minimum measured values on the last sampling day, [NO_2+NO_3] = 7.86 µmol L^{-1} and [PO_4] = 0.57 µmol L^{-1}.

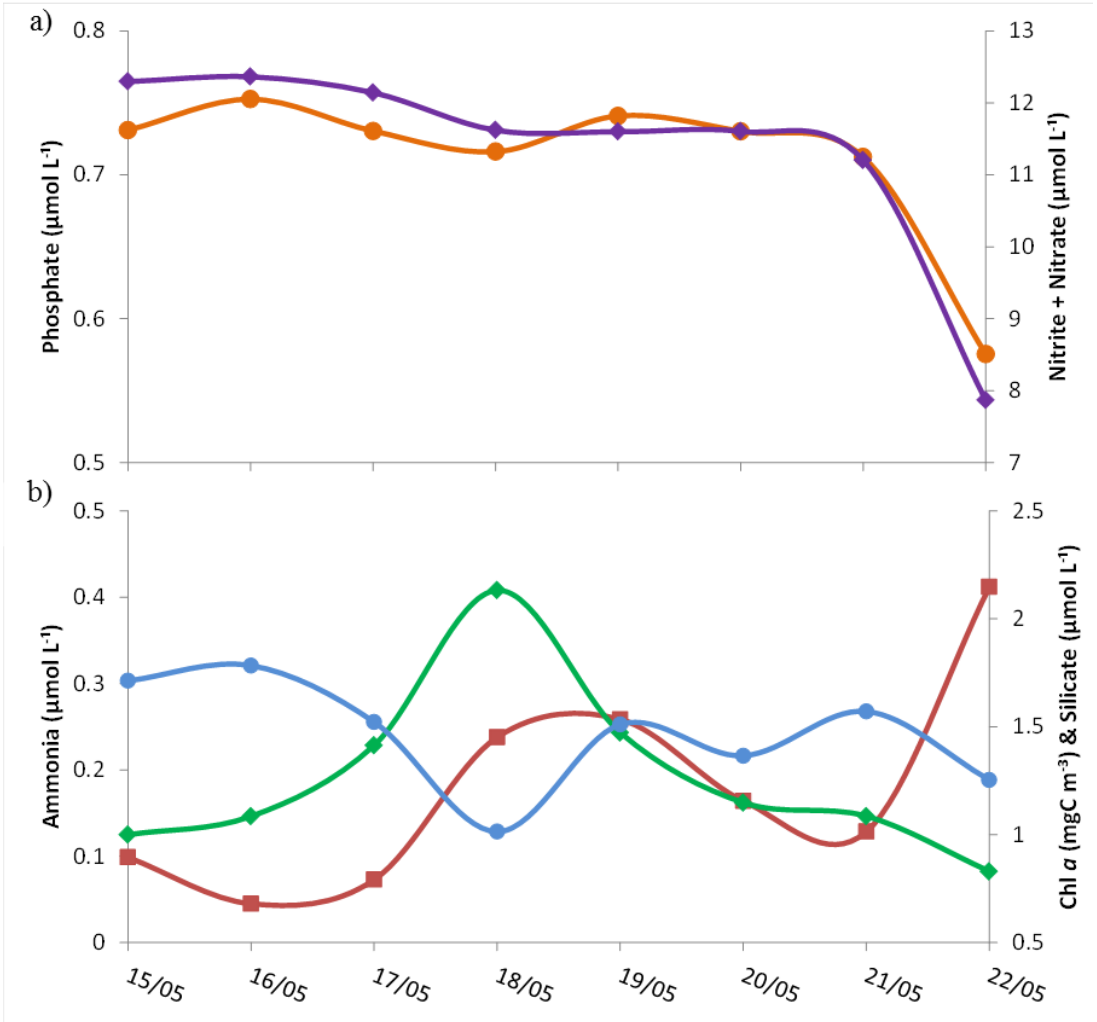

Figure 4.5. Inorganic phosphate (), nitrite+nitrate (), ammonia (), silicate () and chl *a* () concentrations at the sampling depth (55% irradiance, ca 8 m).

The silicate concentrations at the sampling depth were between 1.71 and 1.78 µmol L^{-1} on the first two days, decreasing to a minimum of 1.01 µmol L^{-1} on 18th May (Figure 4.5 (b)). This decrease in silicate concentration was observed on the same date when the chlorophyll *a* concentration reached its highest value of 2.13 mg m^{-3}. Fluorescence data showed that the chlorophyll *a* concentration was high through the mixed layer, at around 18.5°W, on 18th May 2009 (Figure 4.6). NH_4 concentration followed a reverse trend in comparison to other nutrients and although concentrations decreased following the chlorophyll bloom, they showed an increasing trend over all (Figure 4.5 (b)). A concentration of 0.09µmol L^{-1} on the first day and measured as 0.41 µmol L^{-1} at the end of the Lagrangian sampling.

4. 4. CHLOROPHYLL *a*

Figure 4.6 shows the distribution of the chlorophyll *a* in the upper 100 m, along the filament, and Figure 4.5 shows its concentration at the sampling depth.

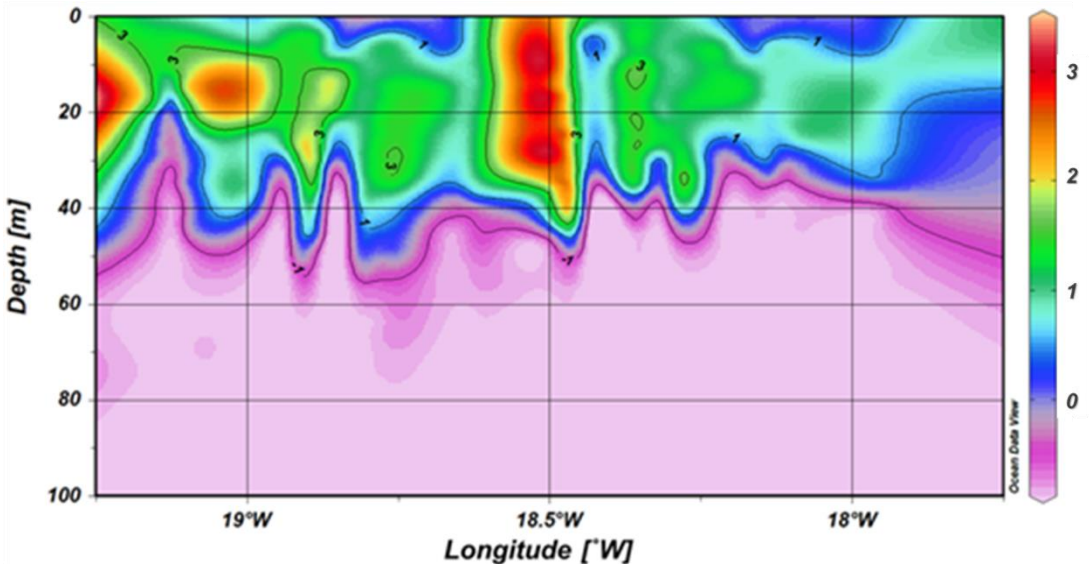

Figure 4.6. Vertical profile of chlorophyll *a* (mg m^{-3}) from 15th to 22nd May 2009. Note the upwelled plume travelled from east (coast) to west (off shore); the direction of the transit is from east to west.

The highest chlorophyll concentration at the sampling depth was 3.09 mg m^{-3}, on 22nd May. The average chlorophyll *a* value on the first 3 days was ca 1.7 mg m^{-3}, whereas on the last 3 days it was ca 2.7 mg m^{-3}. The two samples in the middle of the transect showed a sharp increase in chlorophyll *a* concentration (3.06 mg m^{-3} on the 18th May), followed by a sudden decrease to 1.74 mg m^{-3} on the 19th May. This peak in the chlorophyll *a* concentration was observed on the same day and location as the cold water plume, moved up the water column, only a day before the upwelling filament met NACW front.

Figure 4.7 shows the result of multi-dimensional scale (MDS) analysis of temperature, nutrients and chlorophyll *a*, applied to data gathered from samples collected at the depth of 55% light intensity. Normalised Euclidean distance was used for the calculation of the resemblance matrix.

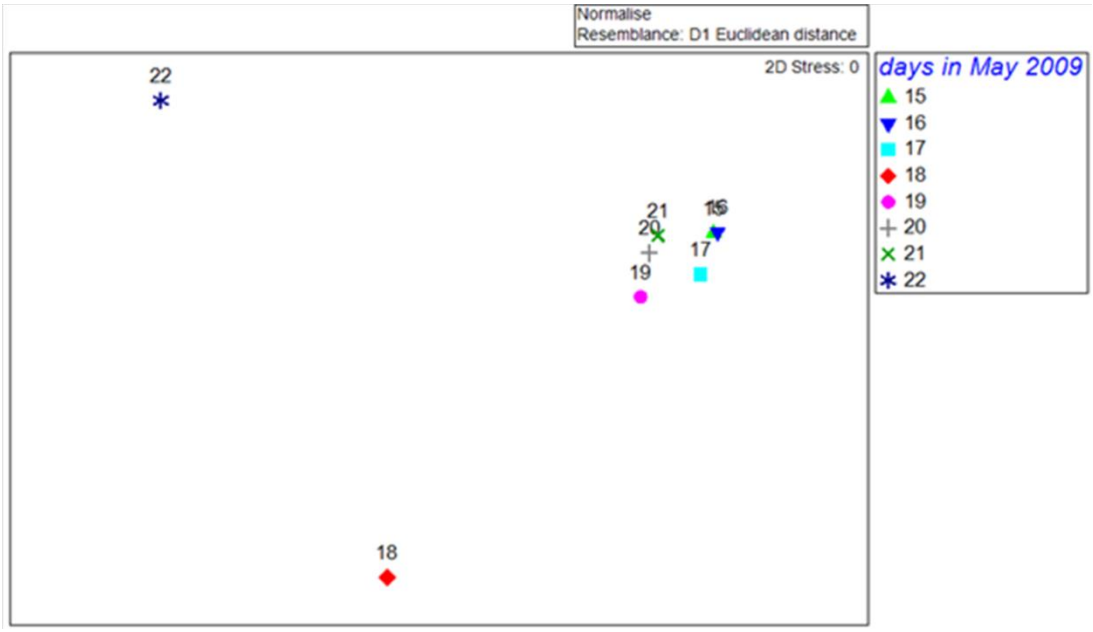

Figure 4.7. MDS plot for the temperature, inorganic nutrients and chlorophyll *a*.

The analysis shows a significant difference between the samples collected on 18th and 22nd May and rest of the samples. The distinct feature observed on 18th May was the increased levels of chlorophyll *a* and decrease in the silicate concentrations (Figure 4.5 and Figure 4.6). On the 22nd May, the data showed decreased levels of temperature, chlorophyll *a*, and inorganic nutrients, except ammonia, which maximum value of 0.41 µmol L^{-1}.

4. 5. EUKARYOTIC AND BACTERIAL ABUNDANCE

Analytical flow cytometry (AFC) was used to measure the abundance of picoeukaryotes, nanoeukaryotes, *Synechococcus*, *Prochlorococcus*, and heterotrophic bacteria. Water samples were collect at pre-dawn from various depths, between 15th

and 22nd May 2009. Figure 4.8 shows the changes in abundance of (a) picoeukaryotes and (b) nanoeukaryotes, in the upper 100 – 150 m of the water column.

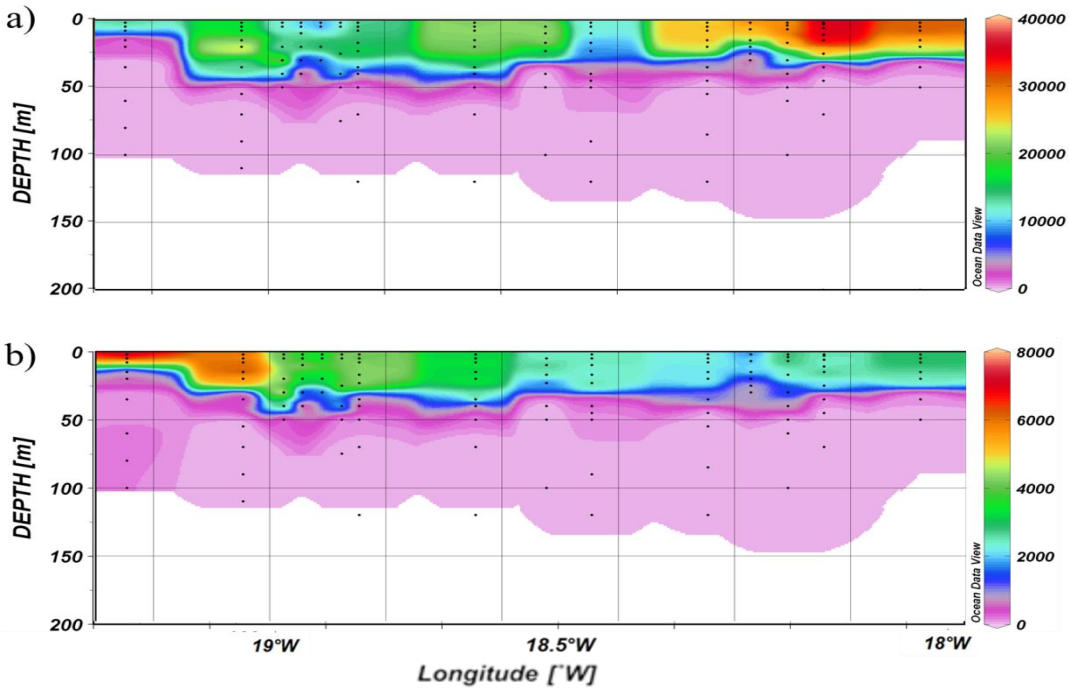

Figure 4.8. Abundance of (a) picoeukaryotes and (b) nanoeukaryotes (cells ml^{-1}) along the transect.

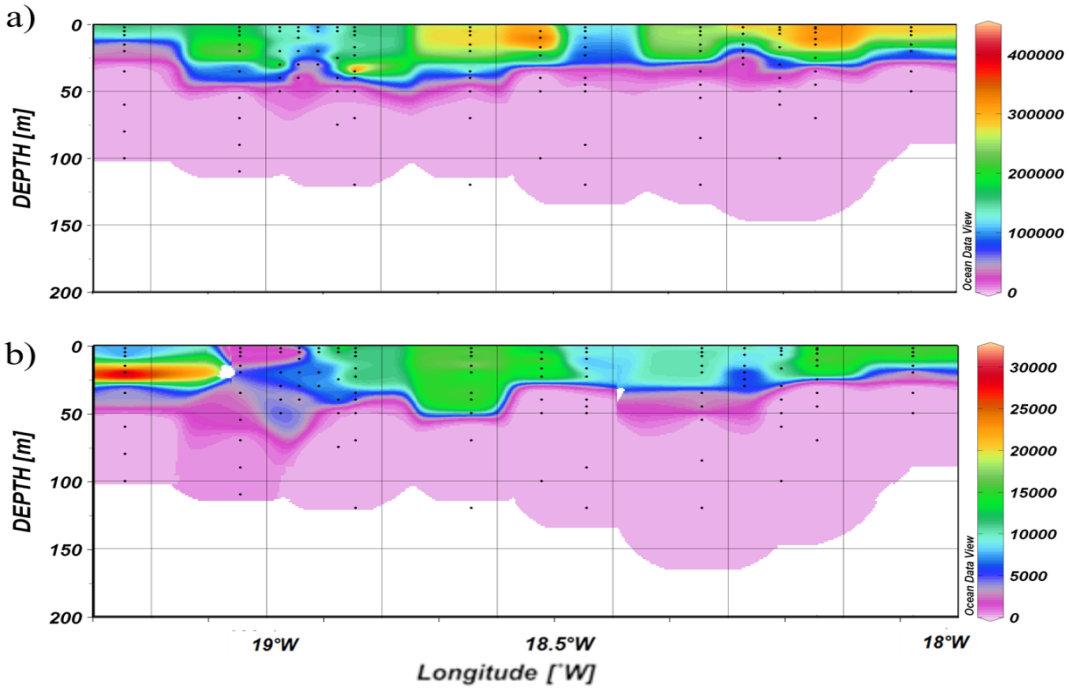

Figure 4.9. Abundance of (a) *Synechococcus* and (b) *Prochlorococcus* (cells ml^{-1}) along the transect.

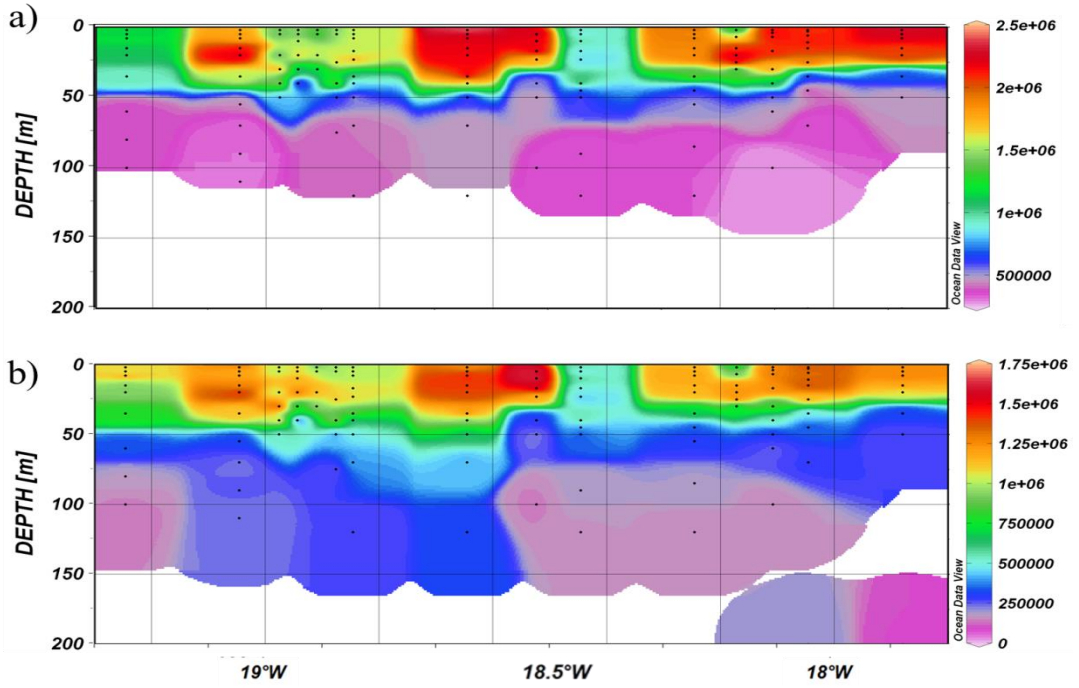

Figure 4.10. Abundance of (a) HNA and (b) LNA bacteria (cells ml^{-1}) along the transect.

The heterotrophic bacterial abundance varied 2.5-fold in the surface water from 1.49 x 10^6 on 18th May to 3.61 x 10^6 on 19th May 2009 (Figure 4.11).

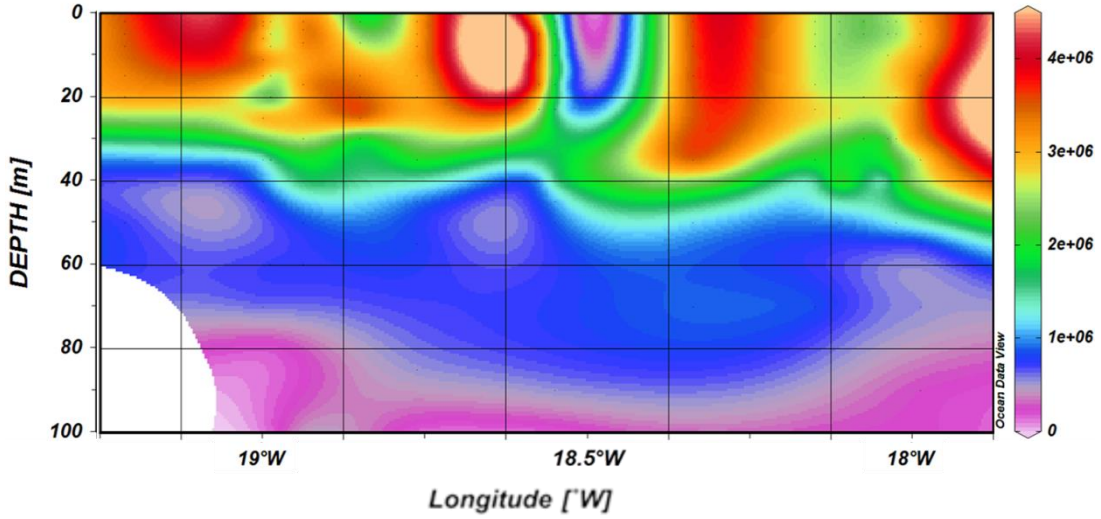

Figure 4.11. Heterotrophic bacterial abundance (cells ml^{-1}).

4. 6. Community Respiration and Production

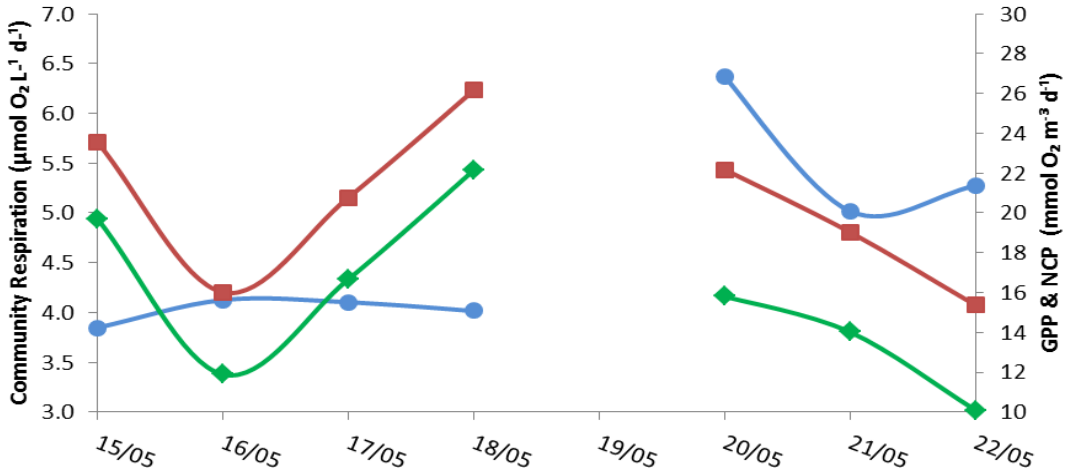

Figure 4.12. Community respiration (—●—), GPP (—■—) and NCP (—◆—) at the 55% light intensity.

4. 7. Bacterial Production

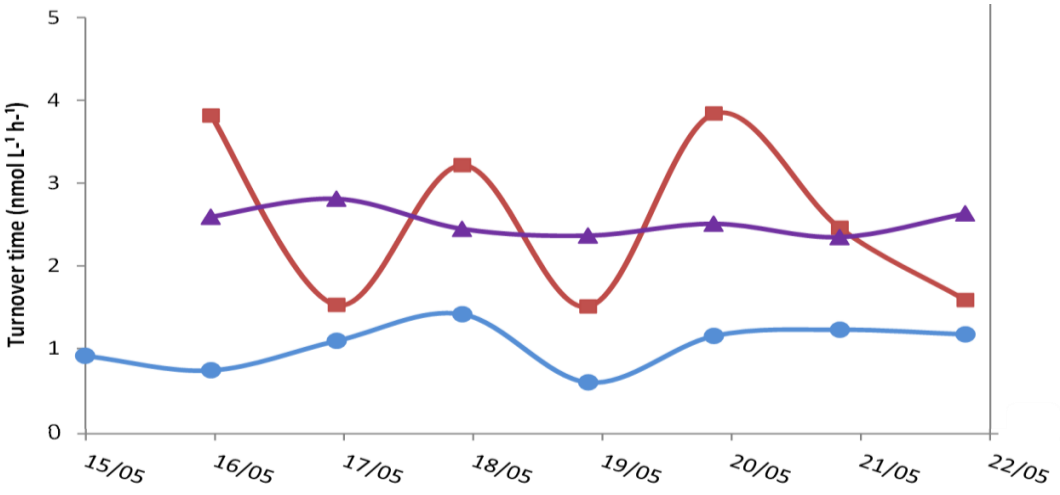

Figure 4.13. Bacterial amino acid turnover times (leucine (blue), methionine (red) and tyrosine (purple)). Samples collected from 55% light intensity, at pre-dawn.

Leucine uptake rates are lower than the methionine and tyrosine uptake rates throughout the transect (Figure 4.13).

4. 8. Bacterial Diversity and the Active Groups

Figure 4.14 shows the relative abundance of the bacterial phyla throughout the study. The bacterial community structure was always dominated by Proteobacteria, with abundances reaching 90% of the microbial community towards the end of the transect. The relative abundance of Bacteroidetes was less than 10% during sampling, except on 16th May, when it was ca 30% of OTUs. Cyanobacterial groups made up 8 to 36% of all OTUs from 15th to 18th May. Their relative abundance decreased to ca 1% of the total community structure on 19th May and remained between 0.5 and 2% for the rest of the sampling.

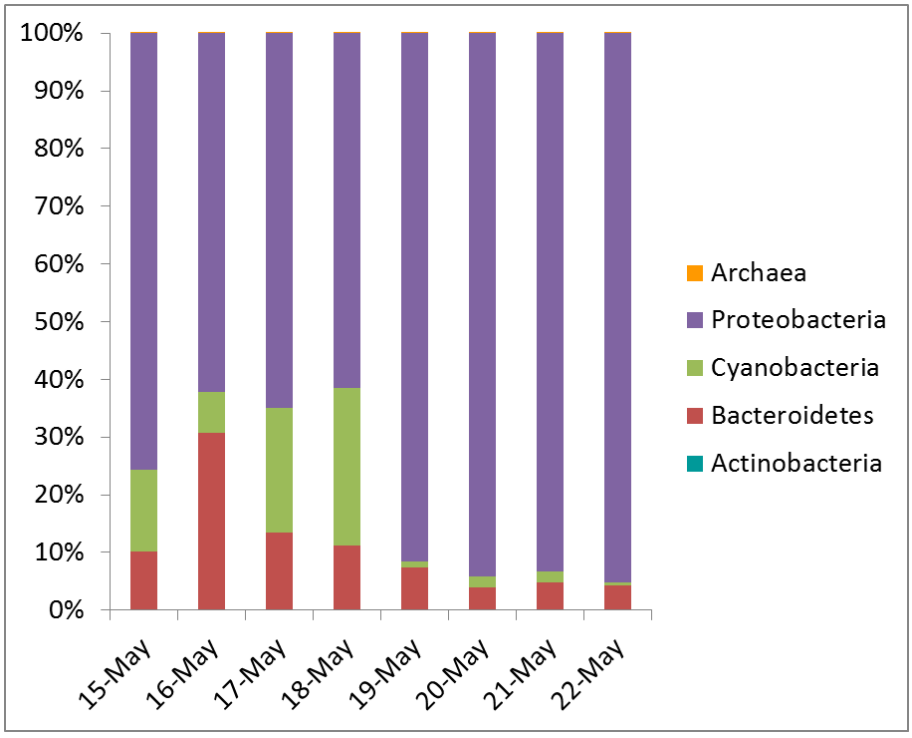

Figure 4.14. Relative Abundance of Archaea and major bacterial groups collected between 15th and 22nd May 2009.

Most of the Proteobacteria sequences belong to the Gammaproteobacteria, with the exception on the 16th May where Alphoproteobacterial sequences made up more than 75% of the OTUs (Figure 4.15).

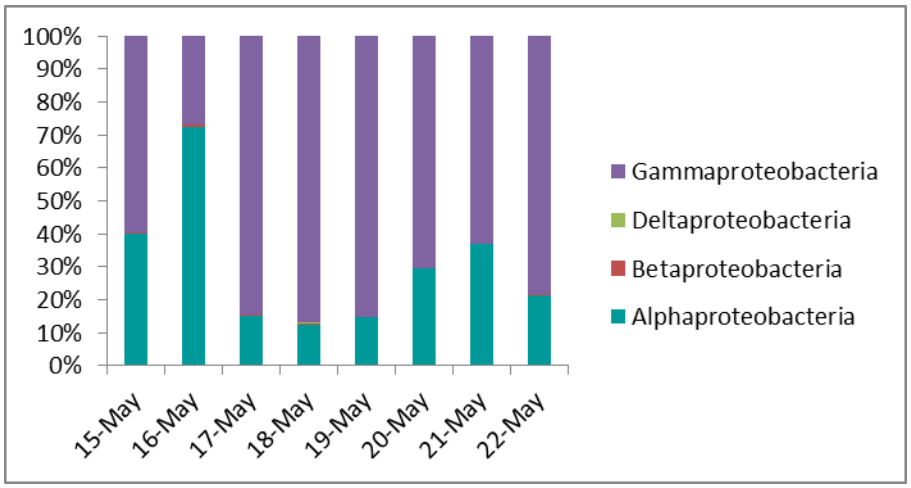

Figure 4.15 Relative abundance of subphyla within the Proteobacteria, collected between 15th and 22nd May 2009.

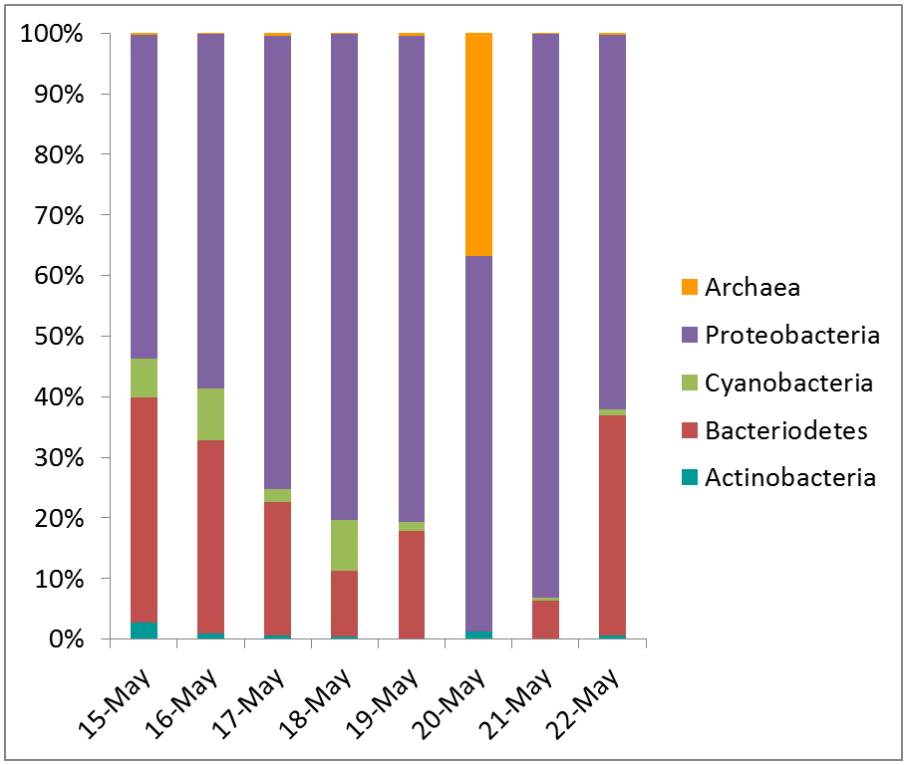

Figure 4.16 Relative abundance of Archaea and major bacterial OTUs, obtained from cDNA, collected between 15th and 22nd May 2009.

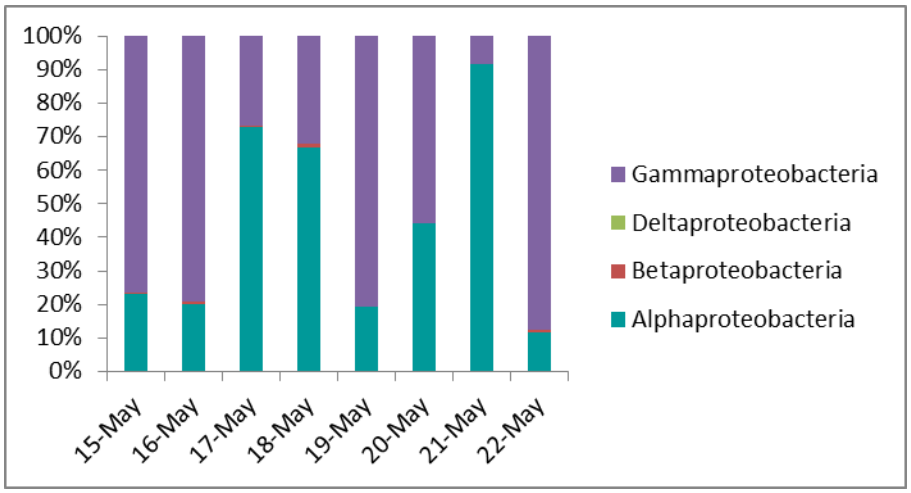

Figure 4.17 Relative abundance of subphyla within the Proteobacteria OTUs, obtained from cDNA, collected between 15th and 22nd May 2009.

5. CONCLUSION AND FUTURE PERSPECTIVES

The study aimed to gain a perspective on the factors affecting the bacterial community composition in the marine environment. The focus was to understand the diversity and the activity of the heterotrophic bacteria in the surface ocean in relation to changing environmental conditions. To be able achieve this, two separate sampling strategies were applied; an annual time series study at a coastal station (station L4, WECO) and a Lagrangian study following an upwelling plume on its track off shore (2nd filament, ICON cruise).

L4 is a well characterised coastal site, located in English Channel which has been monitored as a part of WECO for almost three decades. Since January 2003, the microbial community has been investigated at station L4. Until 2009, the samples were collected monthly, weather permitting. During the time series study, weekly samples were collected from 6th April 2009 to 26th April 2010, from station L4. Despite our best efforts, there are gaps in the data set, mostly due to unfavourable weather conditions. Nevertheless, the data set presents a high resolution molecular and environmental time-series study.

APPENDIX A: MANUFACTURERS' PROTOCOLS

RNA Purification:

RNA was purified using the TURBO DNA-free™ kit (Ambion®, Life Technologies) followed by RNAeasy® plus mini kit (Qiagen).

TURBO DNA-free™ kit contains TURBO DNase, 10X TURBO DNase buffer, DNase inactivation reagent and nuclease-free water.To 100 µl of the nucleic acid extract, 10 µl of 10X TURBO DNase buffer and 1 µl of TURBO DNase was added and mixed. It was then incubated at 37°C for 30 minutes. 10 µl of inactivation reagent was added to the mixture, followed by 5 minutes incubation at room temperature, with frequent mixing. It was centrifuged at 10000 x g (10400 rpm) for 3 minutes. The supernatant containing RNA was transferred into a clean 1.5 ml tube. The sample volume was adjusted to 100 µl by adding RNase-free water and it was stored at -80°C until further analysis.

After the first step of cleaning with TURBO DNA-free, a second purifying step with the RNeasy® plus mini kit was applied to the samples. This kit contains spin columns, gDNA eliminator spin columns, collection tubes, RNase-free water and buffers (RLT and RPE). To 100 µl of TURBO DNA-free™ cleaned nucleic acid extract, 350 µl of the buffer RLT and 250 µl of 100% ethanol were added and mixed gently with pipette. The sample was then transferred into the spin column, in a 2 ml collection tube. It was centrifuged for 15 seconds at 10000 rpm. The flow through was discarded. The spin column was placed in a new 2 ml collection tube and 500 µl of the buffer RPE was added to the spin column. It was again centrifuged for 15 seconds at 10000 rpm and

the flow through was discarded. To the same spin column with the collection tube, 500 µl of 80% ethanol was added. It was centrifuged for 2 minutes at 10000 rpm. The collection tube with the flow through was discarded. The spin column was placed in a clean 2 ml collection tube, centrifuged for 5 minutes at the maximum speed. The collection tube with the flow through was discarded. The spin column was placed in a 1.5 ml collection tube. 14 µl of RNase-free water was added directly to the centre of the spin column. It was centrifuged for 1 minute at maximum speed. The eluted total RNA was kept at -80°C until further analysis.

RNA Quality Assessment:

Assessment is carried out by using the Agilent 2100 Bioanalyser with the Bioanalyser RNA 6000 Nano kit (Agilent Technologies). The system contains the bioanalyser, PC software, a chip priming station, a vortex mixer and requires a 16-pin electrode cartridge (Nano chip) to load the samples. The Bioanalyser RNA 6000 Nano kit was used to run the samples on the system. The kit contains the Nano chips, Nano dye, Nano gel matrix, Nano marker and a ladder. To load the Nano chip, first the gel dye mixture was prepared by mixing 1 µl of the Nano dye with 65 µl of the gel matrix and centrifuging at 13000 x g for 10 minutes at room temperature. The Nano chip was then placed to the chip priming station. 9 µl of the mixture was pipetted into the gel-dye well on the chip, holding the plunger tight, waited 30 seconds exactly and the plunger was released. 5 µl of the Nano marker was added to the ladder and each sample well on the chip. 1 µl of the ladder was pipetted to the ladder well. The sample was aliquoted and denatured for 2 minutes at 70°C, and pipetted into the sample wells (1 µl of sample per well). The chip then was placed into the bioanalyser.

BIBLIOGRAPHY

AGOGUÉ, H., LAMY, D., NEAL, P.R., SOGIN, M.L. & HERNDL, G.J. (2011) Water mass-specificity of bacterial communities in the North Atlantic revealed by massively parallel sequencing. *Molecular Ecology*, 20, 258–274.

ALONSO-SÁEZ, L. & GASOL, J.M. (2007) Seasonal variations in the contributions of different baterial groups to the uptake of low-molecular-weight compounds in Northwestern Mediterranean coastal waters. *Applied and Environmental Microbiology*, 73, 3528–3535.

AMANN, R.I., KRUMHOLZ, L. & STAHL, D.A. (1990) Fluorescent-oligonucleotide probing of whole cells for determinative, phylogenetic, and environmental studies in microbiology. *Journal of Bacteriology*, 172, 762–770.

ARANGUREN-GASSIS, M., TEIRA, E., SERRET, P., MARTÍNEZ-GARCÍA, S. & FERNÁNDEZ, E. (2012) Potential overestimation of bacterial respiration rates in oligotrophic plankton communities. *Marine Ecology Progress Series*, 453, 1–10.

ARAR, E.J. & COLLINS, G.B. (1997) In vitro determination of chlorophyll a and pheophytin a in marine and freshwater algae by fluorescence.

ARÍSTEGUI, J., BARTON, E.D., MONTERO, M.F., GARCÍA-MUÑOZ, M. & ESCÁNEZ, J. (2003) Organic carbon distribution and water column respiration in the NW Africa-Canaries coastal transition zone. *Aquatic Microbial Ecology*, 33, 289–301.

AZAM, F. (1998) Microbial control of oceanic carbon flux: the plot thickens. *Science*, 280, 694–696.

AZAM, F., FENCHEL, T., FIELD, J.G., GRAY, J.S., MEYER-REIL, L.A. & THINGSTAD, F. (1983) The ecological role of water-column microbes in the sea. *Marine Ecology Progress Series*, 10, 257–267.

AZAM, F. & MALFATTI, F. (2007) Microbial structuring of marine ecosystems. *Nature reviews: Microbiology*, 5, 782–791.

AZAM, F. & WORDEN, A.Z. (2004) Microbes, molecules, and marine ecosystems. *Science*, 303, 1622–1624.

BAAS-BECKING, L.G.M. (1934) Geobiologie of inleiding tot de milieukunde. W.P. Van Stockum & Zoon, The Hague, the Netherlands.

BALTAR, F., LINDH, M. V., PARPAROV, A., BERMAN, T. & PINHASSI, J. (2012) Prokaryotic community structure and respiration during long-term incubations. *MicrobiologyOpen*, 1, 214–224.

BARNES, M., TILSTONE, G., SMYTH, T., SUGGETT, D., ASTORECA, R., LANCELOT, C. & KROMKAMP, J. (2014) Absorption-based algorithm of primary production for total and size-fractionated phytoplankton in coastal waters. *Marine Ecology Progress Series*, 504, 73–89.

BARNES, M.K., TILSTONE, G.H., SMYTH, T.J., WIDDICOMBE, C.E., GLÖEL, J., ROBINSON, C., ET AL. (submitted) Drivers and effects of *Karenia mikimotoi* blooms in the Western English Channel (1992-2009). *in press*.

BENSON, B.B. & KRAUSE, D.J. (1984) The concentration and isotopic fractionation of oxygen dissolved in freshwater and seawater in equilibrium with the atmosphere. *Limnology and Oceanography*, 29, 620–632.

BLAXTER, M., MANN, J., CHAPMAN, T., THOMAS, F., WHITTON, C., FLOYD, R. & ABEBE, E. (2005) Defining operational taxonomic units using dna barcode data. *Philosophical Transactions of the Royal Society of London. Series B, Biological Sciences*, 360, 1935–1943.

BLIGHT, S.P., BENTLEY, T.L., LEFEVRE, D., ROBINSON, C., RODRIGUES, R., ROWLANDS, J. & WILLIAMS, P.J.B. (1995) Phasing of autotrophic and heterotrophic plankton metabolism in a temperate coastal ecosystem. *Marine Ecology Progress Series*, 128, 61–75.

BOWLER, C., KARL, D.M. & COLWELL, R.R. (2009) Microbial oceanography in a sea of opportunity. *Nature*, 459, 180–184.

BOYD, P.W., ROBINSON, C., SAVIDGE, G. & WILLIAMS, P.J.B. (1995) Water column and sea-ice primary production during Austral spring in the Bellingshausen Sea. *Deep Sea Research Part II: Topical Studies in Oceanography*, 42, 1177–1200.

BREWER, P.G. & RILEY, J.P. (1965) The automatic determination of nitrate in sea water. *Deep Sea Research*, 12, 765–772.

BROWN, J.R. (2003) Ancient horizontal gene transfer. *Nature Reviews Genetics*, 4, 121–132.

CAMPBELL, B.J., YU, L., HEIDELBERG, J.F. & KIRCHMAN, D.L. (2011) Activity of abundant and rare bacteria in a coastal ocean. *Proceedings of the National Academy of Sciences of the United States of America*, 108, 12776–12781.

CAPORASO, J.G., KUCZYNSKI, J., STOMBAUGH, J., BITTINGER, K., BUSHMAN, F.D., COSTELLO, E.K., ET AL. (2010) QIIME allows analysis of high-throughput community sequencing data. N*ature Methods*, 7, 335–336.

CAPORASO, J.G., PASZKIEWICZ, K., FIELD, D., KNIGHT, R. & GILBERT, J. A (2012) The Western English Channel contains a persistent microbial seed bank. *The ISME journal*, 6, 1089–1093.

CARLSON, C.A., DEL GIORGIO, P.A. & HERNDL, G.J. (2007) Microbes and the dissipation of energy and respiration : from cells to ecosystems. *Oceanography*, 20, 89–100.

CARPENTER, J.H. (1965) The Chesapeake Bay Institute technique for the Winkler dissolved oxygen method. *Limnology and Oceanography*, 10, 141–143.

CARRIT, D.E. & CARPENTER, J.H. (1966) Comparison and evaluation of currently employed modifications of the Winkler method for determining dissolved oxygen in sea water. A NASCO report. *Journal of Marine Research*, 24, 286–318.

CHISHOLM, S.W., FRANKEL, S.L., GOERICKE, R., OLSON, R.J., PALENIK, B., WATERBURY, J.B., ET AL. (1992) Prochlorococcus marinus nov. gen. nov. sp.: an oxyphototrophic marine prokaryote containing divinyl chlorophyll a and b. *Archives of Microbiology*, 157, 297–300.

DELONG, E.F. (1992) Archaea in coastal marine environments. *Proceedings of the National Academy of Sciences of the United States of America*, 89, 5685–5689.

DELONG, E.F. (2009) The microbial ocean from genomes to biomes. *Nature*, 459, 200–206.

DOOLITTLE, W.F. & PAPKE, R.T. (2006) Genomics and the bacterial species problem. *Genome Biology*, 7, 116.

DUCKLOW, H.W., DICKSON, M., KIRCHMAN, D.L., STEWARD, G., ORCHARDO, J., MARRA, J. & AZAM, F. (2000) Constraining bacterial production , conversion efficiency and respiration in the Ross Sea, Antarctica, January-February, 1997. *Deep Sea Research Part II: Topical Studies in Oceanography*, 47, 3227–3247.

EILER, A., LANGENHEDER, S., BERTILSSON, S. & TRANVIK, L.J. (2003) Heterotrophic bacterial growth efficiency and community structure at different natural organic carbon concentrations. *Applied and Environmental Microbiology*, 69, 3701–3709.

FALKOWSKI, P.G., FENCHEL, T. & DELONG, E.F. (2008) The microbial engines that drive earth 's biogeochemical cycles. *Science*, 320, 1034–1039.

FENCHEL, T. (2001) Eppur si muove: many water column bacteria are motile. *Aquatic Microbial Ecology*, 24, 197–201.

FRIEDLINE, C.J., FRANKLIN, R.B., MCCALLISTER, S.L. & RIVERA, M.C. (2012) Bacterial assemblages of the eastern Atlantic Ocean reveal both vertical and latitudinal biogeographic signatures. *Biogeosciences*, 9, 2177–2193.

FUHRMAN, J. A, HEWSON, I., SCHWALBACH, M.S., STEELE, J. A, BROWN, M. V & NAEEM, S. (2006) Annually reoccurring bacterial communities are predictable from ocean conditions. *Proceedings of the National Academy of Sciences of the United States of America*, 103, 13104–13109.

FUHRMAN, J. A, STEELE, J. A, HEWSON, I., SCHWALBACH, M.S., BROWN, M. V, GREEN, J.L. & BROWN, J.H. (2008) A latitudinal diversity gradient in planktonic marine bacteria. *Proceedings of the National Academy of Sciences of the United States of America*, 105, 7774–7778.

FUHRMAN, J.A. (2009) Microbial community structure and its functional implications. *Nature*, 459, 193–199.

FUHRMAN, J.A. (2012) Metagenomics and its connection to microbial community organization. *F1000 Biology Reports*, 4, 1–5.

FUKUDA, R., OGAWA, H., NAGATA, T. & KOIKE, I. (1998) Direct determination of carbon and nitrogen contents of natural bacterial assemblages in marine environments. *Applied and Environmental Microbiology*, 64, 3352–3358.

GASOL, J.M., GIORGIO, P.A., MASSANA, R. & DUARTE, C.M. (1995) Active versus inactive bacteria: size-dependence in a coastal marine plankton community. *Marine Ecology Progress Series*, 128, 91–97.

GASOL, J.M. & MORAN, X.A.G. (1999) Effects of filtration on bacterial activity and picoplankton community structure as assessed by flow cytometry. *Aquatic Microbial Ecology*, 16, 251–264.

GASOL, J.M., ZWEIFEL, U.L., PETERS, F., FUHRMAN, J.A. & HAGSTROM, A. (1999) Significance of size and nucleic acid content heterogeneity as measured by flow cytometry in natural planktonic bacteria. *Applied Environmental Microbiology*, 65, 4475–4483.

GILBERT, J. A. & DUPONT, C.L. (2011) Microbial metagenomics: beyond the genome. *Annual Review of Marine Science*, 3, 347–371.

GILBERT, J.A., FIELD, D., SWIFT, P., NEWBOLD, L., OLIVER, A., SMYTH, T., ET AL. (2009) The seasonal structure of microbial communities in the Western English Channel. *Environmental Microbiology*, 11, 3132–3139.

GILBERT, J.A., STEELE, J.A., CAPORASO, J.G., STEINBRÜCK, L., REEDER, J., TEMPERTON, B., ET AL. (2012) Defining seasonal marine microbial community dynamics. *The ISME journal*, 6, 298–308.

DEL GIORGIO, P.A., COLE, J.J. & CIMBLERIS, A. (1997) Respiration rates in bacteria exceed phytoplankton production in unproductive aquatic systems. *Nature*, 385, 148–151.

GIOVANNONI, S.J., BRITSCHGI, T.B., MOYER, C.L. & FIELD, K.G. (1990) Genetic diversity in Sargasso Sea bacterioplankton. *Nature*, 345, 60–63.

GIOVANNONI, S.J. & STINGL, U. (2005) Molecular diversity and ecology of microbial plankton. *Nature*, 437, 343–348.

GIOVANNONI, S.J. & VERGIN, K.L. (2012) Seasonality in ocean microbial communities. *Science*, 335, 671–676.

GÓMEZ-CONSARNAU, L., LINDH, M. V, GASOL, J.M. & PINHASSI, J. (2012) Structuring of bacterioplankton communities by specific dissolved organic carbon compounds. *Environmental Microbiology*, 14, 2361–2378.

GONZÁLEZ, N., ANADÓN, R. & VIESCA, L. (2003) Carbon flux through the microbial community in a temperate sea during summer: role of bacterial metabolism. *Aquatic Microbial Ecology*, 33, 117–126.

GRASSHOFF, K., KREMLING, K. & EHRHARDT, M. (1976) Chapter 12. Determination of trace elements. In *Methods of Seawater Analysis*, Wiley-VCH, pp. 253–364.

HANSELL, D. A., CARLSON, C. A. & SCHLITZER, R. (2012) Net removal of major marine dissolved organic carbon fractions in the subsurface ocean. *Global Biogeochemical Cycles*, 26.

HANSELL, D.A. & CARLSON, C.A. (2001) Marine dissolved organic matter and the carbon cycle. *Oceanography*, 14, 41–49.

HERNDL, G.J., AGOGUÉ, H., BALTAR, F., REINTHALER, T., SINTES, E. & VARELA, M.M. (2008) Regulation of aquatic microbial processes: the 'microbial loop' of the sunlit surface waters and the dark ocean dissected. *Aquatic Microbial Ecology*, 53, 59–68.

HEWSON, I., PAERL, R.W., TRIPP, H.J., ZEHR, J.P. & KARL, D.M. (2009) Metagenomic potential of microbial assemblages in the surface waters of the central Pacific Ocean tracks variability in oceanic habitat. *Limnology and Oceanography*, 54, 1981–1994.

HOBBIE, J.E., DALEY, R.J. & JASPER, S. (1977) Use of Nuclepore filters for counting bacteria by fluorescence microscopy. *Applied and Environmental Microbiology*, 33, 1225–1228.

HUNT, D.E., LIN, Y., CHURCH, M.J., KARL, D.M., TRINGE, S.G., IZZO, L.K. & JOHNSON, Z.I. (2013) Relationship between abundance and specific activity of bacterioplankton in open ocean surface waters. *Applied and Environmental Microbiology*, 79, 177–184.

KARL, D.M. (2007) Microbial oceanography: paradigms, processes and promise. *Nature reviews. Microbiology*, 5, 759–769.

KARSENTI, E., ACINAS, S.G., BORK, P., BOWLER, C., DE VARGAS, C., RAES, J., ET AL. (2011) A holistic approach to marine ecosystems biology. *PLoS Biology*, 9, 1–5.

KIRCHMAN, D.L., DITTEL, A.I., FINDLAY, S.E.G. & FISCHER, D. (2004) Changes in bacterial activity and community structure in response to dissolved organic matter in the Hudson River , New York. *Aquatic Microbial Ecology*, 35, 243–257.

KIRKWOOD, D.S. (1989) Simultaneous determination of selected nutrients in sea water. In *International Council for the Exploration of the Sea (ICES) Committee Meeting* p. CM1989/C:29.

KNAP, A.., MICHAELS, A., CLOSE, A., DUCKLOW, H. & DICKSON, A. (1994) Protocols for the Joint Global Ocean Flux Study (JGOFS) core measurements.

LANDA, M., COTTRELL, M., KIRCHMAN, D., BLAIN, S. & OBERNOSTERER, I. (2013) Changes in bacterial diversity in response to dissolved organic matter supply in a continuous culture experiment. *Aquatic Microbial Ecology*, 69, 157–168.

LEMÉE, R., ROCHELLE-NEWALL, E., WAMBEKE, F. VAN, PIZAY, M.D., RINALDI, P. & GATTUSO, J.P. (2002) Seasonal variation of bacterial production , respiration and growth efficiency in the open NW Mediterranean Sea. *Aquatic Microbial Ecology*, 29, 227–237.

LOUCAIDES, S., TYRRELL, T., ACHTERBERG, E.P., TORRES, R., NIGHTINGALE, P.D., KITIDIS, V., ET AL. (2012) Biological and physical forcing of carbonate chemistry in an upwelling filament off northwest Africa: Results from a Lagrangian study. *Global Biogeochemical Cycles*, 26, GB3008.

MANTOURA, R.F.C. & WOODWARD, E.M.S. (1983) Optimization of the indophenol blue method for the automated determination of ammonia in estuarine waters. *Estuarine, Coastal and Shelf Science*, 17, 219–224.

MARTÍNEZ-GARCÍA, S., FERNÁNDEZ, E., DEL VALLE, D., KARL, D. & TEIRA, E. (2013) Experimental assessment of marine bacterial respiration. *Aquatic Microbial Ecology*, 70, 189–205.

MARTINY, J.B.H., BOHANNAN, B.J.M., BROWN, J.H., COLWELL, R.K., FUHRMAN, J. A, GREEN, J.L., ET AL. (2006) Microbial biogeography: putting microorganisms on the map. *Nature Reviews. Microbiology*, 4, 102–112.

MARY, I., TARRAN, G., WARWICK, P.E., TERRY, M.J., SCANLAN, D.J., BURKILL, P.H. & ZUBKOV, M. V. (2008) Light enhanced amino acid uptake by dominant bacterioplankton groups in surface waters of the Atlantic Ocean. *FEMS Microbiology Ecology*, 63, 36–45.

McDaniel, L.D., Young, E., Delaney, J., Ruhnau, F., Ritchie, K.B. & Paul, J.H. (2010) High frequency of horizontal gene transfer in the oceans. *Science*, 330, 50.

Minas, H.J., Packart, T.T., Minas, M. & Coste, B. (1982) An analysis of the production-regeneration system in the coastal upwelling area off NW Africa based on oxygen, nitrate and ammonium distributions. *Journal of Marine Research*, 40, 615–641.

Morán, X.A.G., Calvo-Díaz, A. & Ducklow, H.W. (2010) Total and phytoplankton mediated bottom-up control of bacterioplankton change with temperature in NE Atlantic shelf waters. *Aquatic Microbial Ecology*, 58, 229–239.

Müller, A.L., de Rezende, J.R., Hubert, C.R.J., Kjeldsen, K.U., Lagkouvardos, I., Berry, D., (2014) Endospores of thermophilic bacteria as tracers of microbial dispersal by ocean currents. *The ISME journal*, 8, 1153–1165.

Munn, C. (2011) Microbes in the marine environment. In *Marine Microbiology: Ecology and Applications* (ed C. Munn), pp. 1–23, 2nd edition. Garland Science, Abingdon, Oxfordshire.

Neufeld, J.D., Schäfer, H., Cox, M.J., Boden, R., McDonald, I.R. & Murrell, J.C. (2007) Stable-isotope probing implicates *Methylophaga* spp and novel Gammaproteobacteria in marine methanol and methylamine metabolism. *The ISME journal*, 1, 480–491.

Obernosterer, I., Kawasaki, N. & Benner, R. (2003) P limitation of respiration in the Sargasso Sea and uncoupling of bacteria from P regeneration in size-fractionation experiments. *Aquatic Microbial Ecology*, 32, 229–237.

Obernosterer, I., Lami, R., Larcher, M., Batailler, N., Catala, P. & Lebaron, P. (2010) Linkage Between Bacterial Carbon Processing and the Structure of the Active Bacterial Community at a Coastal Site in the NW Mediterranean Sea. *Microbial Ecology*, 59, 428–435.

Olsen, G.J., Lane, D.J., Giovannoni, S.J., Pace, N.R. & Stahl, D. a (1986) Microbial ecology and evolution: a ribosomal RNA approach. *Annual Review of Microbiology*, 40, 337–365.

Pedler, B.E., Aluwihare, L.I. & Azam, F. (2014) Single bacterial strain capable of significant contribution to carbon cycling in the surface ocean. *Proceedings of the National Academy of Sciences of the United States of America*, 111, 7202–7207.

Pedrós-Alió, C. (2012) The rare bacterial biosphere. *Annual Review of Marine Science*, 4, 449–466.

PINGREE, R.D. & GRIFFITHS, D.K. (1978) Tidal fronts on the shelf seas around the British Isles. *Journal of Geophysical Research*, 83, 4615.

PINHASSI, J., AZAM, F., HEMPHÄLÄ, J., LONG, R.A., MARTINEZ, J., ZWEIFEL, U.L. & HAGSTRÖM, A. (1999) Coupling between bacterioplankton species composition, population dynamics, and organic matter degradation. *Aquatic Microbial Ecology*, 17, 13–26.

POMEROY, L.R. (1974) The ocean's food web, a changing paradigm. *BioScience*, 24, 499–504.

POMEROY, L.R., WILLIAMS, P.J.B., AZAM, F. & HOBBIE, J.E. (2007) The microbial loop. *Oceanography*, 20, 28–33.

POMMIER, T., PINHASSI, J. & HAGSTRÖM, Å. (2005) Biogeographic analysis of ribosomal RNA clusters from marine bacterioplankton. *Aquatic Microbial Ecology*, 41, 79–89.

REES, A.P., BROWN, I.J., CLARK, D.R. & TORRES, R. (2011) The Lagrangian progression of nitrous oxide within filaments formed in the Mauritanian upwelling. *Geophysical Research Letters*, 38, L21606.

REES, A.P., HOPE, S.B., WIDDICOMBE, C.E., DIXON, J.L., WOODWARD, E.M.S. & FITZSIMONS, M.F. (2009) Alkaline phosphatase activity in the Western English Channel: Elevations induced by high summertime rainfall. *Estuarine, Coastal and Shelf Science*, 81, 569–574.

REINTHALER, T., WINTER, C. & HERNDL, G.J. (2005) Relationship between bacterioplankton richness , respiration , and production in the southern North Sea. *Applied and Environmental Microbiology*, 71, 2260–2266.

RIVKIN, R.B. & LEGENDRE, L. (2001) Biogenic carbon cycling in the upper ocean: effects of microbial respiration. *Science*, 291, 2398–2400.

ROBINSON, C. (2008) Bacterial respiration. In *Microbial Ecology of the Oceans* (ed D.L. Kirchman), pp. 299–334, 2nd edition. John Wiley & Sons, Inc.

ROBINSON, C., ARCHER, S.D. & WILLIAMS, P.J.B. (1999) Microbial dynamics in coastal waters of east antarctica: plankton production and respiration. *Marine Ecology Progress Series*, 180, 23–36.

ROBINSON, C., STEINBERG, D.K., ANDERSON, T.R., ARÍSTEGUI, J., CARLSON, C.A., FROST, J.R., ET AL. (2010) Mesopelagic zone ecology and biogeochemistry – a synthesis. *Deep Sea Research Part II: Topical Studies in Oceanography*, 57, 1504–1518.

ROBINSON, C. & WILLIAMS, P.J.B. (2005) CHAPTER 9 Respiration and its measurement in surface marine waters. In *Respiration in Aquatic Ecosystems* (eds P.A. del Giorgio & P.J.L.B. Williams), pp. 147–180, 1st edition.

RUSCH, D.B., HALPERN, A.L., SUTTON, G., HEIDELBERG, K.B., WILLIAMSON, S., YOOSEPH, S., ET AL. (2007) The Sorcerer II Global Ocean Sampling (GOS) expedition: Northwest Atlantic through eastern tropical Pacific. *PLoS biology*, 5, e77.

RUSCH, D.B., MARTINY, A.C., DUPONT, C.L., HALPERN, A.L. & VENTER, J.C. (2010) Characterization of Prochlorococcus clades from iron-depleted oceanic regions. *Proceedings of the National Academy of Sciences of the United States of America*, 107, 16184–16189.

SEBASTIÁN, M. & GASOL, J.M. (2013) Heterogeneity in the nutrient limitation of different bacterioplankton groups in the Eastern Mediterranean Sea. *The ISME journal*, 7, 1665–1668.

SHERR, E.B. & SHERR, B.F. (2002) Significance of predation by protists in aquatic microbial food webs. *Antonie van Leeuwenhoek*, 81, 293–308.

SMYTH, T.J., FISHWICK, J.R., AL-MOOSAWI, L., CUMMINGS, D.G., HARRIS, C., KITIDIS, V., (2009) A broad spatio-temporal view of the Western English Channel Observatory. *Journal of Plankton Research*, 32, 585–601.

SOGIN, M.L., MORRISON, H.G., HUBER, J.A., WELCH, D.M., HUSE, S.M., NEAL, P.R., ET AL. (2006) Microbial Diversity in the Deep Sea and the Underexplored 'Rare Biosphere'. *Proceedings of the National Academy of Sciences of the United States of America*, 103, 12115–12120.

SOUTHWARD, A.J., LANGMEAD, O., HARDMAN-MOUNTFORD, N.J., AIKEN, J., BOALCH, G.., JOINT, I., ET AL. (2004) A review of long-term research in the western English Channel. *Advances in Marine Biology*, 47, 1–105.

STAHL, D.A., FLOWERS, J.J., HULLAR, M. & DAVIDSON, S. (2013) Structure and Function of Microbial Communities. In *The Prokaryotes*, Rosenberg, Eugene, DeLong, E.F., Lory, S., Stackebrandt, E., Thompson, F. (Eds.), Springer, pp. 3–30.

STALEY, J.T. & GOSINK, J.J. (1999) Microbial extracellular enzymes and the marine carbon cycle. *Annual Review of Marine Science*, 53, 189–2125.

STEWART, F.J. (2013) Where the genes flow. *Nature Geoscience*, 6, 688–690.

STOCKER, R. & SEYMOUR, J.R. (2012) Ecology and physics of bacterial chemotaxis in the ocean. *Microbiology and Molecular Biology Reviews : MMBR*, 76, 792–812.

SUL, W.J., OLIVER, T.A., DUCKLOW, H.W., AMARAL-ZETTLER, L.A. & SOGIN, M.L. (2013) Marine bacteria exhibit a bipolar distribution. *Proceedings of the National Academy of Sciences of the United States of America*, 110, 2342–2347.

SWAN, B.K., TUPPER, B., SCZYRBA, A., LAURO, F.M., MARTINEZ-GARCIA, M., GONZÁLEZ, J.M., ET AL. (2013) Prevalent genome streamlining and latitudinal divergence of planktonic bacteria in the Surface Ocean. *Proceedings of the National Academy of Sciences of the United States of America*, 110, 11463–11468.

TEIRA, E., MARTÍNEZ-GARCÍA, S., FERNÁNDEZ, E., CALVO-DÍAZ, A. & MORÁN, X.A.G.X. (2010) Lagrangian study of microbial plankton respiration in the subtropical North Atlantic Ocean: bacterial contribution and short-term temporal variability. *Aquatic Microbial Ecology*, 61, 31–43.

THOMAS, T., GILBERT, J. & MEYER, F. (2012) Metagenomics - a guide from sampling to data analysis. *Microbial informatics and experimentation*, 2, 3. BioMed Central Ltd.

TILSTONE, G., SMYTH, T., POULTON, A. & HUTSON, R. (2009) Measured and remotely sensed estimates of primary production in the Atlantic Ocean from 1998 to 2005. *Deep Sea Research Part II: Topical Studies in Oceanography*, 56, 918–930.

TREUSCH, A.H., VERGIN, K.L., FINLAY, L. A, DONATZ, M.G., BURTON, R.M., CARLSON, C. A & GIOVANNONI, S.J. (2009) Seasonality and vertical structure of microbial communities in an ocean gyre. *The ISME journal*, 3, 1148–1163.

TYSON, G.W., CHAPMAN, J., HUGENHOLTZ, P., ALLEN, E.E., RAM, R.J., RICHARDSON, P.M., ET AL. (2004) Community structure and metabolism through reconstruction of microbial genomes from the environment. *Nature*, 428, 37–43.

VENTER, J.C., REMINGTON, K., HEIDELBERG, J.F., HALPERN, A.L., RUSCH, D., EISEN, J.A., ET AL. (2004) Environmental genome shotgun sequencing of the Sargasso Sea. *Science*, 304, 66–74.

WATERBURY, J.B., WATSON, S.W., GUILLARD, R.R.L. & BRAND, L.E. (1979) Widespread occurance of a unicellular, marine, planktonic, cyanobacterium. *Nature*, 277, 293–294.

WHITMAN, W.B., COLEMAN, D.C. & WIEBE, W.J. (1998) Perspective prokaryotes : The unseen majority, *Proceedings of the National Academy of Sciences of the United States of America*, 95, 6578–6583.

WIDDICOMBE, C.E., ELOIRE, D., HARBOUR, D., HARRIS, R.P. & SOMERFIELD, P.J. (2010) Long-term phytoplankton community dynamics in the Western English Channel. *Journal of Plankton Research*, 32, 643–655.

WIETZ, M., GRAM, L., JØRGENSEN, B. & SCHRAMM, A (2010) Latitudinal patterns in the abundance of major marine bacterioplankton groups. *Aquatic Microbial Ecology*, 61, 179–189.

WILLIAMS, P.J.B. & JENKINSON, N.W. (1982) A transportable microprocessor-controlled precise Winkler titration suitable for field station and shipboard use1. *Limnology and Oceanography*, 27, 576–584.

WILLIAMS, P.J.L.B. & DEL GIORGIO, P.A. (2005) Respiration in aquatic ecosystems : history and background. In *Respiration in Aquatic Ecosystems* (eds P.A. del Giorgio & P.J.B. Williams), pp. 1–17, 1st edition. Oxford University Press, New York.

WINKLER, L.W. (1888) Die Bestimmung des in Wasser gelösten Sauerstoffen. *Berichte der Deutschen Chemischen Gesellschaft*, 21, 2843–2855.

WOOLEY, J.C., GODZIK, A. & FRIEDBERG, I. (2010) A primer on metagenomics. *PLoS Computational Biology*, 6, 1–13.

WRIGHT, R.T. & HOBBIE, J.E. (1966) Use of glucose and acetate by bacteria and algae in aquatic ecosystems. *Ecology*, 47, 447–464.

YOKOKAWA, T. & NAGATA, T. (2010) Linking bacterial community structure to carbon fluxes. *Journal of Oceanography*, 66, 1–12.

YOOSEPH, S., NEALSON, K.H., RUSCH, D.B., MCCROW, J.P., DUPONT, C.L., KIM, M., ET AL. (2010) Genomic and functional adaptation in surface ocean planktonic prokaryotes. *Nature*, 468, 60–66.

ZHANG, J.Z. & CHI, J. (2002) Automated analysis of nanomolar concentrations of phosphate in natural waters with liquid waveguides. *Environmental Science and Technology*, 36, 5.

ZUBKOV, M. V., TARRAN, G., MARY, I. & FUCHS, B.M. (2008) Differential microbial uptake of dissolved amino acids and amino sugars in surface waters of the Atlantic Ocean. *Journal of Plankton Research*, 30, 211–220.